



저작자표시-비영리-변경금지 2.0 대한민국

이용자는 아래의 조건을 따르는 경우에 한하여 자유롭게

- 이 저작물을 복제, 배포, 전송, 전시, 공연 및 방송할 수 있습니다.

다음과 같은 조건을 따라야 합니다:



저작자표시. 귀하는 원저작자를 표시하여야 합니다.



비영리. 귀하는 이 저작물을 영리 목적으로 이용할 수 없습니다.



변경금지. 귀하는 이 저작물을 개작, 변형 또는 가공할 수 없습니다.

- 귀하는, 이 저작물의 재이용이나 배포의 경우, 이 저작물에 적용된 이용허락조건을 명확하게 나타내어야 합니다.
- 저작권자로부터 별도의 허가를 받으면 이러한 조건들은 적용되지 않습니다.

저작권법에 따른 이용자의 권리는 위의 내용에 의하여 영향을 받지 않습니다.

이것은 [이용허락규약\(Legal Code\)](#)을 이해하기 쉽게 요약한 것입니다.

[Disclaimer](#)

이학박사 학위논문

**Role of bacterial peptidoglycan
in regulation of bone mass**

세균의 펩티도글리칸에 의한 골량 조절

2019 년 8 월

서울대학교 대학원

치의과학과 면역 및 분자미생물 전공

김 지 선

Role of bacterial peptidoglycan in regulation of bone mass

By

Jiseon Kim

Under the supervision of

Professor Seung Hyun Han, Ph. D.

A dissertation submitted in partial fulfillment of

the requirements for the degree of

Doctor of Philosophy

will be published elsewhere

August 2019

School of Dentistry

Graduate School

Seoul National University

Role of bacterial peptidoglycan in regulation of bone mass

지도교수 한승현
이 논문을 이학박사 학위논문으로 제출함
2019년 6월

서울대학교 대학원
치의과학과 면역 및 분자미생물 전공
김지선

김지선의 박사 학위논문을 인준함
2019년 7월

위원장	석영재	(인)
부위원장	한승현	(인)
위원	윤철희	(인)
위원	강석성	(인)
위원	박주홍	(인)

ABSTRACT

Role of bacterial peptidoglycan in regulation of bone mass

Jiseon Kim

Immunology and Molecular Microbiology

Department of Dental Science

The Graduate School

Seoul National University

Objectives

It has been suggested that gut microbiota, a bacterial community colonized in the intestine, interacts with host and influences on various physiological regulations including bone homeostasis. Peptidoglycans (PGNs) are the most abundant bacterial cell wall components and their fragments released from the gut microbiota can be delivered into the bone marrow and potentially affect the bone metabolism. Therefore, the objective of the present study is to elucidate the role of bacterial PGNs in the regulation of bone metabolism using *in vivo* and *in vitro* models. Under the

research objective, (i) direct effect of PGN on osteoblast or osteoclast differentiation and (ii) indirect effect of PGN on host factors involved in the regulation of bone metabolism were investigated.

Methods

Insoluble PGNs from various *Lactobacillus* spp. and *Bacillus* spp. were purified by sequential treatment with sodium dodecyl sulfate, DNase, RNase, trypsin, trichloroacetic acid, and acetone. Soluble PGNs were prepared by treatment of the purified PGNs with mutanolysin. Nucleotide-binding oligomerization domain (NOD) 1 or NOD2 activation by PGNs was determined by reporter gene assay. Mice were intragastrically given phosphate buffered saline (PBS) or insoluble PGN by oral gavage technique three times weekly for four weeks. In a separate experiment, mice were intraperitoneally or intravenously given PBS or insoluble PGN once weekly for four weeks. Ovariectomy (OVX)-induced osteoporosis mouse model and receptor activator of nuclear factor- κ B ligand (RANKL)-induced osteoporosis mouse model were prepared for *in vivo* studies. Estrogen deficiency was confirmed by measuring body weight, uterus weight, and level of 17β -estradiol in the serum. Bone morphometric parameters (trabecular bone volume, trabecular number, trabecular separation, and trabecular thickness) of femur and lumbar were analyzed by X-ray microcomputed tomography. Differentiation of osteoblast and osteoclast *in vivo* was determined by immunofluorescence staining of runt-related transcription factor 2 (Runx2) and tartrate-resistant acid phosphatase (TRAP) staining, respectively. Calcein AM was intraperitoneally injected to the mice to observe new bone formation and the related parameters were measured by using OsteoMeasure

software. The levels of RANKL, osteoprotegerin, and tumor necrosis factor (TNF)- α in bone marrow extracellular fluid or that of P1NP, TNF- α , interleukin (IL)-6, and IL-1 β in serum were determined by enzyme-linked immunosorbent assay. The mRNA expressions of osteoclast or osteoblast differentiation markers were determined by real-time reverse transcription-polymerase chain reaction. Osteoblast precursors were isolated from calvariae of one-day mice. Bone marrow-derived macrophages (BMMs) were prepared by incubation of bone marrow cells with macrophage colony-stimulating factor (M-CSF) and committed osteoclast precursors were prepared by incubation of BMMs with M-CSF and RANKL. To observe direct effect of PGN, calvarial osteoblast precursors were stimulated with soluble PGNs in the presence of β -glycerophosphate and ascorbic acid. Osteoblast differentiation and function were determined by alkaline phosphatase staining and alizarin red S staining, respectively. BMMs or committed osteoclast precursors were stimulated with PGNs in the presence of M-CSF and/or RANKL. BMMs co-cultured with osteoblasts were stimulated with soluble PGNs in the presence of β -glycerophosphate, ascorbic acid, and 1 α ,25-dihydroxyvitamin D₃.

Results

Intragastric administration of insoluble *L. plantarum* PGN (Lp.PGN) increased trabecular bone volume and trabecular number in both femurs and lumbar vertebrae in OVX-induced osteoporosis mouse model. When the effect of PGNs from various *Lactobacillus* spp. on trabecular bone was further examined, insoluble PGNs isolated from *L. casei*, *L. delbrueckii*, *L. rhamnosus* GG, *L. agilis*, *L. ruminis*, and *L. saerimneri* increased femoral trabecular bone volume and trabecular number in

OVX-induced osteoporosis mouse model. Runx2 immunofluorescence or TRAP staining of paraffin sections of femur showed increased Runx2-positive and decreased TRAP-positive areas on bone surfaces in OVX mice supplemented with Lp.PGN compared to the OVX control mice. In addition, calcein double labeling demonstrated that supplementation of Lp.PGN induced new bone formation. Intraperitoneal or intravenous administration of insoluble or soluble Lp.PGN increased femoral trabecular bone volume and trabecular number in OVX-induced osteoporosis mouse model. In addition, *in vitro* osteoblast differentiation assay demonstrated that soluble Lp.PGN directly induced osteoblast mineralization. On the other hand, soluble Lp.PGN attenuated osteoclast differentiation in BMM/osteoblast co-culture system. Reporter gene assay demonstrated that Lp.PGN preferentially activates NOD2, but not NOD1, and that soluble Lp.PGN more potently activates NOD2 signaling than insoluble Lp.PGN does. Intra-gastric administration of Lp.PGN in NOD2-deficient OVX mice did not exhibit trabecular bone mass changes, while that in wild-type OVX mice increased bone mass. Moreover, Runx2-positive areas were not increased and TRAP-positive areas were not decreased by supplementation with Lp.PGN in NOD2-deficient mice. Moreover, RANKL/OPG ratio was significantly decreased in bone marrow extracellular fluid and the levels of TNF- α and IL-6 were decreased in serum from OVX mice supplemented with Lp.PGN in comparison with that from OVX control mice. In contrast to the Lp.PGN, *B. cereus* PGN (Bc.PGN) and *B. subtilis* PGN (Bs.PGN) preferentially activated NOD1. Intra-gastric administration of Bc.PGN or Bs.PGN decreased trabecular bone volume and/or trabecular number. TRAP stained paraffin sections of femur showed increased TRAP-positive areas on bone surfaces. In addition, Bc.PGN increased osteoclast differentiation from BMMs co-cultured with

osteoblasts. *In vitro* osteoclast differentiation demonstrated that Bc.PGN directly increases the number of TRAP-positive osteoclasts from committed osteoclast precursors. Bc.PGN induced phosphorylation of ERK and specific inhibition of ERK signaling attenuated Bc.PGN-induced osteoclast differentiation.

Conclusion

The present study demonstrates that NOD2-activating PGN inhibits bone loss in osteoporosis condition through increasing osteoblast differentiation and decreasing osteoclast differentiation, whereas NOD1-activating PGN induces bone destruction. These results suggest that gut microbiota-derived PGN fragments could be involved in the regulation of bone metabolism through NOD1 and NOD2 signaling and that the NOD2 ligands could be used as postbiotics for treatment of bone diseases.

Keywords: Bacterial peptidoglycan, NOD1, NOD2, Osteoblast, Osteoclast

Student number: 2011-31195

CONTENTS

Abstract	I
Contents	VI
List of figures	X
List of tables	XIII
Abbreviations	XIV
Chapter I. Introduction	1
1. Bone remodeling	1
2. Osteoclast differentiation	3
3. Osteoblast differentiation	4
4. Osteoporosis	8
5. Gut microbiota and bone regulation	10
6. Probiotics and bone regulation	11
6.1. Modification of gut microbiota	11
6.2. Enhancement of intestinal barrier function	12
6.3. Modulation of immune system	13
7. Peptidoglycan (PGN)	15
7.1. Structure of PGN	15
7.2. PGN degrading enzymes and cleavage sites	17
7.3. PGN detection by NOD proteins	19
8. Objective of the present study	20
Chapter II. Materials and Methods	21

1. Materials	21
2. Preparation of PGN	21
2.1. Bacterial strains and culture condition	21
2.2. Purification of PGN	22
3. <i>In vivo</i> mouse model	23
4. Preparation of osteoclasts and osteoblasts	24
4.1. Preparation of osteoclast and osteoclast differentiation	24
4.2. Preparation of osteoblast and osteoblast differentiation	25
5. Bone morphometric analysis using micro-computed tomography (micro-CT)	26
6. Histological analysis	26
7. Calcein double labeling	27
8. Real-time reverse transcription-polymerase chain reaction (Real- time RT-PCR)	27
9. Transient transfection and reporter gene assay	29
10. Enzyme linked immunosorbent assay (ELISA)	29
11. Western blot analysis	30
12. Immunofluorescence staining	30
13. Statistical analysis	31
Chapter III. Results	32
1. Intragastric administration of Lp.PGN attenuates bone loss induced by estrogen deficiency	32

2. Intra-gastric administration of PGNs isolated from <i>Lactobacillus</i> spp. regulate trabecular bone volume decreased by estrogen deficiency	38
3. Intra-gastric administration of Lp.PGN induces Runx2 decreased by OVX-induced estrogen deficiency	40
4. Intra-gastric administration of Lp.PGN decreases osteoclasts increased by OVX-induced estrogen deficiency	42
5. NOD2 signaling is essential for increase of trabecular bone volume by Lp.PGN	44
6. Intravenous or intraperitoneal administration of Lp.PGN increases trabecular bone volume in OVX-induced osteoporosis mouse model	48
7. Lp.PGN directly induces osteoblast mineralization though NOD2 <i>in vitro</i>	51
8. Lp.PGN indirectly decreases osteoclast differentiation via osteoblasts	54
9. Intra-gastric administration of Lp.PGN decreases TNF- α , IL-6, and RANKL production	56
10. Intra-gastric administration of Lp.PGN increases trabecular bone volumes in RANKL-induced osteoporosis mouse model	60
11. NOD1-activating Bc.PGN and Bs.PGN induce bone destruction	66
12. Bc.PGN induces osteoclast differentiation by direct and indirect mechanisms	69
13. Bc.PGN directly inhibits osteoblast differentiation <i>in vitro</i>	76

Chapter IV. Discussion	78
Chapter V. References	86
국문초록	99

List of Figures

Figure 1.	Bone remodeling cycle	2
Figure 2.	Illustration of osteoclast and osteoblast differentiation	6
Figure 3.	Illustration of basic structure of PGN and cleaving enzymes	16
Figure 4.	Experimental procedure of OVX-induced osteoporosis mouse model	34
Figure 5.	Establishment of osteoporosis mouse model by ovariectomy	35
Figure 6.	Intragastric administration of Lp.PGN increases femoral trabecular bone volume, but not cortical bone volume, in OVX-induced osteoporosis mouse model	36
Figure 7.	Intragastric administration of Lp.PGN increases vertebral trabecular bone volume in OVX-induced osteoporosis mouse model	37
Figure 8.	Intragastric administration of PGNs isolated from <i>Lactobacillus</i> spp. increases femoral trabecular bone volumes in OVX-induced osteoporosis mouse model	39
Figure 9.	Intragastric administration of Lp.PGN induces Runx2 decreased OVX-induced estrogen deficiency	41
Figure 10.	Intragastric administration of Lp.PGN decreases osteoclasts increased by OVX-induced estrogen deficiency	43
Figure 11.	Lp.PGNs selectively activate NOD2	45
Figure 12.	NOD2 signaling is essential for increase of trabecular bone volume by Lp.PGN	46

Figure 13. NOD2 is required for induction of Runx2 and inhibition of osteoclasts by Lp.PGN	47
Figure 14. Intraperitoneal administration of Lp.PGN increases femoral trabecular bone volume in OVX-induced osteoporosis mouse model	49
Figure 15. Intravenous administration of Lp.PGN increases femoral trabecular bone volume in OVX-induced osteoporosis mouse model	50
Figure 16. Lp.PGN induces osteoblast mineralization <i>in vitro</i>	52
Figure 17. NOD2 is required for induction of osteoblast mineralization by Lp.PGN	53
Figure 18. Lp.PGN indirectly attenuates osteoclast differentiation <i>in vitro</i>	55
Figure 19. Intragastric administration of Lp.PGN decreases TNF- α and IL-6 production in serum and bone marrow extracellular fluid	58
Figure 20. Intragastric administration of Lp.PGN decreases RANKL production in bone marrow extracellular fluid	59
Figure 21. Experimental procedure of RANKL-induced osteoporosis mouse model	62
Figure 22. Intragastric administration of Lp.PGN increases femoral trabecular bone volume in RANKL-induced osteoporosis mouse model	63

Figure 23. Intragastric administration of Lp.PGN increases vertebral trabecular bone volume in RANKL-induced osteoporosis mouse model	64
Figure 24. Intragastric administration of Lp.PGN increases bone formation	65
Figure 25. Bc.PGN and Bs.PGN selectively activate NOD1	67
Figure 26. Intragastric administration of NOD1-activating Bc.PGN and Bs.PGN induce bone destruction	68
Figure 27. Bc.PGN increases TRAP-positive osteoclasts <i>in vivo</i>	71
Figure 28. Bc.PGN enhances osteoclast differentiation and expression of NFATc1	72
Figure 29. Phosphorylation of ERK are required for Bc.PGN-induced osteoclast differentiation	73
Figure 30. Bc.PGN induces osteoclast differentiation from BMMs co-cultured with osteoblast precursors	74
Figure 31. Bc.PGN indirectly induces osteoclast differentiation by affecting osteoblasts through NOD1 signaling	75
Figure 32. Bc.PGN inhibits osteoblast differentiation	77
Figure 33. Schematic illustration of the proposed mechanism	85

List of tables

Table 1. Signaling of osteogenic factors	7
Table 2. Major therapeutics for osteoporosis and their side effects	9
Table 3. Probiotic benefits to skeletal health	14
Table 4. PGN fragments that recognized by mammalian sensing molecules	18

Abbreviations

ALP	alkaline phosphatase
BFR	bone formation rate
BMMs	bone marrow-derived macrophages
BMP	bone morphogenetic protein
BMs	bone marrow cells
CARD	caspase activation and recruitment domain
col1α1	collagen type I α 1
CXCL	CXC-chemokine ligand
DMEM	Dulbecco's modified Eagle's medium
ELISA	enzyme-linked immunosorbent assay
ERK	extracellular signal-regulated kinase
FBS	fetal bovine serum
FGF	fibroblast growth factor
FGFR	FGF receptor family of tyrosin kinase receptor
IGF	insulin-like growth factor
IL	interleukin
JNK	c-Jun N-terminal kinase
MAPK	mitogen-activated protein kinase
M-CSF	macrophage colony-stimulating factor
<i>mDAP</i>	<i>meso</i> -diaminopimelic acid
MDP	NAM-D-ala-D-glu
micro-CT	micro-computed tomography
MNCs	multinucleated cells

MRS	de Man, Rogosa and Sharpe
NAG	<i>N</i> -acetylglucosamine
NAM	<i>N</i> -acetylmuramic acid
NFATc1	nuclear factor of activated T cells 1
NF-κB	nuclear factor- κ B
NOD	nucleotide-binding oligomerization domain
OPG	osteoprotegerin
OPN	osteopontin
OVX	ovariectomy
P1NP	procollagen type 1 N propeptide
PBS	phosphate-buffered saline
PGN	peptidoglycan
PGRP	PGN recognition protein
PI3-K	phosphoinositide 3-kinase
RANK	receptor activator of nuclear factor κ B
RANKL	receptor activator of nuclear factor κ B ligand
RT-PCR	reverse transcription-polymerase chain reaction
Runx2	runt-related transcription factor 2
S1P	sphingosine-1-phosphate
SDS	sodium dodecyl sulphate
TBS-T	Tris-buffered saline containing 0.05% Tween-20
TGF	transforming growth factor
TNF	tumor necrosis factor
TRAF	TNF receptor-associated factor

TRAP	tartrate-resistant acid phosphatase
TSB	tryptic soy broth
α-MEM	alpha-minimum essential medium

Chapter I. Introduction

1. Bone remodeling

Bone is continuously remodeled to maintain bone mass and quality by replacing older bone to new bone [1] throughout the lifetime. The bone remodeling process is tightly regulated by bone component cells, such as bone-resorbing osteoclasts and bone-forming osteoblasts [2]. Bone remodeling process is divided into four steps, bone resorption, reversal, bone formation, and mineralization (Fig. 1) [3]. In bone resorption step, osteoclast precursors are recruited into the bone surface and differentiated into mature osteoclasts and fully activated osteoclasts dissolve mineral [4]. When osteoclasts finish the resorption, osteoblast precursors are recruited to the resorbed site by bone matrix releasing factors, insulin-like growth factor (IGF)-1 and transforming growth factor (TGF)- β and by mature osteoclast releasing factors, bone morphogenetic protein (BMP) 6 and sphingosine-1-phosphate (S1P) [5]. The osteoblasts replace the area by participating in new bone formation. At the end of the bone remodeling cycle, bone lining cells cover the bone surface. Biomarkers of bone formation and resorption are released during bone remodeling. Bone formation markers, such as osteocalcin, bone-specific alkaline phosphatase (ALP), and procollagen type 1 N propeptide (P1NP) are detected in serum [6]. Bone resorption markers are tartrate-resistant acid phosphatase (TRAP), C-terminal cross-linking telopeptide of type I collagen, deoxypyridinoline, and pyridonoline [6]. The bone remodeling process can be altered by various factors, including hormones, cytokines, and microbes [3].

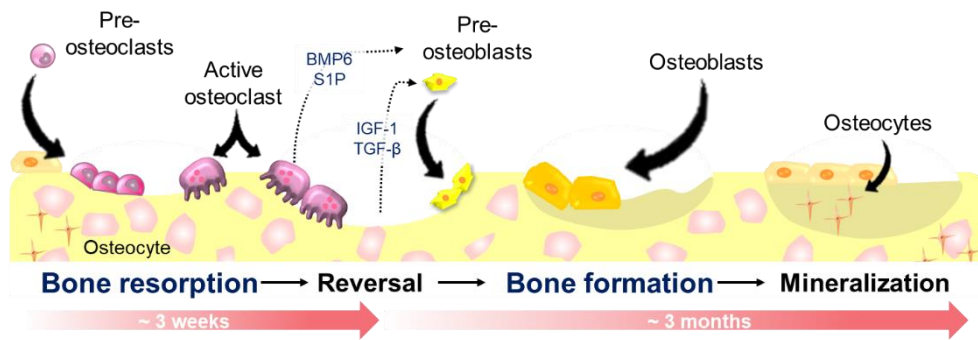


Figure 1. Bone remodeling cycle. The bone remodeling cycle is divided into four phases, bone resorption, reversal, bone formation, and mineralization. Osteoclast precursors are recruited to the bone surface to initiate bone remodeling. Osteoclasts are differentiated into mature osteoclasts and resorb the old or damaged bones. At the end of the resorption phase, BMP6 and S1P are produced by mature osteoclasts and IGF-1 and TGF- β are released from bone matrix. Then, osteoblast precursors are recruited, differentiated, and activated. The process is finished with mineralization. BMP: bone morphogenetic protein, S1P: sphingosine-1-phosphate, IGF: insulin-like growth factor, TGF: transforming growth factor.

2. Osteoclast differentiation

Osteoclasts, derived from the monocyte/macrophage lineage of hematopoietic stem cells, are responsible for bone resorption [7]. Macrophage colony-stimulating factor (M-CSF) and receptor activator of nuclear factor- κ B ligand (RANKL) are important factors required for osteoclast differentiation [7]. M-CSF supports survival and proliferation during osteoclast differentiation by binding to macrophage colony stimulating factor 1 receptor (also known as c-Fms) [8]. RANKL provides a signal for osteoclast differentiation and activation by binding to receptor activator of nuclear factor κ B (RANK) [9]. RANKL controls osteoclast differentiation process from precursors to maturation, including fusion of mononucleated osteoclast precursors into multinucleated cells and expression of osteoclast-specific markers, and attachment of osteoclasts to the bone surfaces, stimulation of resorption, and promotion of osteoclast survival [10]. Association of RANKL and its trimeric receptor RANK induces recruitment of TNF receptor-associated factor (TRAF) 6 [11]. TRAF6 activates signaling molecules and transcription factors, such as mitogen-activated protein kinase (MAPK), nuclear factor- κ B (NF- κ B), c-Fos, and nuclear factor of activated T cells 1 (NFATc1) [7, 12] to induces upregulation of osteoclast-specific molecules, such as TRAP, cathepsin K, and dendritic cell-specific transmembrane protein [9]. Amplification of NFATc1 is induced by co-stimulatory signals including triggering receptor expressed in myeloid cells-2 and osteoclast-associated receptor [13, 14]. An important step in the late stage of osteoclast differentiation is to have specialized morphology to resorb bone matrix called sealing zone and ruffled border [15]. Integrin on the mature osteoclasts recognizes ArgGlyAsp amino-acid motif in the organic matrix of bone to make tight attachment

to the bone surface [16]. The sealing zone creates a bone absorbing space and surrounds another membrane are called ruffled border [17]. Effective bone resorption is dependent on the acidification of the lacunar space below the ruffled border membrane [18].

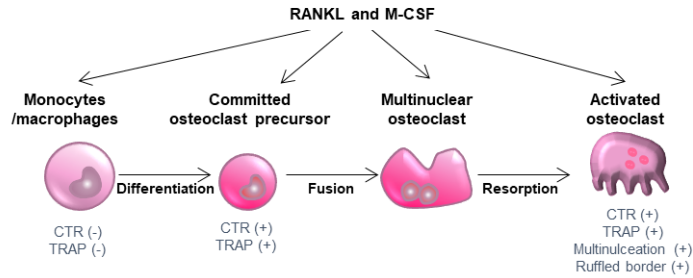
Both RANKL and M-CSF are expressed by osteoblasts, osteocytes and bone marrow stromal cells (Fig. 2A) [19]. RANKL and RANK interaction can be inhibited by osteoprotegerin (OPG) secreted by osteoblasts and osteocytes [7, 20]. Unlike other members of TNF receptor family, OPG is a secreted protein. Association of OPG and RANKL blocks RANKL interaction with RANK on osteoclasts, thereby inhibiting osteoclast differentiation [20]. Therefore, the ratio of RANKL to OPG is one of critical factors for determining osteoclast differentiation. Upregulation of RANKL expression in osteoblasts is induced by various factors, such as $1\alpha,25$ -dihydroxyvitamin D₃, parathyroid hormone, and IL-6 [21]. OPG secretion is promoted by activation of lymphoid enhancer-binding factor 1 by β -catenin signaling in osteoblasts [22].

3. Osteoblast differentiation

Osteoblasts, differentiated from mesenchymal cell lineages, are responsible for bone formation, deposition and mineralization of bone cells [23]. Osteoblast differentiation can be induced by various osteogenic factors, including BMP2, fibroblast growth factor (FGF), and IGF (Table 1) [24, 25]. Osteoblast differentiation can be divided into four steps including proliferation, maturation, mineralization, and apoptosis. Specific transcription factors are activated in each step to induce osteoblast markers (Fig. 2B). The osteogenic factors induce the expression of runt-

related transcription factor 2 (Runx2), a crucial transcription factor for osteoblast differentiation at the early stage [26]. *Runx2* mutant mice exhibit a lack of skeletal mineralization and perinatal lethality due to the lacking of osteoblasts [27]. During osteoblast differentiation, Runx2 regulates the expression of osteogenic specific markers, including ALP, osteopontin (OPN), osteocalcin, and collagen type I α 1 (coll1 α 1) [2]. ALP is an early marker of osteoblast differentiation and important for stabilizing the matrix [28]. Osteocalcin and OPN are non-collagenous matrix proteins upregulated at the late differentiation stage [29]. Coll1 α 1 is one of the bone matrix protein that is expressed at the beginning of osteoblast differentiation [29]. Osteoblasts can regulate bone resorption by production of RANKL and OPG [7, 20].

A. Osteoclast differentiation



B. Osteoblast differentiation

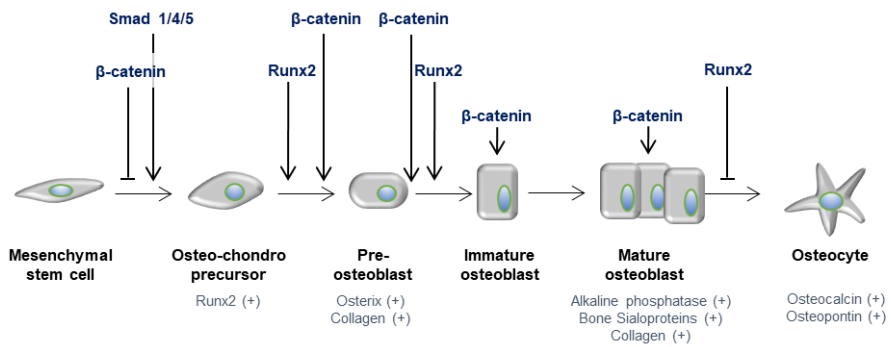


Figure 2. Illustration of osteoclast and osteoblast differentiation. (A) Stages of osteoclast differentiation and osteoclastogenic marker expression. (B) Stages of osteoblast differentiation, main transcription factors, and osteogenic marker expression. Runx2: runt-related transcription factor 2, CTR: calcitonin receptor, TRAP: tartrate-resistant acid phosphatase.

Table 1. Signaling of osteogenic factors [30, 31]

Ligands	Cell source	Receptors	Kinases	Transcription factors	Biological outcome	Ref.
BMPs (members of TGF- β superfamily)	Osteoprogenitor cell, osteoblast, chondrocyte, endothelial cell	A dimer composed of a type I BMP receptor and a type II BMP receptor	Smad 1/5/8 \rightarrow Complex of Smad4-Smad 1/5/8	Runx2	Osteoblast proliferation /differentiation	[32]
FGFs	Macrophage, monocyte, chondrocyte, osteoblast, endothelial cell	FGF receptor family of tyrosin kinase receptors (FGF receptor 1-4)	PLC- γ PI3-K ERK1/2	Runx2	Preosteoblast proliferation /osteoblast differentiation	[33]
IGF-1	Osteoblast, chondrocyte, hepatocyte, endothelial cell	A tetrameric receptor (two IGF-1 receptor α and two IGF-1 receptor β)	ERK PI3-K	Elk1	Osteoblast proliferation /differentiation /survival	[34-37]

4. Osteoporosis

Coupling and balancing between bone formation and bone resorption mean the volume of bone resorbed by osteoclasts almost equal the replaced volume of bone formation, thereby total bone volume is maintained [38]. Therefore, an imbalance of osteoblast and osteoclast differentiation results in bone diseases, such as osteoporosis, osteogenesis imperfect, hyperparathyroidism [39]. Osteoporosis, which means ‘porous bone’ reflecting the state of the phenomenon [40], is a disease related to the low bone mass and commonly occurs in adults older than 50 years [1]. Osteoporosis has been a major health problem causing more than 2 million bone fractures every year according to the International Osteoporosis Foundation [41]. It is one of the serious diseases because patients do not have obvious symptoms until fractures occur and the mortality is 20% within one year after fracture treatment [42]. Recent research reported that 2 in 5 post-menopausal women and 1 in 3 men in the elderly population suffer from osteoporotic fracture in European countries and the United States [43]. Currently, therapeutic drugs developed for treatment of osteoporosis are used to inhibit bone resorption or to induce bone formation (Table 2) [44-49]. However, conventional treatments have some unexpected side effects, such as nausea and rash. Bisphosphonate, one of the agents clinically used for targeting bone resorption, can lead to the osteonecrosis of the jaw [47]. In addition, parathyroid hormone, an anabolic agent for bone formation, is related to the incidence of osteosarcoma [50]. Moreover, although there are many treatment options showing minor side effects, osteoporosis fracture is still increasing. Therefore, it is important to develop new therapeutic targets for osteoporosis.

Table 2. Major therapeutics for osteoporosis and their side effects

Class	Drug (Brand)	Side effects	Ref.
Anti-resorptive medications	Bisphosphonates		
	Alendronate (Fosamax)	Dyspepsia, abdominal pain, musculoskeletal pain	[44]
	Ibandronate (Boniva)	Skin reactions at the injection site (irritation, pain, and swelling), angioedema, facial edema, urticaria, hypersensitivity reactions	[45]
	Risedronate (Actonel)	Rash, pruritus, urticaria, angioedema, bullous reactions, photosensitivity, Stevens Johnson syndrome	[45]
	Zoledronate (Reclast)	Rash, redness, swelling and/or pain at infusion site, osteonecrosis of the jaws	[45, 47]
	Monoclonal antibodies Denosumab (Prolia)	Osteonecrosis of the jaws	[46, 47]
Anti-resorptive medications	Calcitonin Calcitonin (Fortical, Miacalcin)	Nausea, facial flushing	[48]
	SERMs (selective estrogen receptor modulators) Raloxifene (Evista)	Rash, hot flushes, venous thromboembolism	[45, 49]
Bone-forming (anabolic) medications	Parathyroid hormone Teriparatide (Forteo)	Sweating, erythema at injection site, rash	[45]

5. Gut microbiota and bone regulation

Recently, it has been suggested that gut microbiota, a bacterial community colonized in the intestine, interacts with host and influences on various physiological regulations including bone homeostasis. Previous reports suggest that gut microbiota might modulate the bone metabolism by releasing bacterial cell wall components [51], producing metabolites [52], and regulating cytokines [53]. Studies comparing germ-free mice and conventionally raised mice directly indicated the relationship between gut microbiota and bone. One report showed that conventionally raised mice exhibited increased body weight, femur length, trabecular bone mass, and cortical thickness, but not increased adiposity, in comparison with germ-free mice during the juvenile growth period [54, 55]. However, on the other hand, two studies showed that germ-free mice exhibited higher trabecular and/or cortical bone than conventionally raised mice and conventionalized germ-free mice at weaning with a normal gut microbiota [53, 56]. Although the role of gut microbiota in bone metabolism is still controversial, accumulating reports suggest that gut microbiota is one of critical factors regulates bone physiology. This inconsistent results may be due to the differences of composition of gut microbiota by their age, mouse strain (C57BL/6 and BALB/c) [54]. As previous studies suggested that beneficial bacteria enhanced bone density [41] and pathogenic bacteria induced bone loss [57], normal microbiota composition and effect of its cell wall component, such as PGN, could results in these differences. Additionally, studies showing the effect of antibiotics administration on bone regulation also supports the influence of the gut microbiota on bone metabolism. Long-term (6 weeks) administration of antibiotics cocktail of vancomycin, imipenem/cilastatin, and neomycin decreased trabecular bone mass

[58]. However, short-term (2 weeks) administration of antibiotics cocktail of ampicillin and neomycin did not change trabecular bone [59]. A few reports suggested the role of gut microbiota, however, further study is still needed to comprehensively address the correlation between composition of microbiota and microbiota diversity on bone metabolism.

6. Probiotics and bone regulation

The word “Probiotic” is derived from the word ‘pro’ in Latin and the word ‘bios’ in Greek. The definition of probiotics has been proposed “as live microorganisms that when administered in adequate amounts will confer a health benefit on the host” by Food and Agricultural Organization/World health Organization [60]. Recently, it has been suggested that probiotics interact with host and influence on various physiological regulations including bone homeostasis (Table 3). Supplementation with probiotics prevent bone loss induced by estrogen deficiency, inflammation, and intestinal dysbiosis [53, 59, 61]. The proposed mechanisms of supplementation of probiotics in previous reports were changing intestinal microbiota, enhancing barrier function, and regulating immune functions [53, 59]. Probiotics have a great commitment to supporting bone health and are generally considered to be safe. Thus, further studies for understanding mechanisms are needed.

6.1. Modification of gut microbiota

Although ingested probiotics are not able to be maintained in gastrointestinal tract for more than one week, probiotics can modify the microbial composition by several mechanisms, including secretion of antimicrobial agents and digestion of complex

carbohydrates [62, 63]. Probiotics such as *Lactobacillus* spp. produce lactic acids and bacteriocins [62]. Lactic acid can be converted to butyric acid, which has beneficial effect on the gut epithelium and is able to inhibit osteoclast differentiation directly [52]. Bacteriocins are antimicrobial peptides targeting pathogens, including *Staphylococcus aureus* and *Pseudomonas aeruginosa* [64]. Despite the fact that supplementation of probiotics could changed composition of gut microbiota and also increased bone mass, specific species in gut microbiota that links bone health are yet to be determined.

6.2. Enhancement of intestinal barrier function

The intestinal epithelium is essential to provide a barrier that prevents translocation of pathogens and other harmful substances to the bloodstream. Tight junctional proteins expressed between intestinal epithelial cells maintain the paracellular permeability to support barrier function [65]. In addition, the mucus layer, antimicrobial peptides, and other immunoglobulins that are secreted from intestine contribute to healthy gut environment [66]. There are some reports supporting the association between intestinal barrier function and bone mass. Conditions that are related to the dysbiosis and damaged intestinal barrier function, such as intestinal inflammation and estrogen-deficiency, promoted bone loss [53, 67, 68]. Under those conditions, probiotics treatment not only decreased intestinal permeability and serum endotoxin levels, but also increased bone mass. For examples, *L. rhamnosus* GG and VSL#3 supplementation in estrogen-deficient mice decreased serum endotoxin level and gut permeability by increasing junctional protein expression in small intestine,

resulting in prevention of bone loss [53]. These previous studies indicated that decrease of gut permeability potentially is involved in enhancement of bone mass.

6.3. Modulation of immune system

There are pathogens, commensals, beneficial microbes, and dietary components in gastrointestinal tract and gut immune system and gut epithelial cells, especially paneth and goblet cells have to distinguish and differentially respond to them. Intestinal immune system dysregulation is associated with pathological expression of cytokines that are associated with diseases, including inflammatory bowel disease. The differentiation and activation of osteoclasts are known to be correlated with cytokines, for example, pro-inflammatory cytokines, such as TNF- α , interleukin (IL) 6, and IL-1 β , enhance osteoclast differentiation leading to bone destruction [69]. In contrast, IL-10 and TGF- β , known as anti-inflammatory cytokines inhibit osteoclast differentiation and activation [70]. Animal models and patients with inflammatory bowel disease have not only increased levels of cytokines, including TNF- α and IL-1 β , and also exhibit decreased bone mass [71-73]. Previous studies have shown that probiotics can regulate immune function [74, 75]. Supplementation of probiotics reduces TNF- α and RANKL expression induced by estrogen deficiency [53] and increased bone marrow regulatory T cells decreased by estrogen deficiency [76]. While previous results indicate that probiotics can affect bone metabolism through regulation of immune system, further studies are still needed to elucidate the action mechanisms.

Table 3. Probiotic benefits to skeletal health

Strain	Time	Analysis method	Bone effects	Model	Ref.
<i>L. reuteri</i> (ATCC 6475)	4 weeks	μCT	↑ BV/TV ↑ Tb.N ↑ Tb.Th ↑ Osteocalcin ↑ BFR		[77]
<i>L. reuteri</i> (ATCC 6475)	4 weeks	μCT	↑ BV/TV ↓ RANKL mRNA ↓ TRAP5 mRNA	OVX	[78]
<i>L. reuteri</i> (ATCC 6475)	4 weeks	μCT	↑ BV/TV ↑ MAR ↑ Osteocalcin ↑ Wnt10b mRNA	STZ-induced Type I Diabetes	[79]
<i>L. rhamnosus</i> (HN001)	4weeks	μCT	↑ BV/TV ↑ Osteocalcin ↓ RANKL mRNA ↓ TNFα mRNA ↓ IL-17 mRNA	OVX	[53]
<i>L. paracasei</i> (NTU 101) or <i>L. plantarum</i> (NTU 102)- fermented soy Milk	8 weeks	μCT SEM	↑ BV/TV ↑ Tb.N	OVX	[80]
<i>L. paracasei</i> or <i>L. paracasei</i> and <i>L.</i> <i>plantarum</i>	6 weeks	μCT	↑ Cortical BMC ↑ Cortical area ↑ OPG mRNA	OVX	[76]
<i>L. casei</i>	10 weeks	μCT	Prevents wear debris-induced osteolysis		[81]
<i>L. rhamnosus</i> GG	6 week	μCT	↓ Bone loss ↓ Inflammation ↓ Osteoclasts	Periodontitis	[82]
<i>L. gasseri</i> SBT2055	5 week	Histomorphometry	↓ Bone loss ↓ Inflammation	Periodontitis	[83]
<i>L. brevis</i> CD2	< 1 week	Histomorphometry	↓ Bone loss ↓ Inflammation	Periodontitis	[84]

7. Peptidoglycan (PGN)

PGNs are the most abundant bacterial cell wall components and their fragments that are released from the gut microbiota can be delivered into the bone marrow and potentially affect the bone metabolism. PGN is an essential and unique cell wall component of both Gram-positive and Gram-negative bacteria and is conserved composition [85]. PGN polymers provide protection in bacteria, but at the same time PGN fragments are released into the environment in the process of bacterial growth and cell division [86]. PGN fragments are recycled for cell wall biosynthesis but some are also used in bacterial communication and are recognized by host cells to induce immune responses.

7.1. Structure of PGN

PGN structure of Gram-positive and Gram-negative bacteria includes repeated disaccharide backbones, *N*-acetylglucosamine (NAG) and *N*-acetylmuramic acid (NAM), connected by β -(1,4)-glycosidic bonds [87]. Stem peptide chains are attached to the NAM and are composed with _L-alanine, _D-glutamic acid, *meso*-diaminopimelic acid (*mDAP*) or _L-lysine, _D-alanine, and _D-alanine (Fig. 3A). Peptide stem chains of third amino acids are cross-linked by direct linking or by bridge peptides comprised of 2-5 glycine and serine residues [88, 89]. PGNs can be divided into Lys-type and DAP-type by the third amino acid of the stem peptide, _L-lysine and *mDAP*, respectively. Modification to the stem peptide and disaccharide backbone can occur by species specific synthetic or degradative enzyme or growth condition [90].

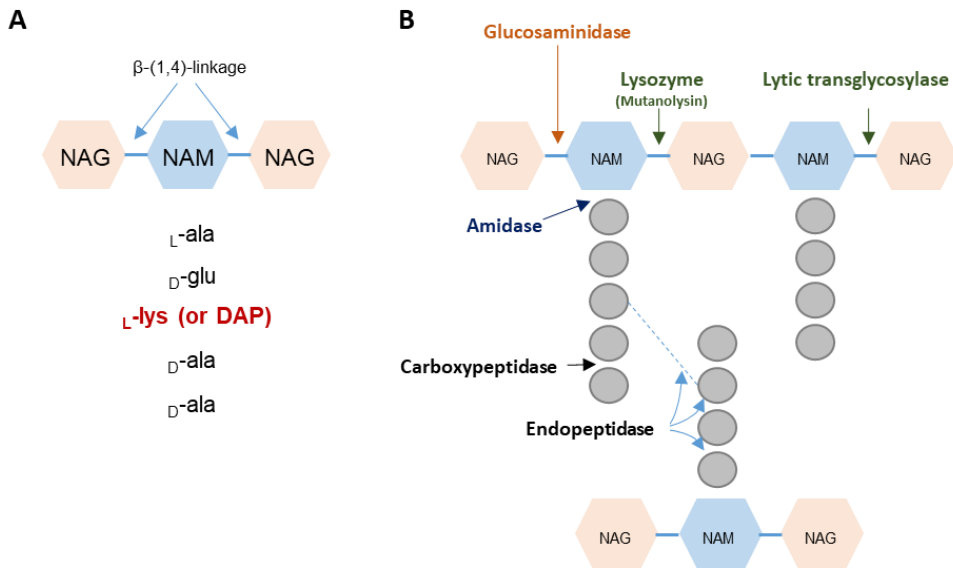


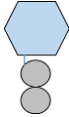

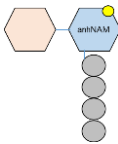
Figure 3. Illustration of basic structure of PGN and cleaving enzymes. (A) Typical structure of PGN (Lys or DAP-type). NAG: *N*-acetylglucosamine, NAM: *N*-acetylmuramic acid, DAP: diaminopimelic acid. (B) Cleavage sites of PGN and cleaving enzymes. Glucosaminidases (orange), amidases (blue), peptidases (black), and muramidases (green).

7.2. PGN degrading enzymes and cleavage sites

Bacteria use several types of PGN hydrolytic enzymes that participate in the assembly and disassembly of bacterial cell walls in the growth and division of bacteria. PGN hydrolytic enzymes bind to and break down PGN (Fig. 3B). Although various enzymes cleave the PGN, it can be classified according to the type of cleaved bond, glycosidases, amidases, and peptidases. Two classes of hydrolytic enzymes digest the PGN glycan backbones. *N*-acetylglucosaminidases cleave the bond between NAG-NAM, while *N*-acetylmuramidases (lysozyme and lytic transglycosylase) cleave the bond between NAM-NAG (Fig. 3B). Muramidase are divided into two groups according to the catalytic mechanism. Lysozyme is a hydrolytic enzyme that degrades glycosidic bond by adding water. In case of lytic transglycosylase, it catalyzes an intramolecular rearrangement for formation of 1, 6-anhydro-*N*-acetylmuramic acid without hydrolytic activity [91, 92]. Amidases hydrolyze amide bond between NAM and the first amino acid and peptidases cleave the link between the amino acids [93]. During growth, different PGN fragments are released by those enzymes (Table 4). For example, about 50% of the PGN fragments is degraded and released during the single generation of growth of *Escherichia coli* [94].

Due to the uniqueness of bacterial PGN, the structures are an excellent target to detect bacteria [95]. Eukaryotes, including mammals, have several PGN recognition molecules and lytic enzymes, such as lysozyme and PGN recognition protein (PGRP) 2 [96]. Lysozyme hydrolyze the β -(1,4)-glycosidic bonds between NAM-NAG, whereas PGRP2 cleaves the amide bond between NAM-L-alanine.

Table 4. PGN fragments recognized by mammalian sensing molecules and their function

PGN fragment	Structure	Sensing molecule	Function	Ref.
Muramyl dipeptide (disaccharide di-, tri-, tetrapeptides)		NOD2	NF-κB innate response activation	[97-99]
Dipeptide D-Glu-mDAP (mono and disaccharide peptides containing this structure)		NOD1	NF-κB innate response activation	[100, 101]
Anhydro-murotetrapeptide (Tracheal cytotoxin, TCT)		PGRP2 PGRP3-4	Hydrolysis of pro-inflammatory PGN fragments Induction of inflammatory response	[102] [103]

7.3. PGN detection by NOD proteins

PGN fragments of non-invasive bacteria are delivered to the cytoplasm through endocytosis, bacterial secretion system, pH-sensing regulatory factor of peptide transporter, or delivered by outer membrane vesicles [104-107]. Nucleotide-binding oligomerization domain (NOD)s, NOD1 and NOD2, are intracellular regulatory proteins that recognize PGNs, one of conserved microorganism-associated molecular patterns. NOD1 and NOD2 proteins contain a carboxy-terminal leucine-rich repeat domain, a central nucleotide binding domain, and amino-terminal caspase activation and recruitment domain (CARD). The difference between NOD1 and NOD2 is the CARD, which interact with receptor-interacting serine/threonine-protein kinase 2, NOD1 contains one CARD, whereas NOD2 contains two CARDS. NOD1 recognizes D -glu-*m*DAP, which generally found in Gram-negative bacteria and some Gram-positive bacteria, such as *Bacillus* spp., *Listeria* spp., and *L. plantarum* [108-110]. NOD2 recognizes NAM- D -ala- D -glu (MDP, muramyl dipeptide), found both in Gram-positive and Gram-negative bacteria [101, 111]. Sensing of PGN fragments by NOD1 or NOD2 results in activation of intracellular signaling pathways, mitogen-activated protein kinase and NF- κ B, resulting in expression of TNF- α , IL-6, CC-chemokine ligand 2, CXC-chemokine ligand (CXCL) 8, CXCL 2, and defensins [112, 113], which are involved in immune responses and antimicrobial activity [114]. In adaptive immune responses, NOD2 signaling drive Th2-type immunity through sensing by dendritic cells although it hardly induces expression of co-stimulatory molecules on dendritic cells [115-117].

8. Objective of the present study

Previous reports suggested that PGN fragments are released during bacterial growth and can be cleaved by lysozyme in the intestinal lumen. Indeed, NOD1 and NOD2 agonists were presented in various Gram-positive and Gram-negative bacteria culture supernatants [118]. In addition, radiolabeled PGN can be detected in the mouse serum and bone marrow, indicating that the PGN fragment released from the intestine can migrate through the mucosal layer and intestinal barrier [119]. Moreover, MDP, one of NOD2 ligands, directly increased bone mass by enhancing osteoblast differentiation and inhibiting osteoclast differentiation [51]. Therefore, a hypothesis that the gut microbiota-derived PGN fragments may contribute to bone regulation was raised.

The objective of the present study is to elucidate the role of bacterial PGN in bone regulation using *in vivo* and *in vitro* model system under the hypothesis that gut microbiota-regulated bone mass could be due to the effect of PGNs. Under the research objective, (i) direct effect of PGN on osteoblast or osteoclast differentiation, and (ii) indirect effect of PGN on regulation of host factors involved in bone regulation were investigated.

Chapter II. Materials and Methods

1. Materials

Recombinant mouse M-CSF and mouse RANKL were purchased from PeproTech (Rocky Hill, NJ, USA). Fetal bovine serum, alpha-minimum essential medium (α -MEM), and Hoechst 33258 were purchased from Gibco (Paisley, UK), Welgene (Daegu, Korea), and Invitrogen (NY, USA), respectively. Penicillin/streptomycin, Dulbecco's modified Eagle's medium (DMEM), and trypsin-EDTA were obtained from HyClone (Logan, UT, USA). Ascorbic acid, β -glycerophosphate, polymyxin B, ALP staining kit, TRAP staining kit, and $1\alpha,25$ -dihydroxyvitamin D₃ were obtained from Sigma-Aldrich (St. Louis, MO, USA). Antibodies specific to Runx2 and alexa fluor 568-conjugated anti-rabbit IgG were obtained from abcam (Cambridge, UK) and Santa Cruz Biotechnology (CA, USA), respectively. Antidodies specific to p38, phospho-p38, extracellular signal-regulated kinase (ERK), phospho-ERK, c-Jun N-terminal kinase (JNK), phospho-JNK were obtained from Cell Signaling Technology (Beverly, MA, USA). Horseradish peroxidase-conjugated anti-rabbit IgG or anti-mouse IgG were purchased from Southern Biotech (Birmingham, AL, USA). SB203580, SP600125, and U0126 were purchased from Calbiochem (La Jolla, CA, USA). Tryptic soy broth (TSB) and de Man, Rogosa and Sharpe (MRS) were purchased from BD Biosciences (San Jose, CA).

2. Preparation of PGN

2.1. Bacterial strains and culture condition

L. plantarum KCTC 10887BP, *L. casei* KCTC 3260, *Lactobacillus agilis* KCTC 3606, *Lactobacillus coleohominis* KCTC 21007, *Lactobacillus mali* KCTC 3596, *Lactobacillus ruminis* KCTC 5781, *Lactobacillus saerimneri* KCTC 5337, and *Bacillus cereus* KCTC 13153 were distributed from Korean Collection for Type Culture (Daejeon, Korea). *Lactobacillus delbrueckii* K552 was kindly provided by Prof. Dae Kyun Chung at Kyung Hee University (Suwon, Republic of Korea). *L. reuteri* ATCC 23272, *L. rhamnosus* GG ATCC 53103, and *Bacillus subtilis* ATCC 6633 were obtained from the American Type Culture. *Lactobacillus acidophilus* KACC 12419 were obtained from Korean Agricultural Culture Collection. *L. delbrueckii*, *L. plantarum*, *L. casei*, *L. rhamnosus* GG, *L. reuteri*, and *L. coleohominis* were grown in MRS at 37°C to mid-log phase in aerobic condition. *L. agilis* was grown in MRS with 0.5% cysteine-hydrochloride at 37°C to mid-log phase in aerobic condition. *L. ruminis*, *L. saerimneri*, and *L. mali* were grown in MRS media at 37°C to mid-log phase in anaerobic condition. *B. subtilis* and *B. cereus* were grown at 37°C to mid-log phase in aerobic condition in TSB and TSB with polymycin B supplement (10 µg/ml), respectively. Bacterial pellets were collected by centrifugation, washed with phosphate-buffered saline (PBS) three times, and stored at -80°C until use.

2.2. Purification of PGN

Bacterial strains were divided into two groups, Lys-type and DAP type, by the third amino acid of the stem peptide (Lys-type: *L. acidophilus*, *L. casei*, *L. delbrueckii*, *L. rhamnosus* GG, *L. reuteri* and DAP-type: *B. subtilis*, *B. cereus*, *L. agilis*, *L. coleohominis*, *L. mali*, *L. ruminis*, *L. saerimneri*. PGN was purified as previously

described with some modifications [120]. The bacterial pellet was washed with 1 M NaCl in PBS and disrupted seven times with glass beads using homogenizer (BeadBeater, Biospec product, OK, USA). The disrupted suspension was collected by centrifugation at $2,000 \times g$ for 10 min. The bacterial lysates were collected by centrifugation at $13,000 \times g$ for 10 min and then removed the supernatant. The pellet was incubated with 0.5% sodium dodecyl sulphate (SDS) in PBS at 60°C for 30 min. Then the pellet was washed five times with PBS. The pellet was suspended in 5 ml of 1 M Tris-HCl (pH 7.0) containing 50 µg DNase and 250 µg RNase and incubated for 2 h at room temperature. After incubation, 50 mM CaCl₂ and 1 mg trypsin were added and incubated at 37°C with shaking for 24 h. After incubation, the pellet was collected by centrifugation at $13,000 \times g$ for 10 min and re-suspended in PBS containing 5% trichloroacetic acid at room temperature with shaking for 24 h. Insoluble PGN was collected and lyophilized. The quantity of insoluble PGN was measured for dry weight. To prepare soluble PGN, 100 µg of insoluble PGN was incubated with 50 U mutanolysin at 37°C with shaking for 24 h. The enzyme was inactivated by incubation at 100°C for 10 min.

3. *In vivo* mouse model

Animal experiments were approved by the Institutional Animal Care and Use Committee of Seoul National University (Approval No. SNU-140512-6 and SNU-160524-3). All mice were housed in a specific pathogen-free facility with a controlled temperature (22–24 °C) and 12-h day/night cycles and were allowed free access to water and food. Wild-type mice and B6.129S1-Nod2^{tm1Flv}/J mice were purchased from Orient Bio (Seongnam, Korea) and Jackson Laboratory (Bar Harbor,

Maine, USA), respectively. Nod1-deficient mice were kindly provided from Jong-Hwan Park at Chonnam National University (Gwangju, Republic of Korea) [121]. To test the effect of PGNs on ovariectomy-induced osteoporosis mouse model, Eleven-week-old C57BL/6 female mice were randomly divided into three groups (sham operation mice, OVX mice, and OVX mice supplemented with PGN). To perform the surgery, double dorsolateral surface incisions (about 0.6 cm) was made after shaving the back of mice, one at a time. Ovaries were completely removed and the incision was sutured as previously described [122]. Three weeks after the operation, mice were intragastrically given PBS or insoluble PGN (30 µg) by oral gavage technique three times weekly for four weeks. To observe direct effect of Lp.PGN, mice were intraperitoneally or intravenously given PBS or insoluble Lp.PGN (30 µg) once weekly for four weeks. For RANKL-induced osteoporosis mouse model, Six-week-old C57BL/6 male mice were randomly divided into two groups and intraperitoneally administered PBS or RANKL daily for three days. One week after the first injection, mice were intragastrically given PBS or insoluble Lp.PGN (30 µg) by oral gavage technique three times weekly for four weeks. In a separate experiment, six-week-old C57BL/6 male mice were randomly divided into three groups and intragastrically given PBS or insoluble Bs.PGN (30 µg) or Bc.PGN (30 µg) by oral gavage technique three times weekly for four weeks.

4. Preparation of osteoclasts and osteoblasts

4.1. Preparation of osteoclast and osteoclast differentiation

Bone marrow cells (BMs) isolated from mouse femurs and tibiae were incubated in α -MEM supplemented with 10% fetal bovine serum (FBS), 100 U/ml penicillin, and

100 µg/ml streptomycin in the presence of 5 ng/ml of M-CSF for 1 day. Non-adherent cells were obtained and induced to differentiate into bone marrow-derived macrophages (BMMs) by incubation with 20 ng/ml of M-CSF for 4 days. BMMs were plated onto a 96-well culture plate at 2×10^4 cells/well and incubated with 20 ng/ml RANKL and 20 ng/ml M-CSF in the presence or absence of soluble Lp.PGN or Bc.PGN. In a separate experiment, BMMs were differentiated into committed osteoclast precursors by incubation with 20 ng/ml RANKL and 20 ng/ml M-CSF for 2 days. The cells were stimulated with soluble Lp.PGN in the presence of 20 ng/ml M-CSF with or without 20 ng/ml RANKL. In co-culture experiments, BMMs (1×10^5) and calvarial osteoblast precursors (1×10^4) plated onto a 48-well culture plate were incubated with 10 nM β -glycerophosphate, 50 µg/ml ascorbic acid, and 100 ng/ml $1\alpha,25$ -dihydroxyvitamin D₃ in the presence or absence of soluble Lp.PGN or Bc.PGN for 12 days. After incubation, the cells were fixed and stained using TRAP staining kit according to the manufacturer's recommendation. TRAP-positive multinucleated cells (MNCs) with three or more nuclei were enumerated as osteoclasts with an inverted phase-contrast microscope.

4.2. Preparation of osteoblast and osteoblast differentiation

Mouse osteoblast precursors were isolated from the calvaria of 1-day-old C57BL/6 mice, as previously described [123]. Briefly, the calvariae were digested in α -MEM containing 1% penicillin/streptomycin, 0.1% collagenase (Wako, Osaka, Japan), 0.2% dispase (Roche, Mannheim, Germany) for 15 min at 37°C with shaking. The digestion procedure was repeated for five times and the supernatant was collected in a same tube except first collection. The collected cells were plated onto a 100 mm

dish at 5×10^5 and incubated for 3 days. Adherent cells were harvested and used as osteoblast precursors. Calvarial osteoblast precursors (2×10^4) were plated onto a 48-well culture plate to be differentiated into osteoblasts by incubation with β -glycerophosphate and ascorbic acid in the presence or absence of soluble Lp.PGN or BcPGN for 12 or 28 days. The cells were fixed and subjected to ALP or alizarin red S staining to determine osteoblast differentiation.

5. Bone morphometric analysis using micro-computed tomography (micro-CT)

The femurs or lumbar vertebrae were isolated from the mice and scanned using X-ray micro-CT (Skyscan1275, Bruker-CT, Kontich, Belgium) at 60 kV, 166 μ A, 1 mm Al filter, and 7 μ m per image pixel size. The micro-CT images were reconstructed by SkyScan NRecon program (version 1.7.3.1) and analyzed by using SkyScan Dataviewer (version 1.5.6.2) and SkyScan CT analyzer software (version 1.17.7.2). Three-dimensional images were created by using SkyScan CT volume program (version 2.1.1.0) or SkyScan CT voxel (version 3.3.0.0). Total 1 mm of trabecular bone region was selected and analyzed from 0.58 mm above the growth plate.

6. Histological analysis

The femurs were fixed and decalcified in 10% EDTA in PBS for 7 days at 4°C. Decalcified femurs were paraffin embedded and sectioned. The paraffin sections were subjected to hematoxylin and eosin, TRAP, or immunofluorescence staining. For immunofluorescence staining, paraffin sections of calcified femur were

permeabilized with 0.3% Triton-X 100 for 40 min. After blocking non-specific binding using 5% bovine serum albumin in PBS with 0.3% Triton-X 100, samples were incubated with mouse anti-Runx2 antibody at 4°C overnight. After washing, samples were incubated with alexa fluor 568-conjugated anti-rabbit IgG antibody followed by Hoechst 33258 staining. Images were obtained using a fluorescence microscope (BX51, Olympus, Tokyo, Japan).

7. Calcein double labeling

Mice were intraperitoneally given 30 µg of insoluble Lp.PGN three times a week for four weeks. Seven and two days before scarification, mice were intraperitoneally administered with 20 mg/kg calcein AM. The femurs were fixed, embedded, and sectioned. The representative images of calcein-labeled femurs were captured under a fluorescence microscope (BX51, Olympus). Mineralizing surface/bone surface, mineral apposition rate, and bone formation rate were measured by using OsteoMeasure software (OsteoMetrics, GA, USA).

8. Real-time reverse transcription-polymerase chain reaction

(Real-time RT-PCR)

Total RNA were isolated from bone, BMs, osteoclasts, and osteoblasts using TRIzol reagent (Thermo Fisher Scientific, CO, USA) according to the manufacturer's instruction. Complementary DNA (cDNA) was reverse-transcribed with random hexamer and reverse transcriptase (Promega Corporation, WI, USA). The mRNA expression levels of Coll1 α 1, ALP, Runx2, OPN, TRAP, NFATc1, Cathepsin K, c-

Fos, RANKL, TNF- α , 18S rRNA, or GAPDH in various tissues or cells were determined by using real-time RT-PCR. The sequences of each primer are as follows:

Col1 α 1; forward 5'-CGACCTCAAGATGTGCCACT-3'		and	reverse 5'-
GACGGCTGAGTAGGGAACAC-3',	ALP;	forward	5'-
CCAACCTCTTTTGTGCCAGAGA-3'	and	reverse	5'-
GGCTACATTGGTGTGAGCTTTT-3',	Runx2;	forward	5'-
AACGATCTGAGATTTGTGGGC-3'	and	reverse	5'-
CCTGCGTGGGATTTCTTGGTT-3',	OPN;	forward	5'-
AGCAAGAAACTCTTCCAAAGCAA-3'	and	reverse	5'-
GTGAGATTCGTCAGATTCATCCG-3',	TRAP;	forward	5'-
TGTGAGGGAGGAGGCGTCTGC-3'	and	reverse	5'-
CGTTCCCAAGAAAGCTCTACC-3',	NFATc1;	forward	5'-
TTCGAGTTCGATCAGAGCGG-3'	and	reverse	5'-
AGGTGACACTAGGGGACACA-3',	Cathepsin K;	forward	5'-
GTGTCCATCGATGCAAGCTTGGCA-3'	and	reverse	5'-
GCTCTCTCCCCAGCTGTTTTTAAT-3',	c-Fos;	forward	5'-
GGGGACAGCCTTTCCTACTA-3'	and	reverse	5'-
CTGTCACCGTGGGGATAAAG-3',	RANKL;	forward	5'-
CCTGATGAAAGGAGGGAGCA-3'	and	reverse	5'-
TGGAATTCAGAATTGCCCGA-3',	TNF- α ;	forward	5'-
CCCTCACACTCAGATCATCTTCT-3'	and	reverse	5'-
GCTACGACGTGGGCTACAG-3',	18S rRNA;	forward	5'-
ATTCGAACGTCTGCCCTATCA-3'	and	reverse	5'-
GTCACCCGTGGTCACCATG-3',	and GAPDH;	forward	5'-

AGGTCGGTGTGAACCGGATTTG-3' and reverse 5'-
TGTAGACCATGTAGTTGAGGTCA-3'.

9. Transient transfection and reporter gene assay

HEK293 cells (2×10^4 cells/ 0.2ml) were plated onto a 96-well culture plate in DMEM overnight. The cells were transfected with pNF- κ B-Luc and pRL-TK *Renilla* luciferase plasmids (Promega, WI, USA) together with the plasmid expressing human NOD1 or NOD2 using LipofectamineTM2000 Transfection Reagent (Invitrogen) for 3 h in DMEM with serum starved condition. After replacing with the fresh DMEM supplemented with 10% FBS, 100 U/ml penicillin, and 100 μ g/ml streptomycin, the cells were further incubated for 24 h. The cells were stimulated with soluble PGNs for additional 16 h. The cells were lysed and the firefly and *Renilla* luciferase activities were analyzed by using the Dual Luciferase Reporter Assay System (Promega) according to the manufacturer's instruction.

10. Enzyme linked immunosorbent assay (ELISA)

Mouse bone marrow in tibiae were pelleted by centrifugation at $3,000 \times g$ for 30 sec, suspended in 400 μ l cold PBS. The supernatant was collected after centrifugation at $13,000 \times g$ for 15 min at 4°C. Mouse serum was collected from blood after incubation for 30 min at room temperature followed by centrifugation at $2,000 \times g$ for 10 min at 4°C. The protein levels of TNF- α , IL-6, IL-1 β , RANKL, or OPG in bone marrow extracellular fluid and serum were measured by using ELISA kits according to the manufacturer's instruction.

11. Western blot analysis

Committed osteoclast precursors were serum-deprived for 3 h and stimulated with Bc.PGN for 15, 30, 60, or 90 min. The cells were washed with PBS and lysed with RIPA buffer (150 mM NaCl, 1% SDS, 1% sodium deoxycholate, 50 mM Tris, and 1% Triton X-100). The lysates were centrifuged at $13,000 \times g$ for 10 min, separated by 10% SDS-polyacrylamide gel electrophoresis, and transferred onto a polyvinylidene difluoride membrane (EMD Millipore, Bedford, MA, USA). After blocking with 5% ski, milk in Tris-buffered saline containing 0.05% Tween-20 (TBS-T), the membrane was incubated with antibodies specific to ERK, phospho-ERK, JNK, phospho-JNK, p-38, phospho-p38, or β -actin at 4°C overnight. The membrane was washed with TBS-T, incubated with horseradish peroxidase-conjugated secondary antibodies for 1 h, and washed with TBS-T. The immunoreactive band was detected by using Chemi imaging system (GeneGnome SRQ system, Syngene, Frederick, MD, USA).

12. Immunofluorescence staining

Cells were fixed with 4% paraformaldehyde and then permeabilized in 0.2% Triton X-100 for 15 min. After blocking with 1% FBS in PBS for 1 h. The cells were incubated with anti-NFATc1 antibody at 4°C overnight. After washing, samples were incubated with alexa fluor 568-conjugated anti-mouse IgG antibody followed by Hoechst 33258 staining. Images were obtained using a fluorescence microscope (BX51, Olympus).

13. Statistical analysis

All experiments were performed at least three times. All quantitative results of *in vivo* studies and *in vitro* studies were expressed as mean values \pm standard error of the mean (SEM) and as mean values \pm standard deviation (SD), respectively. Statistical significance of differences was determined by unpaired t-test or one-way ANOVA. An asterisk (*) indicates a statistically significant difference from the control group at $p < 0.05$

Chapter III. Results

1. Intra-gastric administration of Lp.PGN attenuates bone loss induced by estrogen deficiency

L. plantarum is one of probiotics known to contribute not only to the treatment of various diseases, such as obesity [124], inflammatory bowel disease [125], and cancer [126] but also to the regulation of bone metabolism [55, 76, 80]. Because previous reports suggested that bacterial PGN fragments were delivered into bone marrow [119], to investigate the effect of PGN isolated from *L. plantarum* on prevention of osteoporosis, postmenopausal osteoporosis mouse model was received Lp.PGN by oral gavage for four weeks as shown in Fig. 4. Establishment of OVX-induced estrogen deficiency was confirmed by observation of body weight, 17β -estradiol, and uterus weight. As shown in Fig 5A, body weight significantly increased in the OVX mice compared with sham control mice. OVX decreased the serum level of 17β -estradiol (Fig. 5B) and uterus weight in comparison with the sham control mice (Fig 5C), typical features of OVX [127]. Femurs and vertebrae were isolated and then subjected to micro-CT analysis. Trabecular bone volume and trabecular number in femurs were significantly increased in Lp.PGN-received OVX mice in comparison with the OVX control (Fig. 6A – C). Trabecular separation and trabecular thickness in femurs were not changed (Fig. 6D and E) by Lp.PGN in comparison with the OVX control. Paraffin sections of femurs exhibited similar tendency (Fig. 6F). However, in contrast to the trabecular bone, cortical thickness was not changed in OVX control mice or OVX mice supplemented with Lp.PGN (Fig. 6G). Vertebral trabecular bone volume, trabecular number, and trabecular separation were increased in OVX mice supplemented with Lp.PGN in comparison

with the OVX control mice (Fig. 7A – C, and E), while trabecular separation was decreased in OVX mice supplemented with Lp.PGN in comparison with the OVX control mice (Fig. 7D). These results indicate that intragastric administration of Lp.PGN attenuates bone loss induced by estrogen deficiency.

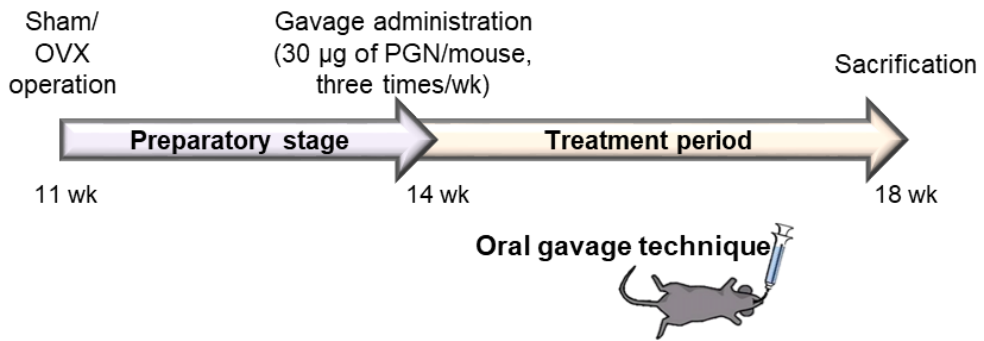


Figure 4. Experimental procedure of OVX-induced osteoporosis mouse model.

Eleven-week-old C57BL/6 mice were randomly divided into three groups and ovariectomized or sham operated. Three weeks after the operation, mice were intragastrically given PGNs three times weekly by oral gavage technique for four weeks.

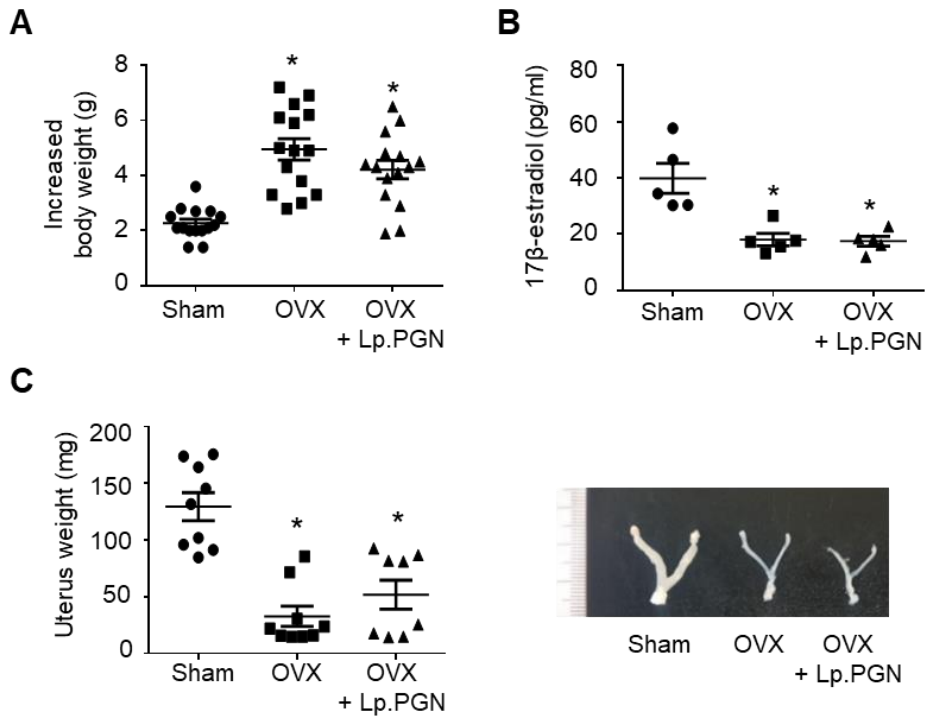


Figure 5. Establishment of osteoporosis mouse model by ovariectomy. Eleven-week-old C57BL/6 female mice were randomly divided into three groups (sham operation, OVX, and OVX supplemented with Lp.PGN). To perform the surgery, double dorsolateral surface incisions (about 0.6 cm) was made after shaving the back of mice, one at a time. Ovaries were completely removed and the incision was sutured. Three weeks after the operation, mice were intragastrically given PBS or insoluble PGN (30 μ g) by oral gavage technique three times weekly for four weeks (A) Body weight gain of mice in each group was measured at week 11 and week 14 and the change was calculated. At the end of the treatment, serum 17 β -estradiol level (B) and uterus weight (C) were measured and photographed. * $p < 0.05$ compared with the sham control group.

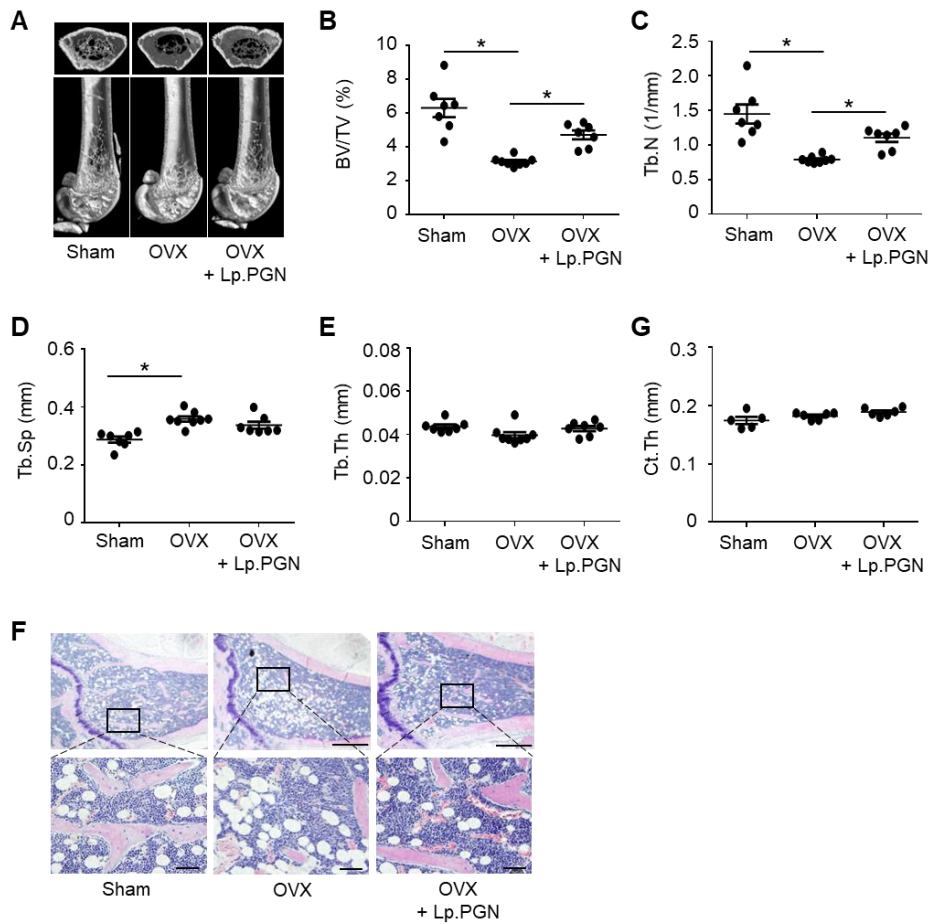


Figure 6. Intra-gastric administration of Lp.PGN increases femoral trabecular bone volume, but not cortical bone volume, in OVX-induced osteoporosis mouse model. Fourteen-week-old OVX mice ($n \geq 5$) were intra-gastrically given 30 μg of insoluble Lp.PGN by oral gavage three times weekly for four weeks. Femurs were scanned by micro-CT and measured trabecular bone parameters using Skyscan programs. (A) Three-dimensional images of the femurs were obtained. BV/TV (B), Tb.N (C), Tb.Sp (D), and Tb.Th (E) were calculated from 3D reconstruction of micro-CT images using the CT analyzer. (F) Paraffin sections of the decalcified femur were subjected to H&E and photographed. Bars = 500 μm (*upper*) or 200 μm (*lower*). BV/TV = trabecular bone volume per total bone volume; Tb.N = trabecular number; Tb.Sp = trabecular separation; Tb.Th = trabecular thickness; Ct.Th = cortical thickness; OVX = ovariectomy. * $p < 0.05$.

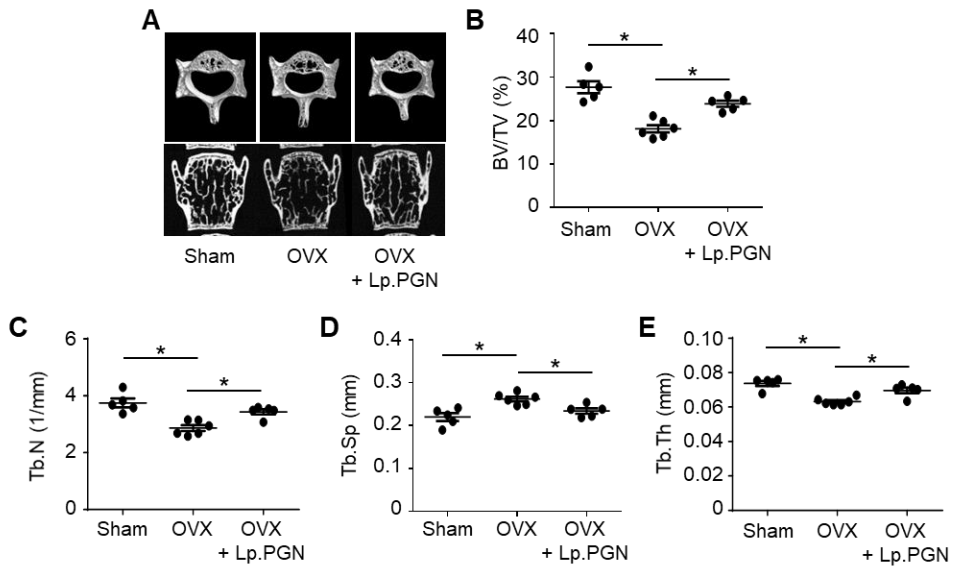


Figure 7. Intra-gastric administration of Lp.PGN increases vertebral trabecular bone volume in OVX-induced osteoporosis mouse model. Fourteen-week-old OVX mice ($n = 5$) were intra-gastrically given 30 μg of insoluble Lp.PGN by oral gavage three times weekly for four weeks. L3 vertebrae were isolated and scanned by micro-CT and measured trabecular bone parameters using Skyscan programs. (A) Three-dimensional images of the L3 were obtained. (B – E) BV/TV, Tb.N, Tb.Sp., and Tb.Th. were calculated from 3D reconstruction of micro-CT images using the CT analyzer. BV/TV = trabecular bone volume per total bone volume; Tb.N = trabecular number; Tb.Sp = trabecular separation; Tb.Th = trabecular thickness. $*p < 0.05$.

2. Intragastric administration of PGNs isolated from *Lactobacillus* spp. regulate trabecular bone volume decreased by estrogen deficiency

To further examine whether the PGNs from other *Lactobacillus* spp. could prevent osteoporosis, PGNs were isolated from various *Lactobacillus* spp. containing Lys-type PGN (*L. acidophilus*, *L. casei*, *L. delbrueckii*, *L. reuteri*, *L. rhamnosus* GG) or DAP-type PGN (*L. agilis*, *L. coleohominis*, *L. mali*, *L. ruminis*, *L. saerimneri*, *L. plantarum*) [128]. OVX mice were received each PGN isolated from various *Lactobacillus* spp. by oral gavage three times weekly for four weeks. Femurs were isolated at the end of experiments and scanned by micro-CT. Bone morphometric analysis of femoral trabecular bone using micro-CT showed that intragastrically administered PGNs from *L. plantarum*, *L. casei*, *L. delbrueckii*, *L. rhamnosus* GG, *L. agilis*, *L. ruminis*, and *L. saerimneri* significantly increased trabecular bone volume and trabecular number (Fig. 8A and B). Trabecular separation and trabecular thickness were not changed by PGNs (Fig. 8C and D). These results suggest that PGNs from *Lactobacillus* spp. may have beneficial effects for protecting bone loss associated with estrogen deficiency.

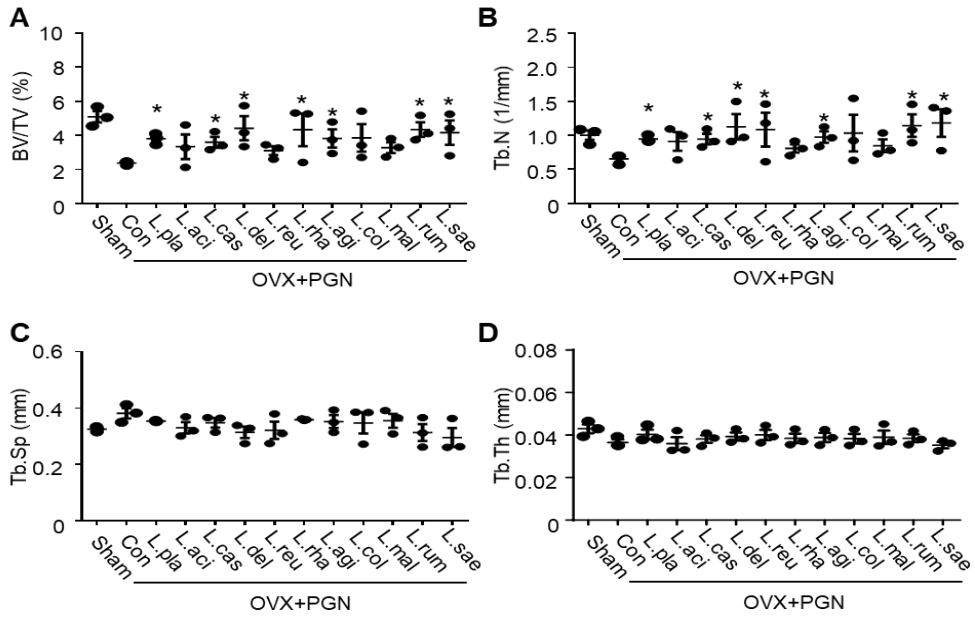


Figure 8. Intra-gastric administration of PGNs isolated from *Lactobacillus* spp. increases femoral trabecular bone volumes in OVX-induced osteoporosis mouse model. Fourteen-week-old OVX mice ($n = 3$) were intra-gastrically given 30 μg of insoluble PGN isolated from various *Lactobacillus* spp. by oral gavage three times a week for four weeks. Femur were scanned by micro-CT and measured trabecular bone parameters using Skyscan programs. BV/TV (A), Tb.N (B), Tb.Sp (C) and Tb.Th (D) were calculated from 3D reconstruction of micro-CT images using the CT analyzer. BV/TV = trabecular bone volume per total bone volume; Tb.N = trabecular number; Tb.Sp = trabecular separation; Tb.Th = trabecular thickness; L.pla = PGN from *L. plantarum*; L.aci = PGN from *L. acidophilus*; L.cas = PGN from *L. casei*; L.del = PGN from *L. delbrueckii*; L.reu = PGN from *L. reuteri*; L.rha = PGN from *L. rhamnosus* GG; L.agi = PGN from *L. agilis*; L.col = PGN from *L. coleohominis*; L.mal = PGN from *L. mali*; L.rum = PGN from *L. ruminis*; L.sae = PGN from *L. saerimneri*. Sham = sham-operated control mice, Con = OVX control mice. * $p < 0.05$.

3. Intra-gastric administration of Lp.PGN induces Runx2 decreased by OVX-induced estrogen deficiency

To verify whether the effect of Lp.PGN on bone metabolism is mediated by regulation of osteoblast differentiation, the paraffin sections of femurs were subjected to immunofluorescence staining. Immunofluorescence staining demonstrated that protein level of Runx2, an essential transcription factor for osteoblast differentiation, was increased in OVX mice supplemented with Lp.PGN in comparison with the OVX control mice (Fig. 9A and B). In addition, serum level of P1NP indicating new bone formation was elevated by Lp.PGN (Fig. 9C). The mRNA levels of *coll1 α 1* and *Runx2* were increased in OVX mice received Lp.PGN in comparison with the OVX, but the changes were not significant (Fig. 9D and E). These results indicate that intra-gastric administration of Lp.PGN attenuates bone loss by regulating the activity of osteoblasts.

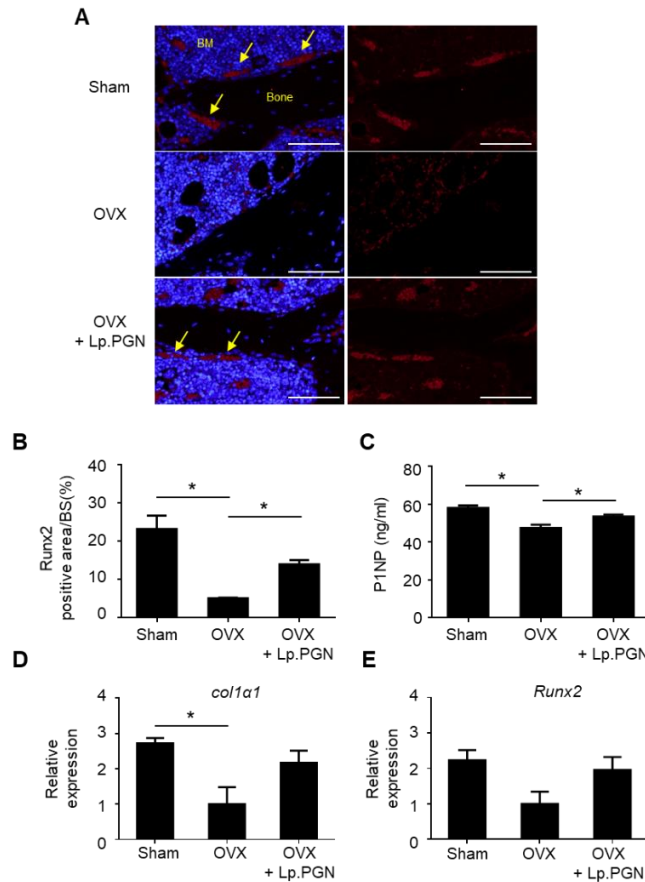


Figure 9. Intra-gastric administration of Lp.PGN induces Runx2 decreased OVX-induced estrogen deficiency. Fourteen-week-old OVX mice ($n = 5$) were intragastrically given 30 μg of insoluble Lp.PGN by oral gavage three times weekly for four weeks. (A and B) The paraffin sections of the decalcified femurs were subjected to immunofluorescence staining using a specific antibody to Runx2. Runx2-positive areas on bone surface with yellow arrows were measured using Image J program. Bars = 100 μm ; arrows = Runx2 positive area; red = Runx2; blue = nuclei. (C) Serum samples were collected to measure the expression of P1NP by ELISA. (D and E) Total RNA in whole tibiae was isolated and mRNA expression levels of *col1a1*, Runx2, OPN, and 18S rRNA were determined by real-time RT-PCR. $*p < 0.05$.

4. Intra-gastric administration of Lp.PGN decreases osteoclasts increased by OVX-induced estrogen deficiency

Next, to examine whether supplementation with Lp.PGN also regulates osteoclast differentiation, the paraffin sections of femurs were subjected to TRAP staining. The femur sections subjected to TRAP staining showed the decreased TRAP-positive surface areas in OVX mice supplemented with Lp.PGN compared to the OVX control mice (Fig. 10A and B). The mRNA levels of TRAP and NFATc1 were significantly decreased in OVX mice received Lp.PGN compare to the OVX control mice (Fig. 10C and D). The mRNA expression of cathepsin K also showed a trend toward decreased level in OVX mice received Lp.PGN in comparison with the OVX control mice (Fig. 10E). These results indicate that intra-gastric administration of Lp.PGN attenuates bone loss by regulating the activity of osteoclasts.

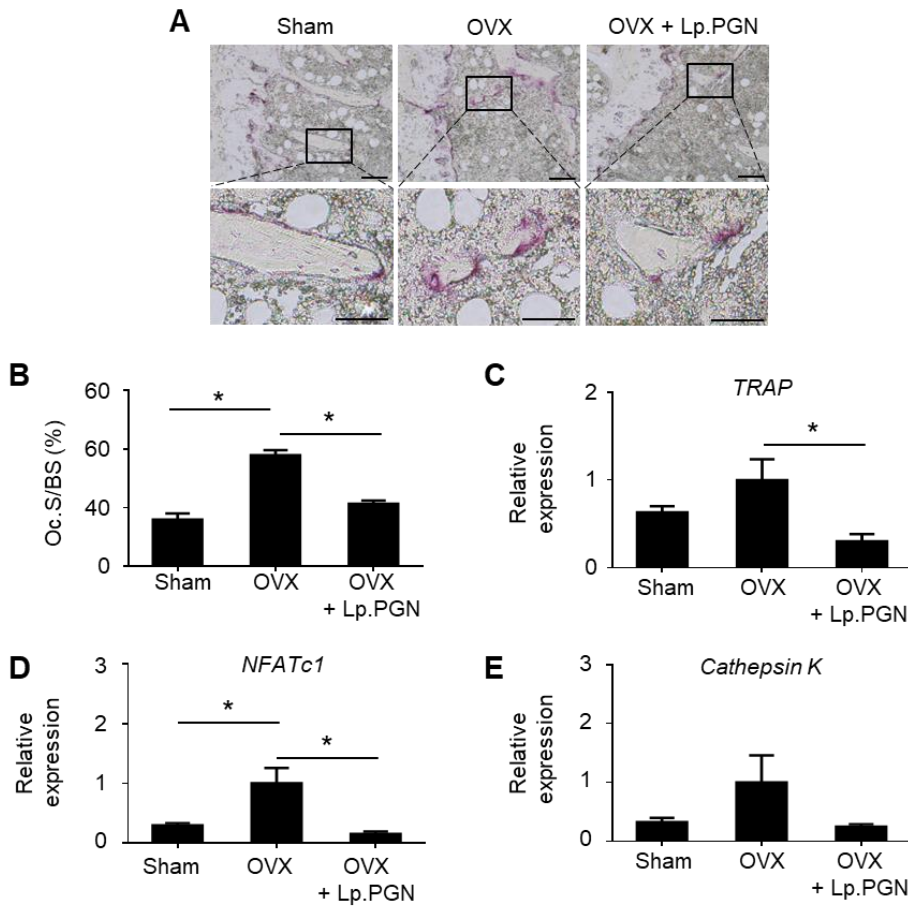


Figure 10. Intra-gastric administration of Lp.PGN decreases osteoclasts increased by OVX-induced estrogen deficiency. Fourteen-week-old OVX mice ($n = 5$) were intra-gastrically given 30 μg of insoluble Lp.PGN by oral gavage three times weekly for four weeks. (A and B) The paraffin sections of the femur were subjected to TRAP staining. TRAP-positive areas (osteoclast surface) on bone surface were measured using Image J program. Bars = 200 μm (*upper*) or 100 μm (*lower*). (C – E) Total RNA in bone marrow was isolated and mRNA expression levels of TRAP, NFATc1, cathepsin K, and 18S rRNA were determined by real-time RT-PCR. $*p < 0.05$.

5. NOD2 signaling is essential for increase of trabecular bone volume by Lp.PGN

PGN fragments containing their conserved D -glu-*m*DAP or NAM- D -ala- D -glu are recognized by NOD1 or NOD2, respectively [129]. Although Lp.PGN contains *m*DAP moiety, *L. plantarum*, insoluble and soluble Lp.PGN are known to activate NOD2 signaling due to the modification [118, 130]. To test which receptor recognizes Lp.PGN, NOD1- or NOD2-dependent NF- κ B activation was determined by using a reporter gene assay. As shown in Fig. 11, both insoluble and soluble Lp.PGN selectively induced NOD2-dependent NF- κ B activation in a dose-dependent manner. Therefore, to further examine whether NOD2 is involved in prevention of estrogen deficiency-induced bone loss by Lp.PGN, OVX and sham control mice were prepared in wild-type and NOD2-deficient mice (Fig. 12E and F). Mice were intragastrically given PBS or insoluble Lp.PGN, and then femurs were scanned by micro-CT. Supplementation with Lp.PGN did not increase femoral trabecular bone volume and trabecular number in NOD2-deficient mice (Fig. 12A – D). Consistent with bone morphometric results, Runx2-positive areas were not increased and TRAP-positive areas were not decreased by supplementation with Lp.PGN in NOD2-deficient mice (Fig. 13A and B). Collectively, these results suggest that intragastric administration of Lp.PGN increases trabecular bone volume through NOD2-dependent pathway.

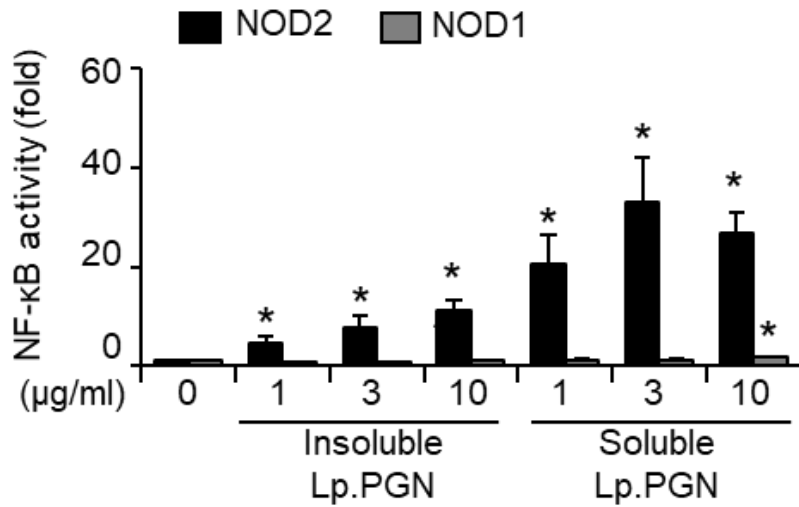


Figure 11. Lp.PGNs selectively activate NOD2. HEK 293 cells (2×10^4 cells/ 0.2 ml) were plated onto a 96-well culture plate in DMEM overnight. The cells were transiently transfected with a plasmid expressing human NOD1 or NOD2 in the presence of firefly luciferase reporter plasmid regulated by NF-κB transcription factor and pRL-TK *Renilla* luciferase plasmid as an internal control of transfection for 3 h in serum starved condition. After replacing with the fresh DMEM, the cells were further incubated for 24 h. The cells were stimulated with soluble or insoluble Lp.PGN fragments at 0, 1, 3, or 10 μg/ml for 16 h. After incubation, the cells were lysed and measured firefly or *Renilla* luciferase activities. Firefly luciferase activity was normalized to *Renilla* luciferase activity. * $p < 0.05$.

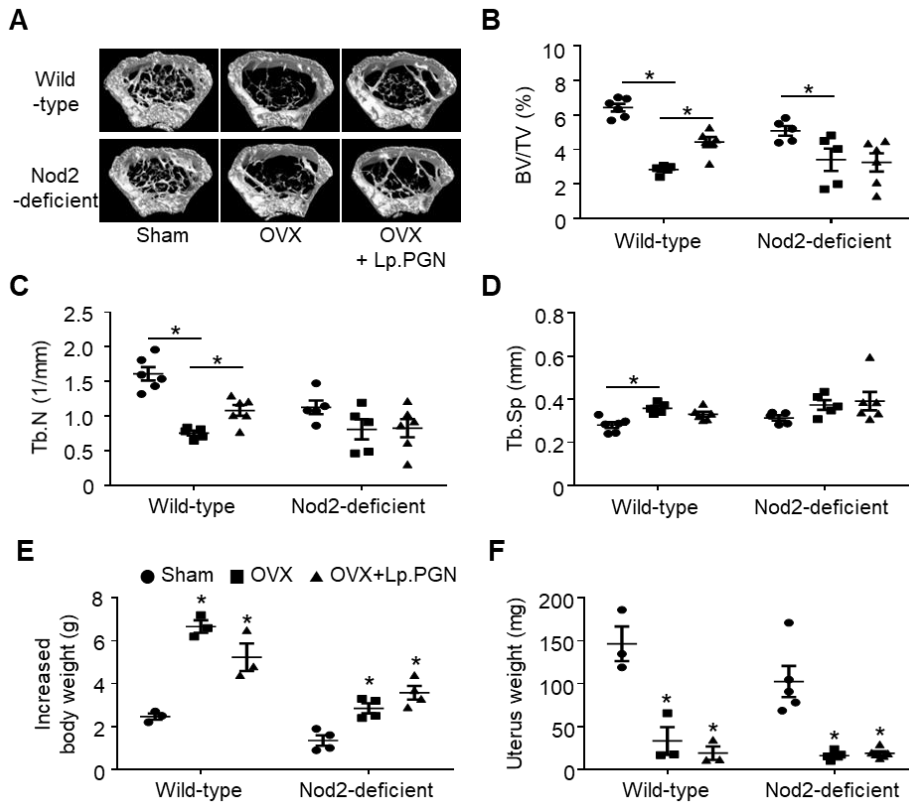


Figure 12. NOD2 signaling is essential for increase of trabecular bone volume by Lp.PGN. Fourteen-week-old OVX mice ($n = 5$) were intragastrically given 30 μg of insoluble Lp.PGN by oral gavage three times weekly for four weeks. Femurs were scanned by micro-CT and measured trabecular bone parameters using Skyscan programs. (A) Three-dimensional images of the femurs were obtained. BV/TV (B), Tb.N (C), and Tb.Sp (D) were calculated from 3D reconstruction of micro-CT images using the CT analyzer. (E) Body weight gain of mice in each group was measured at week 11 and week 14 and the change was calculated. At the end of the treatment, uterus weight (F) were measured. $*p < 0.05$ compared with the sham control group. BV/TV = trabecular bone volume per total bone volume; Tb.N = trabecular number; Tb.Sp = trabecular separation; OVX = ovariectomy. $*p < 0.05$.

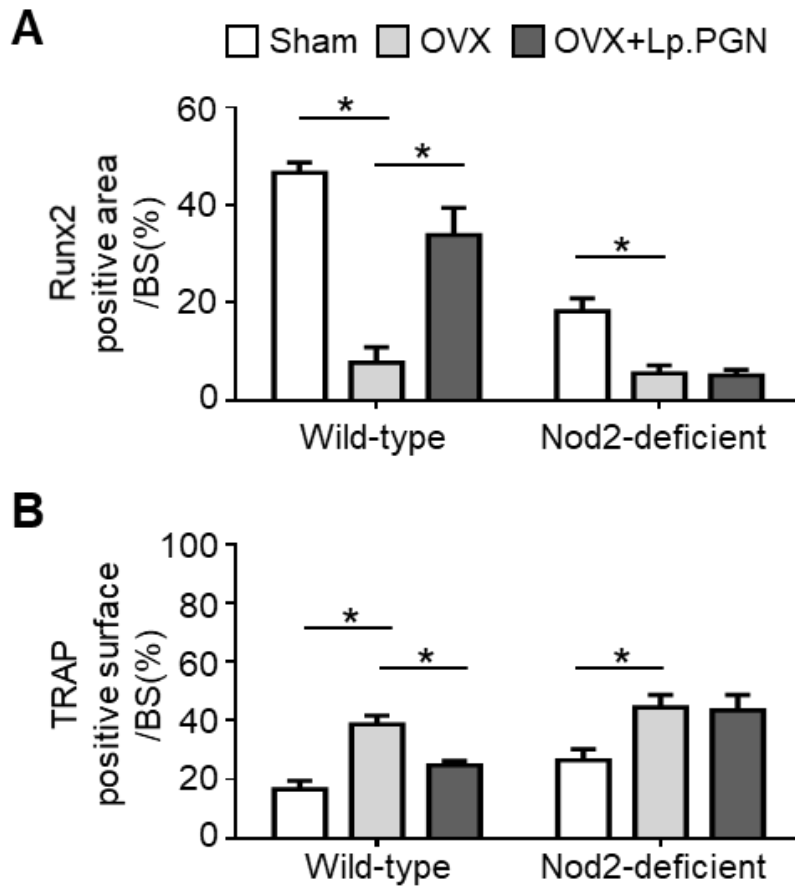


Figure 13. NOD2 is required for induction of Runx2 and inhibition of osteoclasts by Lp.PGN. Fourteen-week-old OVX mice were intragastrically given 30 μ g of insoluble Lp.PGN by oral gavage three times weekly for four weeks. The paraffin sections of the decalcified femur from wild-type or NOD2-deficient mice were subjected to immunofluorescence staining using a specific antibody to Runx2 or subjected to TRAP staining. Runx2-positive areas (A) and TRAP-positive areas (B) appeared on bone surface were measured using Image J program. BS = bone surface. * $p < 0.05$.

6. Intravenous or intraperitoneal administration of Lp.PGN increases trabecular bone volume in OVX-induced osteoporosis mouse model

Next, Lp.PGN was administered intravenously or intraperitoneally to confirm that the beneficial effect of Lp.PGN is by Lp.PGN acting on the intestine or not. Because lysozyme which cleave the bond between NAM-NAG of glycan chain in PGN, is present in body fluid including serum and intestine [130, 131], Lp.PGN fragments are thought to be present to the systemic circulation. In addition, previous reports suggested that intraperitoneal administration of MDP, an active moiety of peptidoglycan, increased bone mass [51, 132]. As the results shown in Fig. 14, OVX mice intraperitoneally administered Lp.PGN exhibited increased trabecular bone volume and trabecular number, while trabecular separation was not changed in comparison with OVX mice. OVX mice intravenously administered insoluble Lp.PGN showed increased trabecular bone volume, whereas trabecular number and trabecular separation is not altered in comparison with OVX mice (Fig. 15). These results indicate that Lp.PGN directly alleviates bone loss.

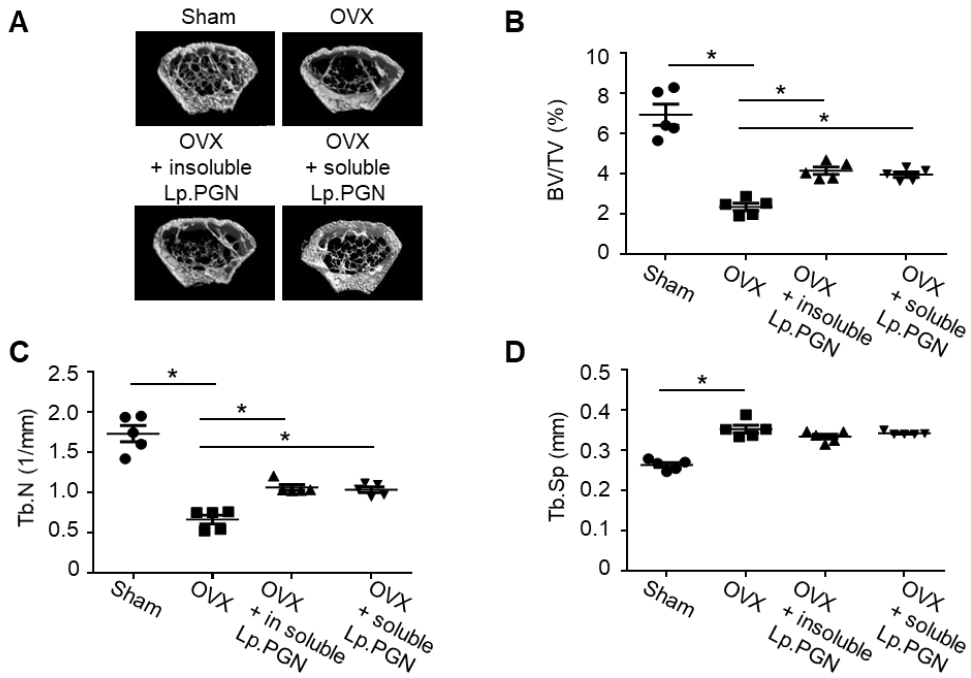


Figure 14. Intrapерitoneal administration of Lp.PGN increases femoral trabecular bone volume in OVX-induced osteoporosis mouse model. Fourteen-week-old OVX mice ($n = 5$) were intraperitoneally given 30 μg of insoluble Lp.PGN or soluble Lp.PGN once weekly for four weeks. Femurs were scanned by micro-CT and measured trabecular bone parameters using Skyscan programs. (A) Three-dimensional images of the femur were obtained. BV/TV (B), Tb.N (C), and Tb.Sp (D) were calculated from 3D reconstruction of micro-CT images using the CT analyzer. BV/TV = trabecular bone volume per total bone volume; Tb.N = trabecular number; Tb.Sp = trabecular separation; Tb.Th = trabecular thickness. $*p < 0.05$.

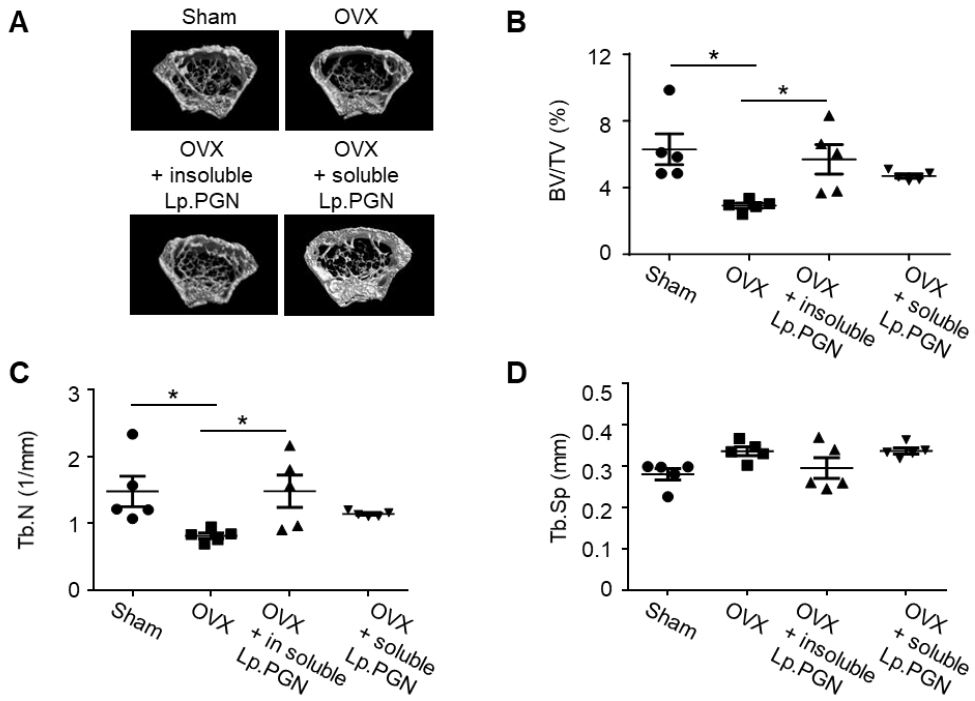


Figure 15. Intravenous administration of Lp.PGN increases femoral trabecular bone volume in OVX-induced osteoporosis mouse model. Fourteen-week-old OVX mice ($n = 5$) were intravenously given 30 μg of insoluble Lp.PGN or soluble Lp.PGN once weekly for four weeks. Femurs were scanned by micro-CT and measured trabecular bone parameters using Skyscan programs. (A) Three-dimensional images of the femurs were obtained. BV/TV (B), Tb.N (C), and Tb.Sp (D) were calculated from 3D reconstruction of micro-CT images using the CT analyzer. BV/TV = trabecular bone volume per total bone volume; Tb.N = trabecular number; Tb.Sp = trabecular separation; Tb.Th = trabecular thickness. $*p < 0.05$.

7. Lp.PGN directly induces osteoblast mineralization through NOD2 *in vitro*

To further examine the effect of Lp.PGN on osteoblast differentiation *in vitro*, soluble Lp.PGN was prepared by incubation with mutanolysin. When osteoblasts are fully differentiated, the cells produce calcium deposits, a critical functional process for bone formation. As shown in Fig. 16A, alizarin red S staining and spectrophotometric analysis demonstrated that soluble Lp.PGN dose-dependently increased the absorbance of alizarin red S. Consistent with the formation of calcium deposits, Lp.PGN induced mRNA expression of OPN, which is expressed in osteoblasts during bone formation (Fig. 16B). Furthermore, due to the selective activation of NOD2-mediated signaling by Lp.PGN (Fig. 11), osteoblast precursors were isolated from wild-type and NOD2-deficient mice and then stimulated with soluble Lp.PGN in the presence of ascorbic acid and β -glycerophosphate. As expected, spectrophotometric analysis showed that the absorbance of calcium deposits is not increased by Lp.PGN in NOD2-deficient cells (Fig 17A and B). Collectively, these results imply that soluble Lp.PGN fragments directly induce osteoblast differentiation and bone formation through NOD2-dependent manner.

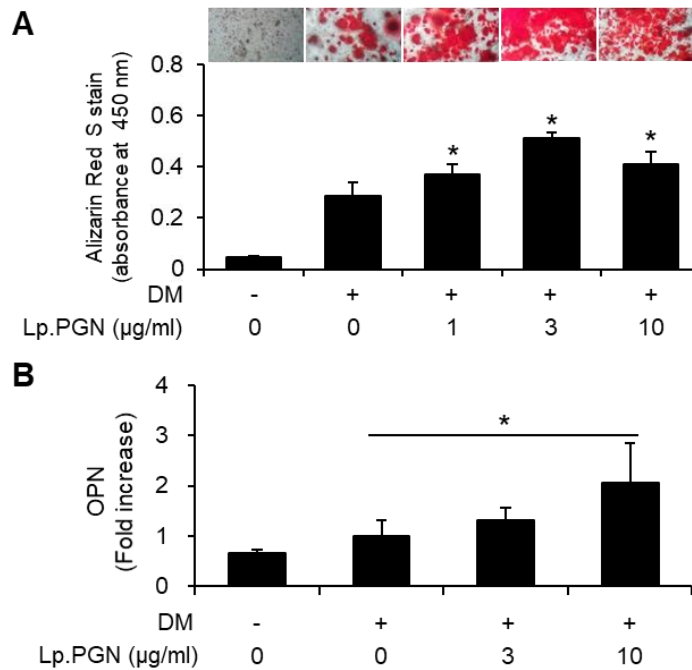


Figure 16. Lp.PGN induces osteoblast mineralization *in vitro*. (A) Calvarial osteoblast precursors were differentiated into osteoblasts by incubation with β -glycerophosphate and ascorbic acid in the presence of soluble Lp.PGN at 0, 1, 3, or 10 $\mu\text{g/ml}$ for 28 days. The cells were fixed and subjected to alizarin Red S staining to determine osteoblast differentiation. Representative images were obtained under an inverted phase-contrast microscope. Alizarin Red S was dissolved in a solution containing 20% methanol and 10% acetic acid and optical density was measured at 450 nm for quantifying precipitate. (B) Calvarial osteoblast precursors were differentiated into osteoblasts by incubation with β -glycerophosphate and ascorbic acid in the presence of soluble Lp.PGN at 0, 3, or 10 $\mu\text{g/ml}$ for 3 days. Total RNA was isolated and mRNA expression levels of OPN and GAPDH were determined by real-time RT-PCR. DM = differentiation medium containing 10 mM β -glycerophosphate and 50 $\mu\text{g/ml}$ ascorbic acid. * $p < 0.05$ compared to the differentiation medium only treated group.

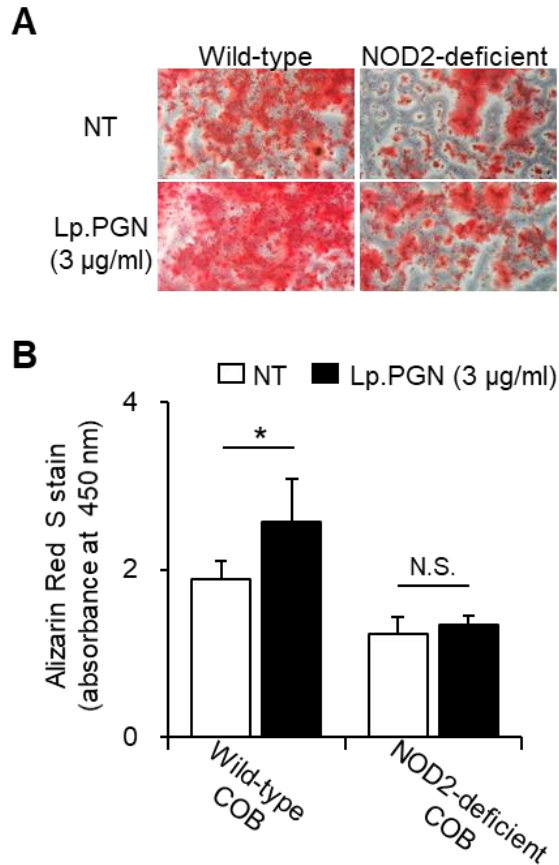


Figure 17. NOD2 is required for induction of osteoblast mineralization by Lp.PGN. Calvarial osteoblast precursors isolated from wild-type or NOD2-deficient mice were differentiated into osteoblasts by incubation with β -glycerophosphate and ascorbic acid in the presence or absence of soluble Lp.PGN at 3 μ g/ml for 28 days. The cells were fixed and subjected to Alizarin Red S staining to determine osteoblast differentiation. (A) Representative images were obtained under an inverted phase-contrast microscope. (B) Alizarin Red S was dissolved in a solution containing 20% methanol and 10% acetic acid and optical density was measured at 450 nm for quantifying precipitate. NT = non-treatment; N.S. = no significant difference. * $p < 0.05$.

8. Lp.PGN indirectly decreases osteoclast differentiation via osteoblasts

Osteoporosis mice supplementation with Lp.PGN exhibited decreased TRAP-positive surfaces in trabecular bone area. To determine if Lp.PGN directly regulates osteoclast differentiation, the effect of Lp.PGN on osteoclasts at different culture conditions of cells, including BMMs, committed osteoclast precursors, and BMM/osteoblast co-culture, were examined. Soluble Lp.PGN scarcely induced the number of TRAP-positive MNCs differentiated from BMMs or committed osteoclast precursors (Fig. 18A and B). However, when BMMs were co-cultured with osteoblast precursors in the presence or absence of Lp.PGN, the number of TRAP-positive MNCs was decreased by Lp.PGN in a dose-dependent manner (Fig. 18C). These results indicate that Lp.PGN indirectly regulate osteoclast differentiation via osteoblasts. Therefore, mRNA expression of RANKL in osteoblasts precursors in the presence of Lp.PGN was determined by real-time RT-PCR. Indeed, when osteoblasts were stimulated with Lp.PGN, the mRNA expression of RANKL were decreased (Fig. 18D). These results suggest that Lp.PGN indirectly attenuates osteoclast differentiation through regulation of RANKL expression in osteoblasts.

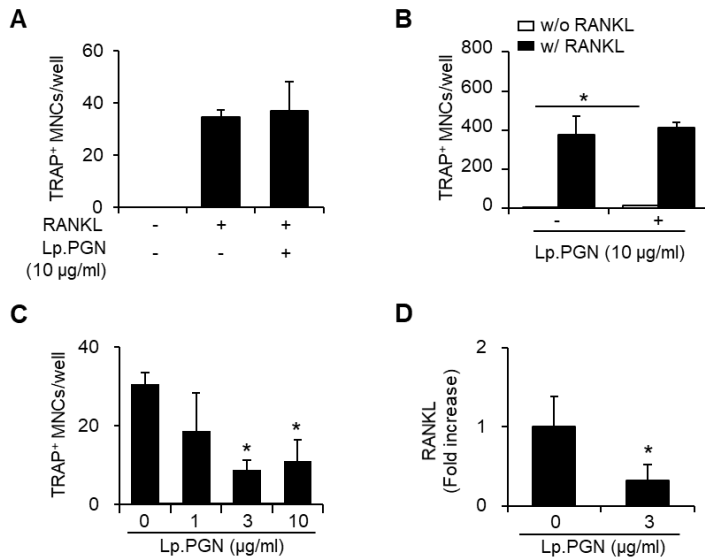


Figure 18. Lp.PGN indirectly attenuates osteoclast differentiation *in vitro*. (A)

BMMs were differentiated into osteoclasts by incubation with M-CSF and RANKL

in the presence or absence of soluble Lp.PGN at 10 µg/ml for 4 days. (B) BMMs

were differentiated into committed osteoclast precursors by incubation with M-CSF

and RANKL for 2 days. The cells were washed once with fresh medium and

differentiated into osteoclasts with M-CSF and/or RANKL in the presence or

absence of soluble Lp.PGN at 10 µg/ml for 2 days. (C) BMMs were differentiated

into osteoclasts by co-culture with calvarial osteoblast precursors. The cells were

incubated with β-glycerophosphate, ascorbic acid, and 1α,25-dihydroxyvitamin D₃

in the presence or absence of soluble Lp.PGN at 0, 1, 3, or 10 µg/ml for 12 days. The

cells were fixed and subjected to TRAP staining. TRAP-positive MNCs with three

or more nuclei were enumerated. (D) Calvarial osteoblast precursors were

differentiated into osteoblasts by incubation with β-glycerophosphate and ascorbic

acid in the presence or absence of soluble 3 µg/ml for 1 day. Total RNA was isolated

and mRNA expression levels of RANKL and GAPDH was determined by real-time

RT-PCR. **p* < 0.05.

9. Intra-gastric administration of Lp.PGN decreases TNF- α , IL-6, and RANKL production

Osteoclast differentiation is regulated by various factors, including pro-inflammatory cytokines, RANKL, and OPG in bone microenvironments [69]. In addition, TNF- α inhibits bone formation by attenuating osteoblast differentiation from precursors and inducing osteoclast differentiation [133]. Previous report suggested that supplementation of probiotics decrease expression of pro-inflammatory cytokines and RANKL which are involved in inducing osteoclast differentiation [53]. Thus, under the speculation that Lp.PGN might be involved in attenuation of TNF- α , IL-6, and IL-1 β , representative pro-inflammatory cytokines, and RANKL [134-136], protein levels of TNF- α , IL-6, IL-1 β , RANKL, and OPG in serum or bone marrow extracellular fluid were detected. Indeed, the levels of TNF- α were significantly decreased in both bone marrow extracellular fluid and serum obtained from OVX mice supplemented with Lp.PGN in comparison with that from OVX control mice (Fig. 19A and B). The level of IL-6 was decreased, while that of IL-1 β was not changed, in serum obtained from OVX mice supplemented with Lp.PGN in comparison with the OVX control mice (Fig. 19C and D). Moreover, the level of RANKL was decreased in bone marrow extracellular fluid obtained from OVX mice supplemented with Lp.PGN in comparison with that from OVX control mice (Fig. 20A). Although the level of OPG was not altered in OVX mice or OVX mice supplemented with Lp.PGN (Fig. 20B), RANKL/OPG ratio, an important determinant of osteoclast activation and bone loss, was significantly decreased in OVX mice supplemented with Lp.PGN in comparison with OVX control mice (Fig.

20C). These results indicate that supplementation with Lp.PGN inhibits osteoclast differentiation through down-regulation of TNF- α , IL-6 and RANKL.

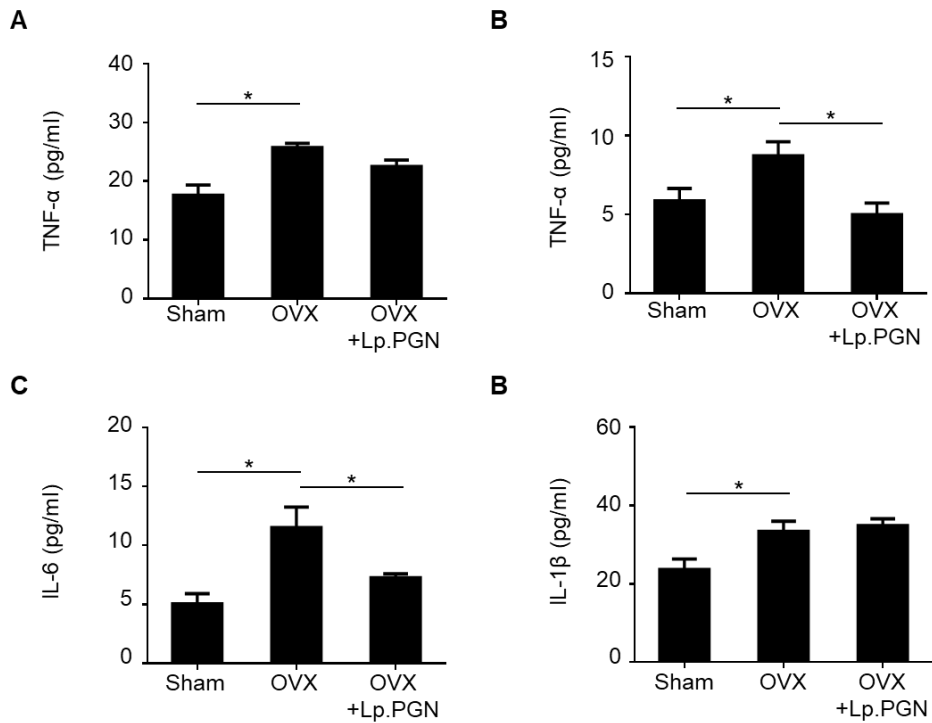


Figure 19. Intra-gastric administration of Lp.PGN decreases TNF- α and IL-6 production in serum and bone marrow extracellular fluid. Fourteen-week-old OVX mice were intragastrically given 30 μ g of insoluble Lp.PGN three times weekly for four weeks. Bone marrow extracellular fluids (A) and serum (B – D) were obtained to measure the level of TNF- α , IL-6, and IL-1 β by ELISA. * $p < 0.05$.

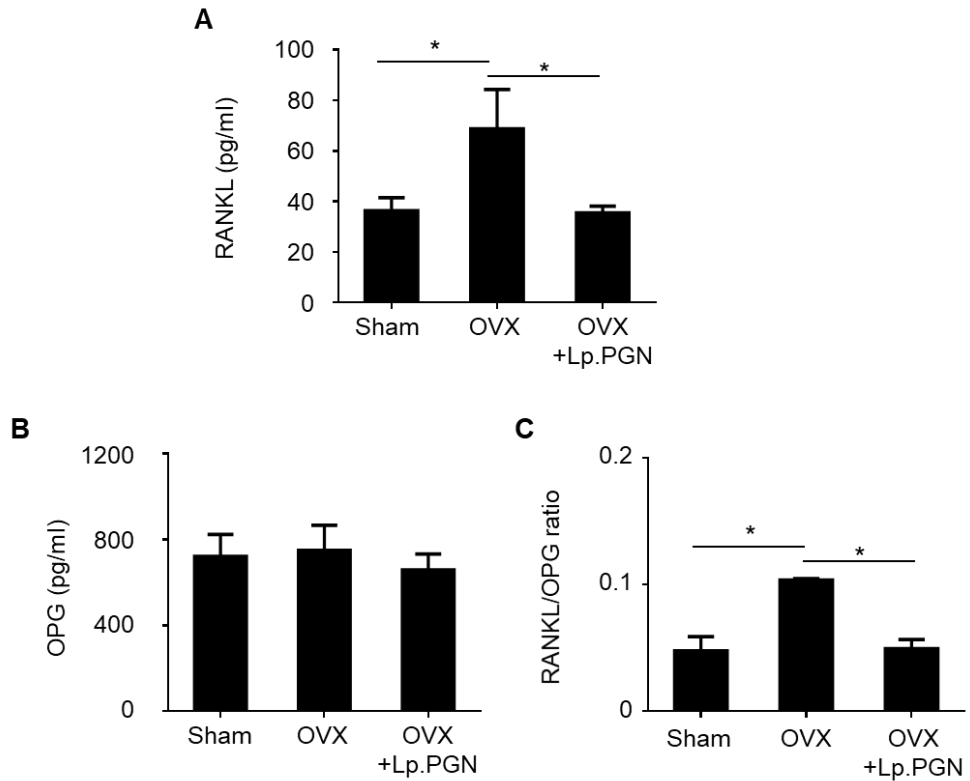


Figure 20. Intra-gastric administration of Lp.PGN decreases RANKL production in bone marrow extracellular fluid. Fourteen-week-old OVX mice were intra-gastrically given 30 μ g of insoluble Lp.PGN three times weekly for four weeks. Bone marrow extracellular fluids were obtained to measure the levels of RANKL (A), and OPG (B) by ELISA. (C) RANKL/OPG ratio was calculated. $*p < 0.05$.

10. Intra-gastric administration of Lp.PGN increases trabecular bone volumes in RANKL-induced osteoporosis mouse model

In some previous reports indicated that the beneficial effect of probiotics on bone quality depends on gender. Therefore, to examine whether supplementation with Lp.PGN could also influence bone metabolism in normal and RANKL-induced bone loss condition in male, mice intraperitoneally administered RANKL or PBS were given Lp.PGN by oral gavage (Fig. 21). RANKL-administered mice exhibited decreased trabecular bone volume and trabecular number and increased trabecular separation (Fig. 22A – D). Similar to the results from OVX model, intragastrical supplementation with Lp.PGN increased femoral trabecular bone volume in comparison with control group (Fig. 22A and B). Trabecular number was increased and trabecular separation was decreased in mice supplementation with Lp.PGN in RANKL-administered group (Fig. 22C and D). Consistently, lumbar vertebral trabecular bone volume was also increased in mice supplementation with Lp.PGN in RANKL-administrated group (Fig. 23A and B). Moreover, to observe whether the increase of trabecular bone volume is due to the new bone formation, mice were intraperitoneally administered 20 mg/kg of calcein seven and two days before femur isolation. As shown in Fig. 24A – D, the percentage of mineralizing surface, mineral apposition rate, and bone formation rate was increased in RANKL-administered mice supplemented with Lp.PGN in comparison with RANKL-administered mice. PBS-administered mice supplemented with Lp.PGN showed trend toward to increase mineralizing surface, mineral apposition rate, and bone formation rate without significance in comparison with PBS-administered control mice. These

results suggest that beneficial effect of Lp.PGN is not limited to the gender difference and supplementation of Lp.PGN increases new bone formation.

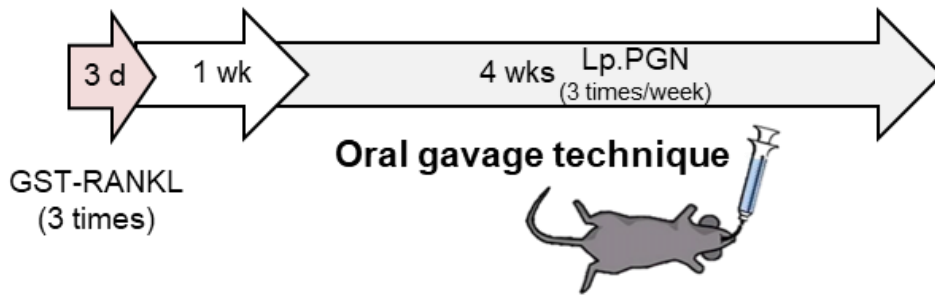


Figure 21. Experimental procedure of RANKL-induced osteoporosis mouse model. Six-week-old C57BL/6 male mice were randomly divided into four groups and were intraperitoneally administered RANKL or PBS once daily for three days. One week after the RANKL injection, mice were intragastrically given PGNs by oral gavage technique for four weeks.

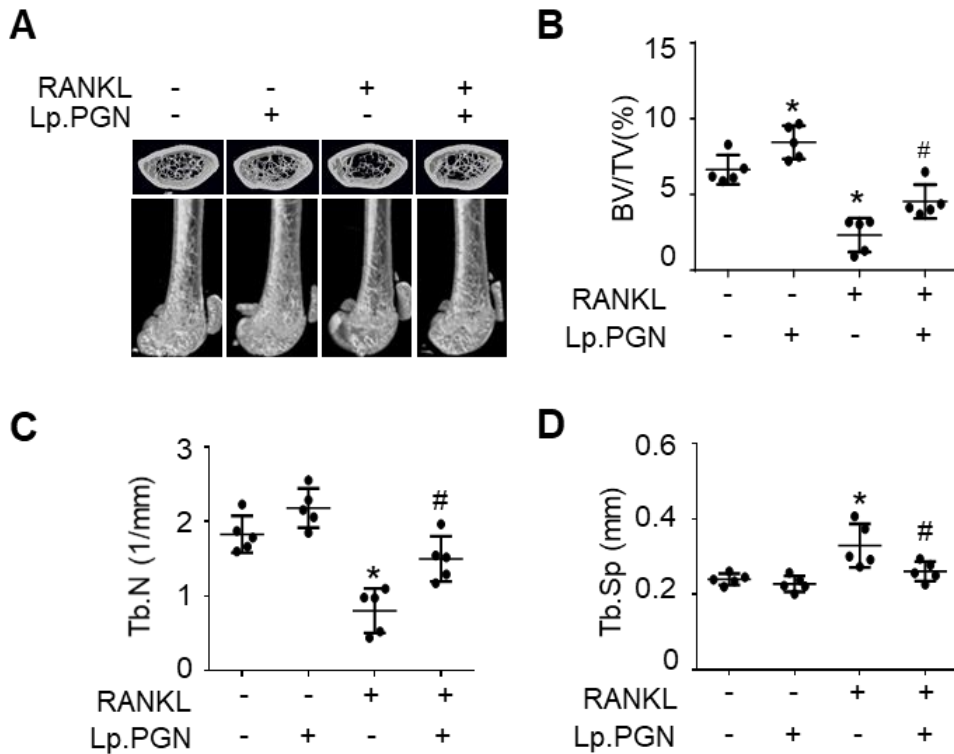


Figure 22. Intra-gastric administration of Lp.PGN increases femoral trabecular bone volume in RANKL-induced osteoporosis mouse model. Seven-week-old male mice ($n = 5$) were intra-gastrically given 30 μg of insoluble Lp.PGN three times weekly for four weeks. (A – D) Femurs were scanned by micro-CT and measured trabecular bone parameters using Skyscan programs. (A) Three-dimensional images of the femurs were obtained. BV/TV (B), Tb.N (C), and Tb.Sp (D) were calculated from 3D reconstruction of micro-CT images using the CT analyzer. BV/TV = trabecular bone volume per total bone volume; Tb.N = trabecular number; Tb.Sp = trabecular separation. * $p < 0.05$, compare to the control group; # $p < 0.05$, compare to the RANKL-treated group.

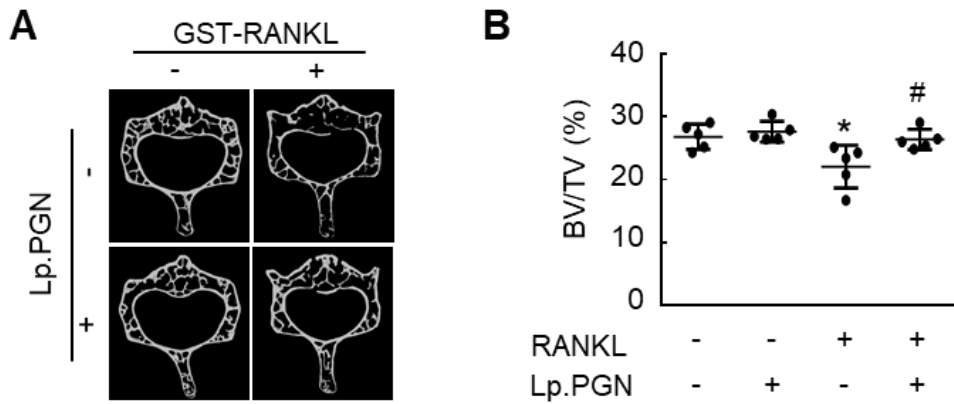


Figure 23. Intra-gastric administration of Lp.PGN increases vertebral trabecular bone volume in RANKL-induced osteoporosis mouse model. Seven-week-old male mice ($n = 5$) were intraperitoneally given 30 μg of insoluble Lp.PGN three times weekly for four weeks. L3 vertebrae were isolated and scanned by micro-CT and measured trabecular bone parameters using Skyscan programs. (A) Three-dimensional images of the L3 were obtained. (B) BV/TV was calculated from 3D reconstruction. BV/TV = trabecular bone volume per total bone volume. $*p < 0.05$, compare to the control group; $\#p < 0.05$, compare to the RANKL-treated group.

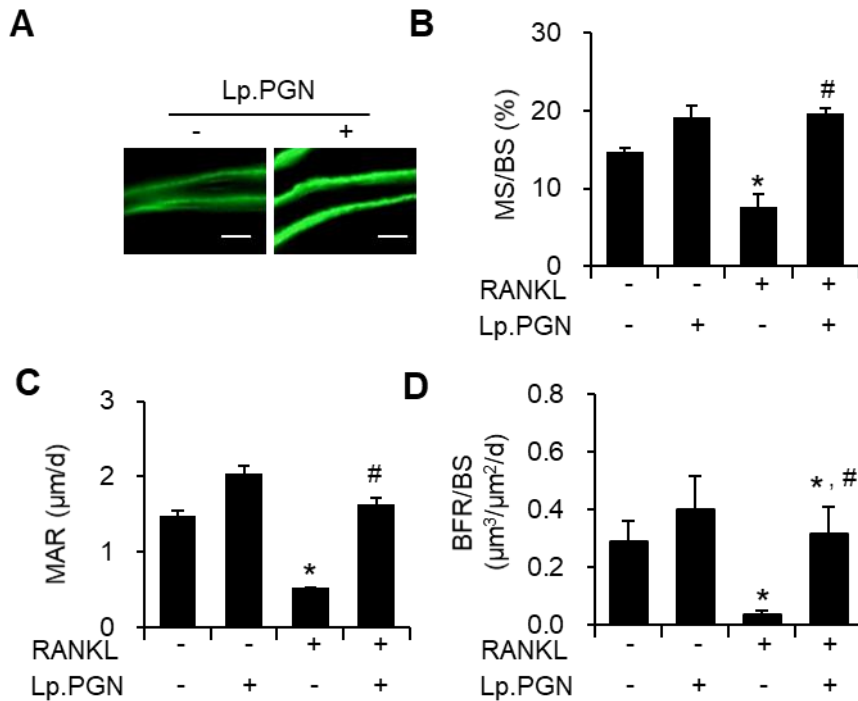


Figure 24. Intra-gastric administration of Lp.PGN increases bone formation.

Seven-week-old male mice were intraperitoneally given 30 μg of insoluble Lp.PGN three times weekly for four weeks. Seven and two days before sacrifice, mice were intraperitoneally administered with calcein AM. The resin sections of the femurs were obtained and then representative images of calcein-labeled bones were captured under a confocal microscope (A). (B – D) MS/BS, MAR and BFR/BS were measured by using OsteoMeasure software. MS/BS = mineralising surface per bone surface; MAR = mineral apposition rate; BFR/BS = Expressing bone formation rate per unit of bone surface. * $p < 0.05$, compare to the control group; # $p < 0.05$, compare to the RANKL-treated group.

11. NOD1-activating Bc.PGN and Bs.PGN induce bone destruction

Lp.PGN results arise the question of whether intragastric administration of NOD1-activating PGN could regulate bone metabolism. Accumulating reports suggested that NOD1 signaling mediated bone destruction, such as periodontitis [137, 138]. Thus, under the hypothesis that intragastric supplementation with NOD1-activating PGN could induce bone loss, *B. cereus* PGN (Bc.PGN) and *B. subtilis* PGN (Bs.PGN) were purified and NOD1 and NOD2 activation was examined using soluble PGN. Fig. 25 showed that Bc.PGN and Bs.PGN selectively induced NOD1 activation. Next, to observe the effect of NOD1 activating PGN on bone regulation, both PGNs were intragastrically administered for four weeks and then bone morphometric changes of femoral trabecular bone was analyzed using micro-CT. As expected, mice supplemented with Bc.PGN decreased trabecular bone mass (Fig. 26A) and mice supplemented with Bc.PGN or Bs.PGN decreased trabecular number (Fig. 26B). Trabecular separation and trabecular thickness were not changed by supplementation with Bc.PGN or Bs.PGN (Fig. 26C and D). Three-dimensional images and paraffin sections of femurs also exhibited lower bone area in comparison with control (Fig. 26 E and F). These results indicate that intragastric administration of NOD1-activating Bc.PGN and Bs.PGN induce bone loss.

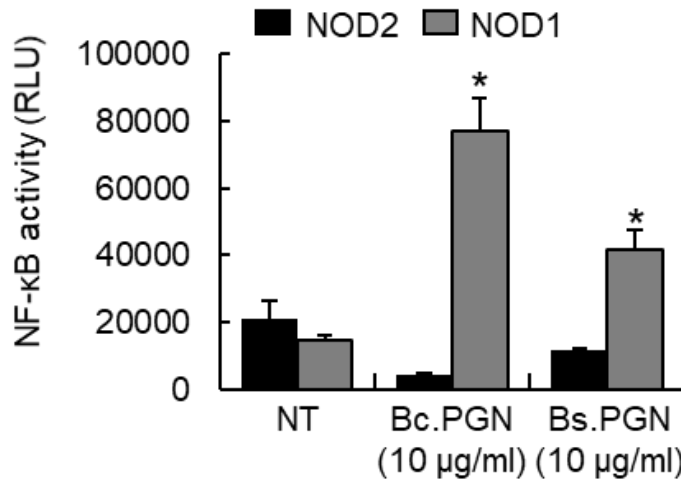


Figure 25. Bc.PGN and Bs.PGN selectively activate NOD1. HEK 293 cells (2×10^4 cells/ 0.2 ml) were plated onto a 96-well culture plate in DMEM overnight. The cells were transiently transfected with a plasmid expressing human NOD1 or NOD2 in the presence of firefly luciferase reporter plasmid regulated by NF- κ B transcription factor and pRL-TK *Renilla* luciferase plasmid as an internal control of transfection for 3 h in serum starved condition. After replacing with the fresh DMEM, the cells were further incubated for 24 h. The cells were stimulated with soluble Bc.PGN or Bs.PGN at 0 or 10 μ g/ml for 16 h. After incubation, the cells were lysed and measured firefly or *Renilla* luciferase activities. Firefly luciferase activity was normalized to *Renilla* luciferase activity. * $p < 0.05$.

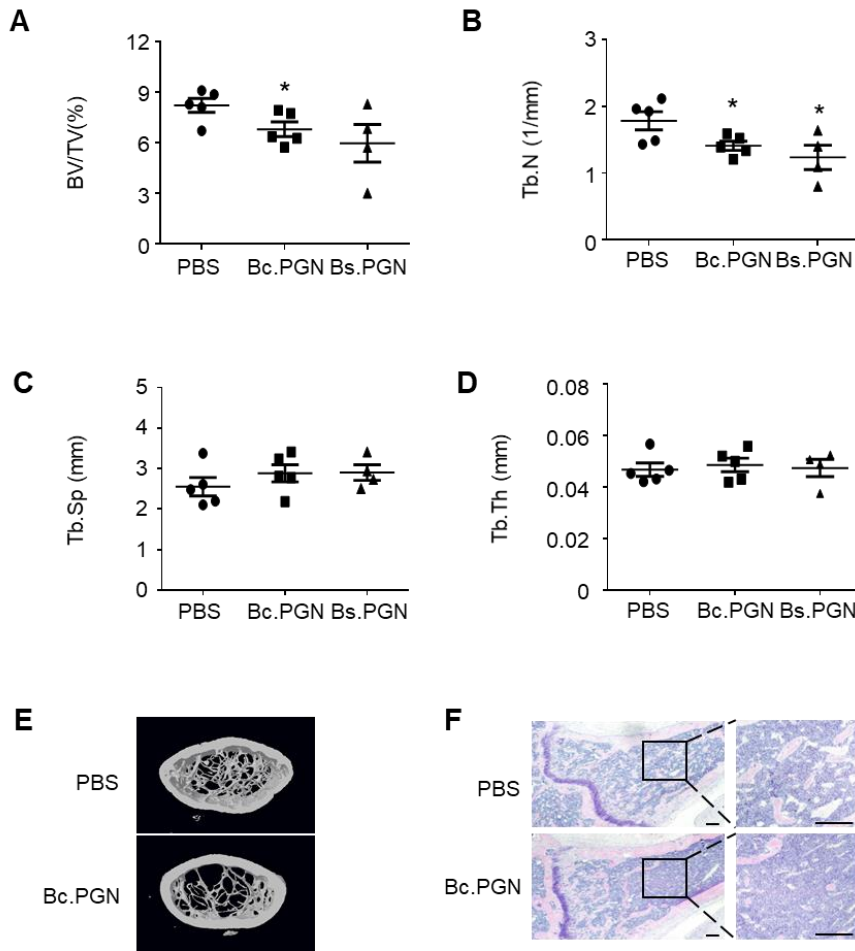


Figure 26. Intra-gastric administration of NOD1-activating Bc.PGN and Bs.PGN induce bone destruction. Seven-week-old male mice were intra-gastrically given PBS ($n = 5$) or 30 μg of Bs.PGN ($n = 4$) or Bc.PGN ($n = 5$) three times weekly for four weeks. Femurs were scanned by micro-CT and measured trabecular bone parameters using Skyscan programs. BV/TV (A), Tb.N (B), Tb.Sp (C), and Tb.Th (D) were calculated from 3D reconstruction of micro-CT images using the CT analyzer. (E) Three-dimensional images of the femur were obtained. (F) Paraffin sections of the decalcified femur were subjected to H&E and photographed. Bars = 200 μm . BV/TV = trabecular bone volume per total bone volume; Tb.N = trabecular number; Tb.Th = trabecular thickness; Tb.Sp = trabecular separation. * $p < 0.05$.

12. Bc.PGN induces osteoclast differentiation by direct and indirect mechanisms

Because *B. cereus* was reported to be causative bacteria of osteomyelitis [139] and intragastric administration of Bc.PGN showed significant bone destruction, paraffin sections of femur from Bc.PGN-administered mice were subjected to TRAP staining. TRAP staining showed increased TRAP-positive surface compared to the control (Fig. 27A and B). As Bc.PGN increased TRAP-positive areas in femur, committed osteoclast precursors were differentiated into osteoclasts in the presence or absence of Bc.PGN *in vitro*. TRAP staining showed that Bc.PGN dose-dependently increased the number of TRAP-positive MNCs (Fig. 28A and B). In addition, immunofluorescence staining of NFATc1 demonstrated that Bc.PGN induced NFATc1 expression and its translocation into the nucleus (Fig. 28C). Since MAPKs activation is associated with osteoclastogenesis [140], phosphorylation of ERK, JNK, and p38 by Bc.PGN was determined by Western blot analysis. Bc.PGN induced phosphorylation of ERK and the maximal phosphorylation of ERK was observed at 90 min (Fig. 29A). In addition, pre-treatment of a specific inhibitor of ERK (U0126) decreased the number of TRAP-positive MNCs induced by Bc.PGN (Fig. 29B). These results suggest that Bc.PGN directly induces osteoclast differentiation via ERK signaling pathways.

Next, because Lp.PGN indirectly regulated osteoclast differentiation by regulating RANKL expression in osteoblasts, the effect of Bc.PGN on osteoclast differentiation from BMMs co-cultured with osteoblast precursors was examined. Similar to *in vivo* TRAP staining results, when BMMs were co-cultured with osteoblast precursors, soluble Bc.PGN increased the number of TRAP-positive MNCs (Fig. 30A and B).

In addition, when osteoblasts were stimulated with Bc.PGN, the mRNA expression of RANKL was increased (Fig 30C). To determine whether the increase of osteoclast number in co-culture is mediated by osteoblasts, BMMs were differentiated from BMs obtained from wild-type and NOD1-deficient mice and the cells were co-culture with wild-type osteoblast precursors to induce osteoclast differentiation in the presence or absence of Bc.PGN. As shown in Fig. 31, the number of TRAP-positive osteoclast was increased by Bc.PGN in both wild-type and NOD1-deficient BMMs co-cultured with clavalial osteoblast precursors. Because Bc.PGN induced osteoclast differentiation of BMMs derived from NOD1-deficient mice, these findings suggest that Bc.PGN also indirectly induces osteoclast differentiation. Taken together, these results indicate that Bc.PGN induces osteoclast differentiation by direct and indirect mechanisms via positive regulation of RANKL.

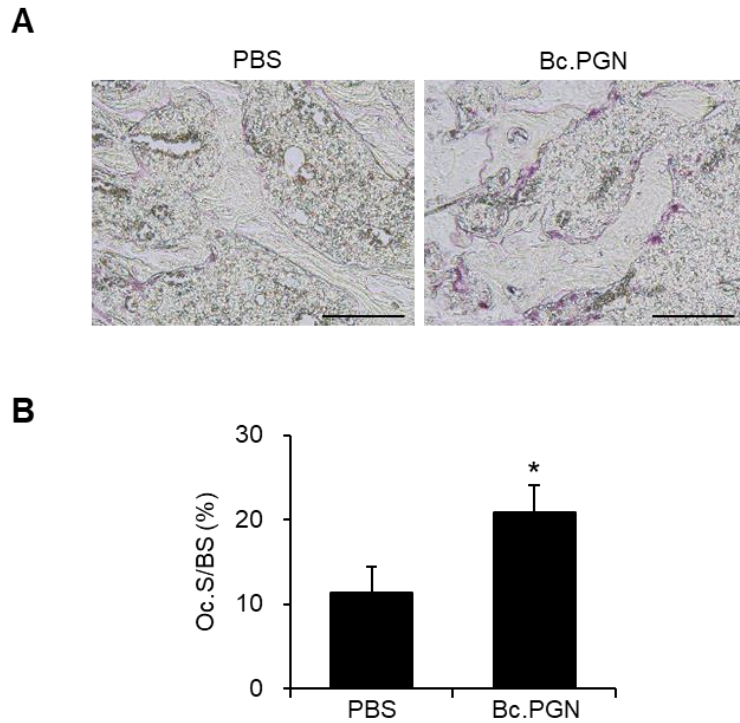


Figure 27. Bc.PGN increases TRAP-positive osteoclasts *in vivo*. Seven-week-old male mice were intragastrically given PBS ($n = 5$) or 30 μg of Bc.PGN ($n = 5$) three times weekly for four weeks. The paraffin sections of the decalcified femurs were subjected to TRAP staining. TRAP-positive areas (osteoclast surface) appeared on bone surface were measured using Image J program. Bars = 200 μm . * $p < 0.05$.

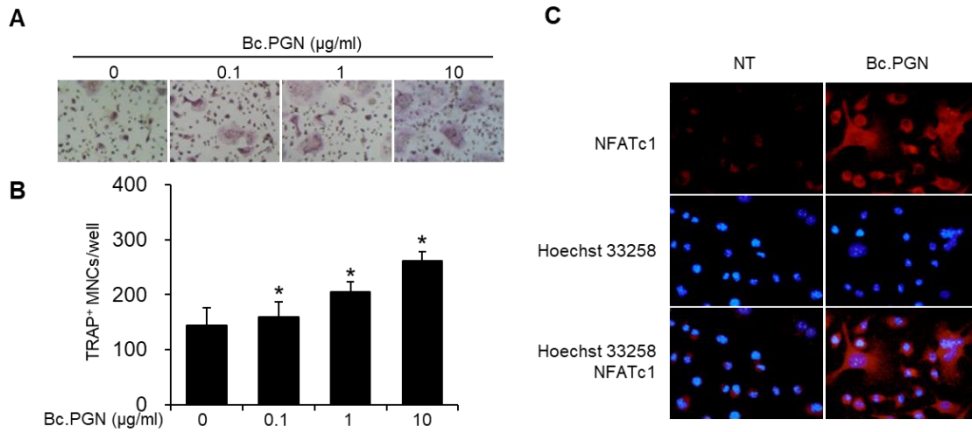


Figure 28. Bc.PGN enhances osteoclast differentiation and expression of NFATc1. (A and B) BMMs were differentiated into committed osteoclast precursors by incubation with M-CSF and RANKL for 2 days. The cells were washed once with fresh medium and differentiated into osteoclasts with M-CSF in the presence of Bc.PGN at 0, 0.1, 1, or 10 µg/ml for 2 days. The cells were fixed and subjected to TRAP staining. Representative images were obtained under an inverted phase-contrast microscope (A) and TRAP-positive MNCs with three or more nuclei were enumerated (B). (C) Committed osteoclast precursors were stimulated with 10 µg/ml of Bc.PGN for 2 days. The cells were fixed and stained with specific antibody to NFATc1, followed by Hoechst 33258. The images of cells were captured under a confocal microscope. * $p < 0.05$.

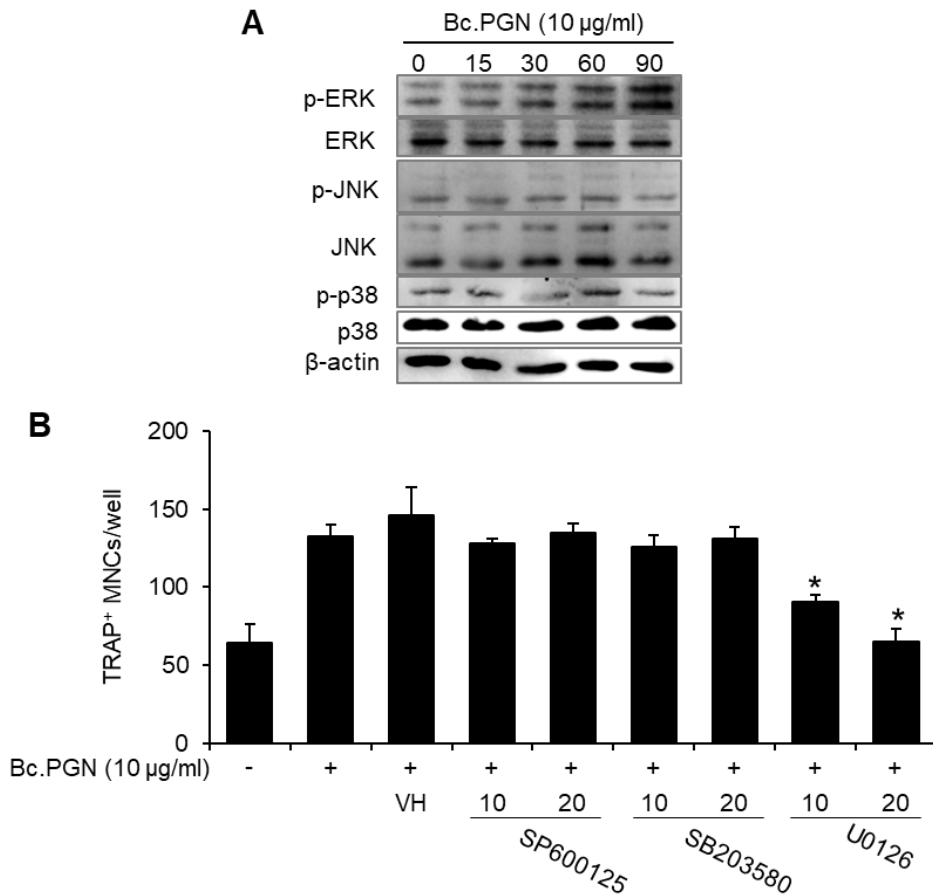


Figure 29. Phosphorylation of ERK are required for Bc.PGN-induced osteoclast differentiation. (A) Committed osteoclast precursors were serum-deprived for 3 h and then stimulated with Bc.PGN for 15, 30, 60, or 90 min. Immunoblots were performed with antibodies specific to phosphorylated or non-phosphorylated forms of MAP kinases, including ERK, p38 kinase, and JNK. (B) Committed osteoclast precursors were pre-treated with the inhibitors of p38, ERK, or JNK for 1 h and then the cells were stimulated with Bc.PGN for 24 h. The cells were stained for TRAP and TRAP-positive MNCs were enumerated. VH: vehicle control. * $p < 0.05$.

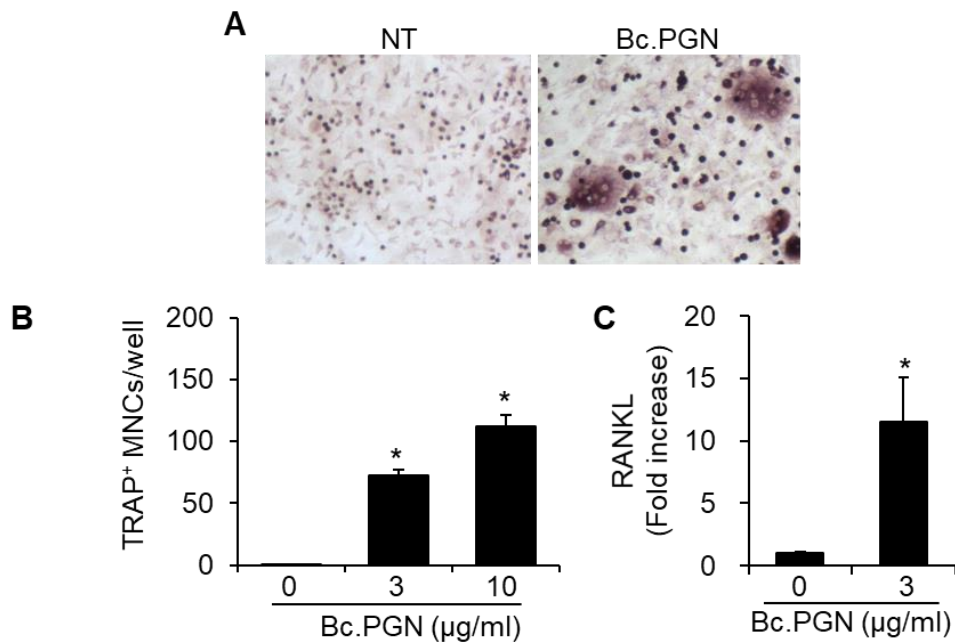


Figure 30. Bc.PGN induces osteoclast differentiation from BMMs co-cultured with osteoblast precursors. BMMs were differentiated into osteoclasts by co-culture with calvarial osteoblast precursors. The cells were incubated with β -glycerophosphate, ascorbic acid, and $1\alpha,25$ -dihydroxyvitamin D_3 in the presence or absence of soluble Bc.PGN at 0, 3, or 10 $\mu\text{g/ml}$ for 12 days. The cells were fixed and subjected to TRAP staining. TRAP-positive MNCs with three or more nuclei were enumerated. (C) Calvarial osteoblast precursors were differentiated into osteoblasts by incubation with β -glycerophosphate and ascorbic acid in the presence or absence of soluble Bc.PGN 3 $\mu\text{g/ml}$ for 1 day. Total RNA was isolated and mRNA expression levels of RANKL and GAPDH was determined by real-time RT-PCR. * $p < 0.05$.

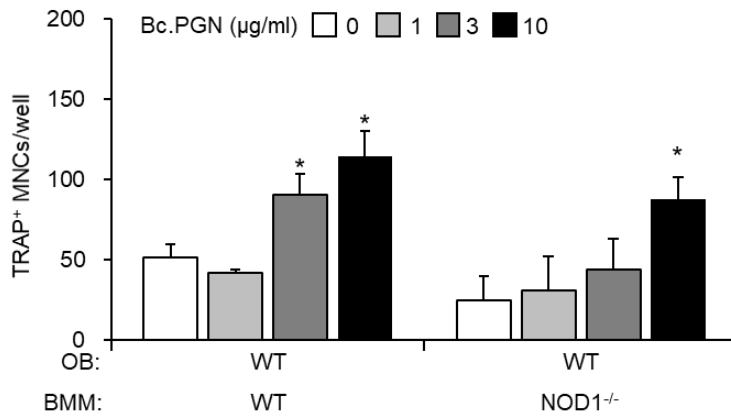


Figure 31. Bc.PGN indirectly induces osteoclast differentiation by affecting osteoblasts through NOD1 signaling. BMMs isolated from wild-type or NOD1-deficient mice were differentiated into osteoclasts by co-culture with calvarial osteoblast precursors isolated from wild-type mice. The cells were incubated with β -glycerophosphate, ascorbic acid, and $1\alpha,25$ -dihydroxyvitamin D₃ in the presence or absence of soluble Bc. PGN at 0, 3, or 10 μ g/ml for 12 days. The cells were fixed and subjected to TRAP staining. TRAP-positive MNCs with three or more nuclei were enumerated. * $p < 0.05$.

13. Bc.PGN directly inhibits osteoblast differentiation *in vitro*

Because Bc.PGN-induced osteoclast differentiation was mediated by regulating osteoblasts through NOD1 signaling in Fig. 30, the effect of Bc.PGN on regulation of osteoblast differentiation was tested. Calvarial osteoblast precursors were stimulated with soluble Bc.PGN and osteoblast differentiation was determined by ALP staining. ALP staining indicated that Bc.PGN decreased osteoblast differentiation (Fig. 32A). Then, the expression of osteoblast differentiation marker was determined by real-time RT-PCR. In addition, mRNA expression levels of ALP and Runx2 were also decreased by Bc.PGN in comparison with control (Fig. 32B). These results suggest that Bc.PGN not only increases osteoclast differentiation but also inhibits osteoblast differentiation.

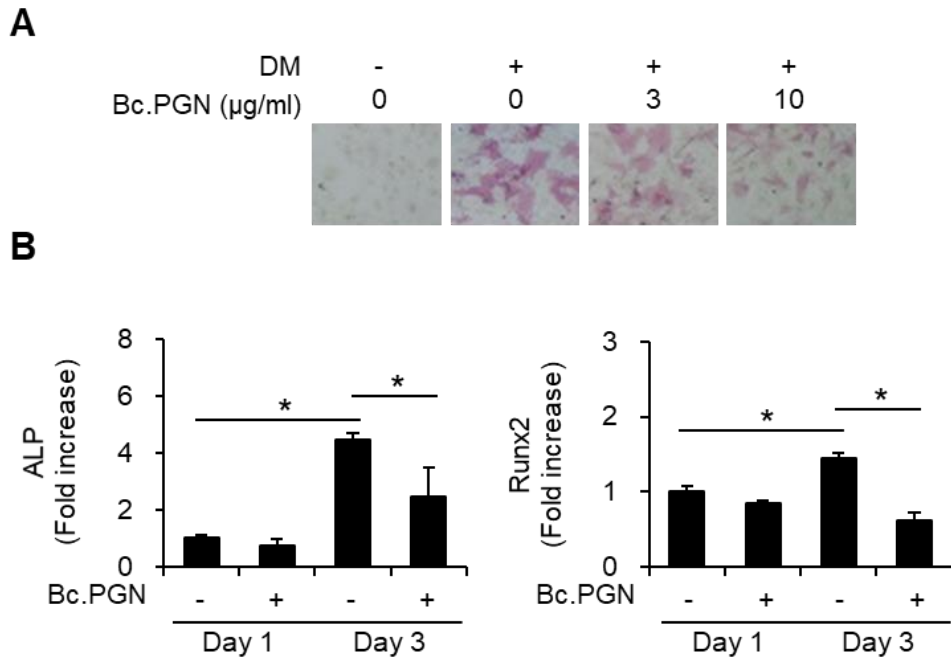


Figure 32. Bc.PGN inhibits osteoblast differentiation. (A) Calvarial osteoblast precursors were differentiated into osteoblasts by incubation with β -glycerophosphate and ascorbic acid in the presence of soluble Bc.PGN at 0, 3, or 10 $\mu\text{g/ml}$ for 12 days. The cells were fixed and subjected to ALP staining to determine osteoblast differentiation. Representative images were obtained under an inverted phase-contrast microscope. (B) Calvarial osteoblast precursors were stimulated with β -glycerophosphate and ascorbic acid in the presence or absence of soluble Bc.PGN (3 $\mu\text{g/ml}$) for 1 or 3 day(s). Total RNA was isolated and mRNA expression levels of ALP, Runx2, and GAPDH were determined by real-time RT-PCR. DM = differentiation medium containing 10 mM β -glycerophosphate and 50 $\mu\text{g/ml}$ ascorbic acid. * $p < 0.05$ compared to the differentiation medium only treated group.

Chapter IV. Discussion

The study demonstrated that Lp.PGN enhanced bone formation and inhibited bone resorption, whereas Bc.PGN inhibited bone formation and enhanced bone resorption. Intra-gastric administration of Lp.PGN enhanced bone mass in OVX- or RANKL-induced osteoporosis mouse model. Supplementation of Lp.PGN increased bone formation and decreased bone resorption through NOD2-dependent manner. In addition, Lp.PGN decreased levels of osteoclastogenic cytokines, TNF- α and RANKL in bone marrow extracellular fluid. In contrast, intra-gastric administration of Bc.PGN, which was recognized by NOD1, induced bone loss through enhancing osteoclast differentiation. Bc.PGN induced osteoclast differentiation by direct and indirect mechanisms. Therefore, the study suggests that bacterial PGN fragments could be involved in the regulation of bone metabolism through NOD1 and NOD2 (Fig. 33).

PGNs from some *Lactobacillus* spp. inhibited bone loss in osteoporosis model. The beneficial effect of probiotics, especially *Lactobacillus* spp. has been reported recent years. *L. reuteri* and *L. rhamnosus* GG increased bone volume in OVX-induced osteoporosis mouse model by reducing RANKL expression [53, 78]. In addition, *L. rhamnosus* GG inhibited alveolar bone loss by reducing osteoclast number [82] and *L. gasseri* also decreased *Porphyromonas gingivalis*-induced alveolar bone loss by suppression of *P. gingivalis*-induced IL-6 and TNF- α expressions [83]. These previous results could be due to the effect of probiotics releasing PGN fragments because intraperitoneal administration of an active moiety of PGN alleviated bone mass through increase of expression and transcription activity of Runx2 in

osteoblasts [51]. However, in this study, among PGNs from *Lactobacillus* spp., PGNs purified from *L. plantarum*, *L. casei*, *L. delbrueckii*, *L. rhamnosus* GG, *L. agilis*, *L. ruminis*, *L. saerimneri* inhibited bone loss in osteoporosis mouse model. This differential effects could be due to the structural differences of PGNs, including (1) variation in stem peptide and its third amino acid (Lys-type or DAP-type), (2) variation in interpeptide bridge, (3) modification of glycan strand [89, 141]. The stem peptide composition in most *Lactobacillus* spp. is $L\text{-Ala-}\gamma\text{-D-Glx-L-Lys-D-Ala-D-Ala}$. *L. acidophilus*, *L. casei*, *L. delbrueckii*, *L. reuteri*, *L. rhamnosus* GG share $L\text{-Lys-D-Asn}$, while *L. plantarum*, *L. agilis*, *L. coleohominis*, *L. mali*, *L. ruminis*, *L. saerimneri* share DAP without interpeptide bridge [128]. Therefore, the differential effect of PGNs seems to be due to the glycan strand modification or differences in released PGN fragments, not the stem peptide or interpeptide bridge. According to the previous report, intragastric administration of PGN from *L. salivarius* protected colitis, but PGN from *L. acidophilus* did not. Structural analysis showed PGN fragments from *L. salivarius* additionally had M-tri-Lys and mice intraperitoneally administered M-tri-Lys exhibited protective effect against colitis [135]. Thus, how PGN is cleaved by the enzyme is thought to be important and PGN fragments from *L. plantarum*, *L. casei*, *L. delbrueckii*, *L. rhamnosus* GG, *L. agilis*, *L. ruminis*, *L. saerimneri* could contain more M-tri-Lys structure than other *Lactobacillus* spp. used in this study.

Lp.PGN fragments directly affected bone cells to increase bone mass. In this study, femur section from OVX mice supplemented with Lp.PGN by oral gavage exhibited increased Runx2 expression and decreased TRAP-positive area in comparison with OVX control. The results might be due to the direct effects of Lp.PGN fragments

that are released from the intestine. Consistent with the *in vivo* results, soluble Lp.PGN treatment of calvarial osteoblast precursors showed increased calcium deposition. In addition, soluble Lp.PGN treatment decreased osteoclast differentiation via osteoblasts through the down-regulation of RANKL expression. Moreover, intravenous administration of Lp.PGN increased bone mass in OVX-induced osteoporosis model, indicating the direct effect of Lp.PGN fragments. A previous report demonstrated that PGN fragments are detected in bloodstream and bone marrow using *E. coli* with [³H]-DAP labeled PGN and reporter gene assay showed that NOD2 activators are in serum [119]. Within the intestine lumen, paneth cells produce lysozyme which cleaves the bond between NAM-NAC of PGN [66]. Then, PGN fragments that are cleaved by lysozyme in the intestine may be subsequently translocated via M cells and reached to the bone marrow where osteoblasts and osteoclasts existed [142]. It has been reported that soluble molecules with a molecular weight of less than 33,000 can be transmitted through the intestinal epithelium to the bloodstream [143]. Although PGN fragments might exist with different size and the exact molecular weight is unknown, when soluble Lp.PGN was separated in SDS-PAGE gel and was subjected to silver staining, the band size ranged below 7 kDa (*data not shown*). Thus, presumably PGN fragments could be delivered to the bloodstream through the intestinal epithelium. Consistent with the speculation, one report showing that *L. reuteri*-conditioned media inhibited osteoclast differentiation *in vitro* suggested that antimicrobial or immunomodulatory molecules, such as reuterin, which are produced from *L. reuteri* might inhibit osteoclast differentiation by crossing the intestinal epithelium and affect systemically [78]. Therefore, this study suggests that PGN fragments from bacteria might directly affect osteoblast differentiation *in vivo*, at least partially.

Current study observed that Lp.PGN supplementation inhibited bone loss induced by OVX through regulation of RANKL level in bone marrow extracellular fluid. RANKL is an essential factor that promotes osteoclast differentiation by binding to RANK expressed in osteoclast precursor and produced by mesenchymal cells including osteoblasts in bone environment [20]. Since up-regulations of RANKL expression and RANKL/OPG ratio typically appear in osteoporotic conditions, including aging, menopause, and an inflammatory bowel disease [53, 78, 144, 145], RANKL expression is important in inhibition of osteoporosis. In this study, Lp.PGN treatment decreased the number of TRAP-positive MNCs differentiated from BMMs in co-culture with osteoblasts and decreased mRNA expression of RANKL in osteoblasts. In addition, RANKL/OPG ratio was down-regulated by Lp.PGN supplementation. These results are concordant with the previous report showing that MDP reduced the number of TRAP-positive MNCs and intraperitoneal administration of MDP decreased RANKL in bone marrow extracellular fluid [51]. Similar to this study, *L. reuteri* and *L. rhamnosus* GG decreased RANKL expression in osteoporosis mouse model [53, 78]. Therefore, the study suggest that probiotics-released PGN fragments could be one of the important factors involved in beneficial effect of probiotics on bone regulation and that PGNs could protect RANKL-related osteoporotic bone diseases.

Supplementation of Lp.PGN decreased TNF- α production in serum and bone marrow extracellular fluid. Previously probiotics treatment altered intestinal microbiota change and the authors suggested that the change in intestinal microbiota might be associated with anti-inflammatory effects [78]. Since many previous

reports indicated that the interaction between NOD2 and intestinal bacteria maintains gut homeostasis [146, 147], NOD2 induction by Lp.PGN was expected to affect intestinal microorganisms. However, pyrosequencing analysis based on 16S rRNA gene of fecal sample from cecum showed no major population change between sham control, OVX control, and OVX mice supplemented with Lp.PGN (*data not shown*). Notably, because not only intragastric administration of Lp.PGN but also intraperitoneal and intravenous administration of Lp.PGN inhibited OVX-induced osteoporosis, presumably reduction of pro-inflammatory cytokine expression could be because of systemic circulation of Lp.PGN fragments. Down-regulation of pro-inflammatory cytokines by NOD2 ligand was shown in previous reports. Mice infected with *P. gingivalis* exhibited lower TNF- α , IL-6 and IL-17 in serum when compared with NOD2-deficient mice infected with *P. gingivalis* [132]. In addition, intraperitoneal administration of MDP down-regulated serum TNF- α and alveolar bone loss. Another study showed that MDP induced IRF4 expression in liver and white adipose tissue leading to decrease TNF- α [134]. Therefore, this study suggests that PGN fragments from probiotics could be involved in regulation of pro-inflammatory cytokines.

Because *B. subtilis* is known to be important starter strain in fermented soybean food such as natto, Bs.PGN-induced bone loss addresses a question if consumption of fermented soybean food negatively affect bone mass. In this study, Bc.PGN preferentially activated NOD1 and intragastric administration of Bc.PGN decreased trabecular bone mass. Consistent with the results, Jiao *et al.* demonstrated that NOD1 stimulating bacteria mediated alveolar bone resorption accompanied by TNF- α and RANKL expression [137]. Thus, PGN fragments from *B. subtilis* could induce bone

loss. However, there are many other components and fermented products, such as isoflavones in fermented soybean food [148]. Soy isoflavones known as phytoestrogen were demonstrated to have various biological functions including prevention of osteoporosis [149-151]. For instance, daily intake of genistein, one of isoflavone phytoestrogen that may interact with nuclear estrogen receptors, increased femoral bone mineral density in a randomized double blind placebo controlled study [152]. Moreover, previous report showed that increased hip and femoral bone marrow density by intake of fermented soybean food in postmenopausal women [153]. Therefore, the negative effect of PGN isolated from *B. subtilis* in this study is considered to be different from the bone mass changes in intake of fermented soybean food.

NOD2 and NOD1 signalings appeared to be important for bone regulation. Mice supplemented with Lp.PGN, which preferentially activated NOD2 signaling, exhibited increased bone mass, while mice supplemented with Bc.PGN or Bs.PGN, which preferentially activated NOD1 signaling, exhibited decreased bone mass. These results considerably raise question that why bone cells respond PGN fragments. There are more than 10^{14} microorganisms in gastrointestinal tract and bacteria release PGN fragments during growing [154]. Since hosts are constantly exposed to the PGN fragments released by the bacteria, they may have evolved to use stimuli rather than respond sensitively. Although the exact concentration of PGN fragments in the bloodstream is unknown, the fact that MDP alone does not induce inflammatory responses, whereas only when MDP and lipoteichoic acid are present together at high concentration, inflammation is induced [155, 156]. These previous results support the speculation that the inflammation is thought to be induced when

the host recognizes that bacteria present in the bloodstream. Because each NOD1 and NOD2 signaling have opposite effects on bone mass modulation, the ratio of NOD1-activating PGN and NOD2-activating PGN in the blood may be important for bone regulation and bone homeostasis. It would be meaningful further study to compare the PGN fragments and their ability to activate NOD1 and NOD2 through feces or serum from healthy and patients with bone disease. Therefore, regulation of osteoclast or osteoblast differentiation by PGN fragments activating NOD1 or NOD2 suggested in this study can be an important mechanism for understanding gut microbiota and bone metabolism regulation from a biological point of view. It could be an important target for bone disease treatment.

In conclusion, the study shows that NOD2-activating PGN inhibits bone loss in osteoporosis condition through increasing osteoblast differentiation and decreasing osteoclast differentiation, whereas NOD1-activating PGN induces bone destruction. Therefore, these results suggest that gut microbiota-derived PGNs could be involved in the regulation of bone metabolism through NOD1 and NOD2 signaling and that the NOD2 ligands could be used as postbiotics for treatment of bone diseases.

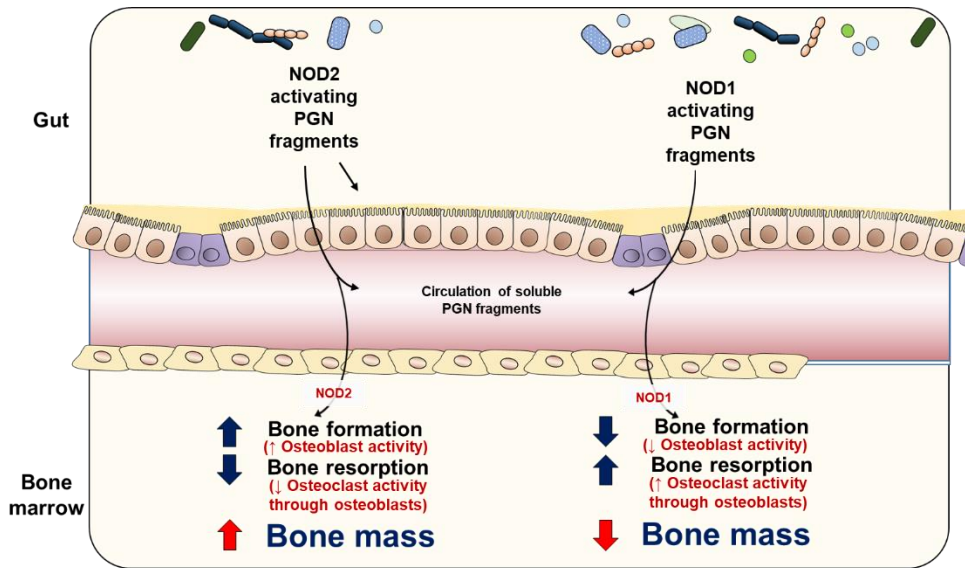


Figure 33. Schematic illustration of the proposed mechanism. Intra-gastric supplementation of NOD2-activating PGN fragments enhances bone mass through enhancement of osteoblast activation and inhibition of osteoclast differentiation via osteoblasts, while NOD1-activating PGN fragments induces bone loss through induction of osteoclast differentiation and inhibition of osteoblast differentiation. Thus, raised suggestion is that gut microbiota-derived PGNs could be involved in the regulation of bone metabolism through NOD1 and NOD2 signaling.

Chapter V. References

1. Sozen, T., L. Ozisik, and N.C. Basaran, *An overview and management of osteoporosis*. Eur J Rheumatol, 2017. 4(1): p. 46-56.
2. Long, F., *Building strong bones: molecular regulation of the osteoblast lineage*. Nat Rev Mol Cell Biol, 2011. 13(1): p. 27-38.
3. Raggatt, L.J. and N.C. Partridge, *Cellular and molecular mechanisms of bone remodeling*. J Biol Chem, 2010. 285(33): p. 25103-8.
4. Li, Z., K. Kong, and W. Qi, *Osteoclast and its roles in calcium metabolism and bone development and remodeling*. Biochem Biophys Res Commun, 2006. 343(2): p. 345-50.
5. Kular, J., et al., *An overview of the regulation of bone remodelling at the cellular level*. Clin Biochem, 2012. 45(12): p. 863-73.
6. Kuo, T.R. and C.H. Chen, *Bone biomarker for the clinical assessment of osteoporosis: recent developments and future perspectives*. Biomark Res, 2017. 5: p. 18.
7. Teitelbaum, S.L., *Bone resorption by osteoclasts*. Science, 2000. 289(5484): p. 1504-8.
8. Tanaka, S., et al., *Macrophage colony-stimulating factor is indispensable for both proliferation and differentiation of osteoclast progenitors*. J Clin Invest, 1993. 91(1): p. 257-63.
9. Lacey, D.L., et al., *Osteoprotegerin ligand is a cytokine that regulates osteoclast differentiation and activation*. Cell, 1998. 93(2): p. 165-76.
10. Jimi, E., et al., *Osteoclast differentiation factor acts as a multifunctional regulator in murine osteoclast differentiation and function*. J Immunol, 1999. 163(1): p. 434-42.
11. Armstrong, A.P., et al., *A RANK/TRAF6-dependent signal transduction pathway is essential for osteoclast cytoskeletal organization and resorptive function*. J Biol Chem, 2002. 277(46): p. 44347-56.
12. Takayanagi, H., et al., *Induction and activation of the transcription factor NFATc1 (NFAT2) integrate RANKL signaling in terminal differentiation of osteoclasts*. Dev Cell, 2002. 3(6): p. 889-901.

13. Kim, N., et al., *A novel member of the leukocyte receptor complex regulates osteoclast differentiation*. J Exp Med, 2002. 195(2): p. 201-9.
14. Humphrey, M.B., et al., *TREM2, a DAP12-associated receptor, regulates osteoclast differentiation and function*. J Bone Miner Res, 2006. 21(2): p. 237-45.
15. Takito, J., S. Inoue, and M. Nakamura, *The Sealing Zone in Osteoclasts: A Self-Organized Structure on the Bone*. Int J Mol Sci, 2018. 19(4).
16. McHugh, K.P., et al., *Mice lacking beta3 integrins are osteosclerotic because of dysfunctional osteoclasts*. J Clin Invest, 2000. 105(4): p. 433-40.
17. Stenbeck, G., *Formation and function of the ruffled border in osteoclasts*. Semin Cell Dev Biol, 2002. 13(4): p. 285-92.
18. Schlesinger, P.H., et al., *Characterization of the osteoclast ruffled border chloride channel and its role in bone resorption*. J Biol Chem, 1997. 272(30): p. 18636-43.
19. Wada, T., et al., *RANKL-RANK signaling in osteoclastogenesis and bone disease*. Trends Mol Med, 2006. 12(1): p. 17-25.
20. Fakhry, M., et al., *Molecular mechanisms of mesenchymal stem cell differentiation towards osteoblasts*. World J Stem Cells, 2013. 5(4): p. 136-48.
21. O'Brien, C.A., *Control of RANKL gene expression*. Bone, 2010. 46(4): p. 911-9.
22. Glass, D.A., 2nd, et al., *Canonical Wnt signaling in differentiated osteoblasts controls osteoclast differentiation*. Dev Cell, 2005. 8(5): p. 751-64.
23. Raisz, L.G., *Physiology and pathophysiology of bone remodeling*. Clin Chem, 1999. 45(8 Pt 2): p. 1353-8.
24. Kaewsrichan, J., et al., *Sequential induction of marrow stromal cells by FGF2 and BMP2 improves their growth and differentiation potential in vivo*. Arch Oral Biol, 2011. 56(1): p. 90-101.
25. Guerra-Menendez, L., et al., *IGF-I increases markers of osteoblastic activity and reduces bone resorption via osteoprotegerin and RANK-ligand*. J Transl Med, 2013. 11: p. 271.

26. Komori, T., et al., *Targeted disruption of Cbfa1 results in a complete lack of bone formation owing to maturational arrest of osteoblasts*. Cell, 1997. 89(5): p. 755-64.
27. Choi, J.Y., et al., *Subnuclear targeting of Runx/Cbfa/AML factors is essential for tissue-specific differentiation during embryonic development*. Proc Natl Acad Sci U S A, 2001. 98(15): p. 8650-5.
28. Huang, W., et al., *Signaling and transcriptional regulation in osteoblast commitment and differentiation*. Front Biosci, 2007. 12: p. 3068-92.
29. Stein, G.S., et al., *Runx2 control of organization, assembly and activity of the regulatory machinery for skeletal gene expression*. Oncogene, 2004. 23(24): p. 4315-29.
30. Devescovi, V., et al., *Growth factors in bone repair*. Chir Organi Mov, 2008. 92(3): p. 161-8.
31. Burr, D.B. and M.R. Allen, *Basic and applied bone biology*. 2013, Amsterdam: Elsevier/Academic Press. xv, 373 pages.
32. Wu, M., G. Chen, and Y.P. Li, *TGF-beta and BMP signaling in osteoblast, skeletal development, and bone formation, homeostasis and disease*. Bone Res, 2016. 4: p. 16009.
33. Takei, Y., T. Minamizaki, and Y. Yoshiko, *Functional diversity of fibroblast growth factors in bone formation*. Int J Endocrinol, 2015. 2015: p. 729352.
34. Sun, S.Y., et al., *Activation of Akt and eIF4E survival pathways by rapamycin-mediated mammalian target of rapamycin inhibition*. Cancer Res, 2005. 65(16): p. 7052-8.
35. Kawai, M. and C.J. Rosen, *The insulin-like growth factor system in bone: basic and clinical implications*. Endocrinol Metab Clin North Am, 2012. 41(2): p. 323-33, vi.
36. Zhang, W., et al., *Effects of insulin and insulin-like growth factor 1 on osteoblast proliferation and differentiation: differential signalling via Akt and ERK*. Cell Biochem Funct, 2012. 30(4): p. 297-302.
37. Youssef, A., D. Aboalola, and V.K. Han, *The Roles of Insulin-Like Growth Factors in Mesenchymal Stem Cell Niche*. Stem Cells Int, 2017. 2017: p. 9453108.

38. Andersen, T.L., et al., *Understanding coupling between bone resorption and formation: are reversal cells the missing link?* Am J Pathol, 2013. 183(1): p. 235-46.
39. Kenkre, J.S. and J. Bassett, *The bone remodelling cycle*. Ann Clin Biochem, 2018. 55(3): p. 308-327.
40. Schapira, D. and C. Schapira, *Osteoporosis - the Evolution of a Scientific Term*. Osteoporosis International, 1992. 2(4): p. 164-167.
41. Schepper, J.D., et al., *Probiotics in Gut-Bone Signaling*. Adv Exp Med Biol, 2017. 1033: p. 225-247.
42. Schnell, S., et al., *The 1-year mortality of patients treated in a hip fracture program for elders*. Geriatr Orthop Surg Rehabil, 2010. 1(1): p. 6-14.
43. Wright, N.C., et al., *The recent prevalence of osteoporosis and low bone mass in the United States based on bone mineral density at the femoral neck or lumbar spine*. J Bone Miner Res, 2014. 29(11): p. 2520-6.
44. Ozaras, N. and A. Rezvani, *Diffuse skeletal pain after administration of alendronate*. Indian J Pharmacol, 2010. 42(4): p. 245-6.
45. Musette, P., et al., *Treatment of osteoporosis: recognizing and managing cutaneous adverse reactions and drug-induced hypersensitivity*. Osteoporos Int, 2010. 21(5): p. 723-32.
46. Kyrgidis, A. and K.A. Toulis, *Denosumab-related osteonecrosis of the jaws*. Osteoporos Int, 2011. 22(1): p. 369-70.
47. Voss, P.J., et al., *Osteonecrosis of the jaw in patients transitioning from bisphosphonates to denosumab treatment for osteoporosis*. Odontology, 2018. 106(4): p. 469-480.
48. Woo, T. and J.D. Adachi, *Role of bisphosphonates and calcitonin in the prevention and treatment of osteoporosis*. Best Pract Res Clin Rheumatol, 2001. 15(3): p. 469-81.
49. D'Amelio, P. and G.C. Isaia, *The use of raloxifene in osteoporosis treatment*. Expert Opinion on Pharmacotherapy, 2013. 14(7): p. 949-956.
50. Nikitovic, D., et al., *Parathyroid hormone/parathyroid hormone-related peptide regulate osteosarcoma cell functions: Focus on the extracellular matrix (Review)*. Oncol Rep, 2016. 36(4): p. 1787-92.

51. Park, O.J., et al., *Muramyl Dipeptide, a Shared Structural Motif of Peptidoglycans, Is a Novel Inducer of Bone Formation through Induction of Runx2*. J Bone Miner Res, 2017. 32(7): p. 1455-1468.
52. Lucas, S., et al., *Short-chain fatty acids regulate systemic bone mass and protect from pathological bone loss*. Nat Commun, 2018. 9(1): p. 55.
53. Li, J.Y., et al., *Sex steroid deficiency-associated bone loss is microbiota dependent and prevented by probiotics*. J Clin Invest, 2016. 126(6): p. 2049-63.
54. Jones, R.M., J.G. Mülle, and R. Pacifici, *Osteomicrobiology: The influence of gut microbiota on bone in health and disease*. Bone, 2018. 115: p. 59-67.
55. Schwarzer, M., et al., *Lactobacillus plantarum strain maintains growth of infant mice during chronic undernutrition*. Science, 2016. 351(6275): p. 854-7.
56. Sjogren, K., et al., *The gut microbiota regulates bone mass in mice*. J Bone Miner Res, 2012. 27(6): p. 1357-67.
57. Wu, H.J., et al., *Gut-residing segmented filamentous bacteria drive autoimmune arthritis via T helper 17 cells*. Immunity, 2010. 32(6): p. 815-27.
58. Hathaway-Schrader, J.D., et al., *Antibiotic Perturbation of Gut Microbiota Dysregulates Osteoimmune Cross Talk in Postpubertal Skeletal Development*. Am J Pathol, 2019. 189(2): p. 370-390.
59. Schepper, J.D., et al., *Probiotic Lactobacillus reuteri Prevents Postantibiotic Bone Loss by Reducing Intestinal Dysbiosis and Preventing Barrier Disruption*. J Bone Miner Res, 2019. 34(4): p. 681-698.
60. Food and Agriculture Organization of the United Nations. and World Health Organization., *Probiotics in food : health and nutritional properties and guidelines for evaluation*. FAO food and nutrition paper., 2006, Rome: Food and Agriculture Organization of the United Nations : World Health Organization. viii, 50 p.
61. Collins, F.L., et al., *Lactobacillus reuteri 6475 Increases Bone Density in Intact Females Only under an Inflammatory Setting*. PLoS One, 2016. 11(4): p. e0153180.

62. Lebeer, S., J. Vanderleyden, and S.C. De Keersmaecker, *Genes and molecules of lactobacilli supporting probiotic action*. Microbiol Mol Biol Rev, 2008. 72(4): p. 728-64, Table of Contents.
63. McCabe, L.R. and N. Parameswaran, *Advances in Probiotic Regulation of Bone and Mineral Metabolism*. Calcif Tissue Int, 2018. 102(4): p. 480-488.
64. Mokoena, M.P., *Lactic Acid Bacteria and Their Bacteriocins: Classification, Biosynthesis and Applications against Uropathogens: A Mini-Review*. Molecules, 2017. 22(8).
65. Lee, S.H., *Intestinal permeability regulation by tight junction: implication on inflammatory bowel diseases*. Intest Res, 2015. 13(1): p. 11-8.
66. Allaire, J.M., et al., *The Intestinal Epithelium: Central Coordinator of Mucosal Immunity: (Trends in Immunology 39, 677-696, 2018)*. Trends Immunol, 2019. 40(2): p. 174.
67. Collins, F.L., et al., *Temporal and regional intestinal changes in permeability, tight junction, and cytokine gene expression following ovariectomy-induced estrogen deficiency*. Physiol Rep, 2017. 5(9).
68. Irwin, R., et al., *Intestinal inflammation without weight loss decreases bone density and growth*. Am J Physiol Regul Integr Comp Physiol, 2016. 311(6): p. R1149-R1157.
69. Kim, J., et al., *Lipoproteins are an important bacterial component responsible for bone destruction through the induction of osteoclast differentiation and activation*. J Bone Miner Res, 2013. 28(11): p. 2381-91.
70. Yi, L., et al., *Gene Modification of Transforming Growth Factor beta (TGF-beta) and Interleukin 10 (IL-10) in Suppressing Mt Sonicate Induced Osteoclast Formation and Bone Absorption*. Med Sci Monit, 2018. 24: p. 5200-5207.
71. Ciucci, T., et al., *Bone marrow Th17 TNFalpha cells induce osteoclast differentiation, and link bone destruction to IBD*. Gut, 2015. 64(7): p. 1072-81.
72. Ali, T., et al., *Osteoporosis in inflammatory bowel disease*. Am J Med, 2009. 122(7): p. 599-604.

73. Metzger, C.E., et al., *Inflammatory Bowel Disease in a Rodent Model Alters Osteocyte Protein Levels Controlling Bone Turnover*. J Bone Miner Res, 2017. 32(4): p. 802-813.
74. Klaenhammer, T.R., et al., *The impact of probiotics and prebiotics on the immune system*. Nat Rev Immunol, 2012. 12(10): p. 728-34.
75. Frei, R., M. Akdis, and L. O'Mahony, *Prebiotics, probiotics, synbiotics, and the immune system: experimental data and clinical evidence*. Curr Opin Gastroenterol, 2015. 31(2): p. 153-8.
76. Ohlsson, C., et al., *Probiotics protect mice from ovariectomy-induced cortical bone loss*. PLoS One, 2014. 9(3): p. e92368.
77. McCabe, L.R., et al., *Probiotic use decreases intestinal inflammation and increases bone density in healthy male but not female mice*. J Cell Physiol, 2013. 228(8): p. 1793-8.
78. Britton, R.A., et al., *Probiotic L. reuteri treatment prevents bone loss in a menopausal ovariectomized mouse model*. J Cell Physiol, 2014. 229(11): p. 1822-30.
79. Zhang, J., et al., *Loss of Bone and Wnt10b Expression in Male Type 1 Diabetic Mice Is Blocked by the Probiotic Lactobacillus reuteri*. Endocrinology, 2015. 156(9): p. 3169-82.
80. Chiang, S.S. and T.M. Pan, *Antiosteoporotic effects of Lactobacillus - fermented soy skim milk on bone mineral density and the microstructure of femoral bone in ovariectomized mice*. J Agric Food Chem, 2011. 59(14): p. 7734-42.
81. Wang, Z., et al., *Probiotics protect mice from CoCrMo particles-induced osteolysis*. Int J Nanomedicine, 2017. 12: p. 5387-5397.
82. Gatej, S.M., et al., *Probiotic Lactobacillus rhamnosus GG prevents alveolar bone loss in a mouse model of experimental periodontitis*. J Clin Periodontol, 2018. 45(2): p. 204-212.
83. Kobayashi, R., et al., *Oral administration of Lactobacillus gasseri SBT2055 is effective in preventing Porphyromonas gingivalis-accelerated periodontal disease*. Sci Rep, 2017. 7(1): p. 545.

84. Maekawa, T. and G. Hajishengallis, *Topical treatment with probiotic Lactobacillus brevis CD2 inhibits experimental periodontal inflammation and bone loss*. J Periodontal Res, 2014. 49(6): p. 785-91.
85. Cava, F. and M.A. de Pedro, *Peptidoglycan plasticity in bacteria: emerging variability of the murein sacculus and their associated biological functions*. Curr Opin Microbiol, 2014. 18: p. 46-53.
86. Typas, A., et al., *From the regulation of peptidoglycan synthesis to bacterial growth and morphology*. Nat Rev Microbiol, 2011. 10(2): p. 123-36.
87. Bourhis, L.L. and C. Werts, *Role of Nods in bacterial infection*. Microbes Infect, 2007. 9(5): p. 629-36.
88. Guan, R., et al., *Structural basis for peptidoglycan binding by peptidoglycan recognition proteins*. Proc Natl Acad Sci U S A, 2004. 101(49): p. 17168-73.
89. Vollmer, W., D. Blanot, and M.A. de Pedro, *Peptidoglycan structure and architecture*. FEMS Microbiol Rev, 2008. 32(2): p. 149-67.
90. Humann, J. and L.L. Lenz, *Bacterial peptidoglycan degrading enzymes and their impact on host muropeptide detection*. J Innate Immun, 2009. 1(2): p. 88-97.
91. Thunnissen, A.M., et al., *Structure of the 70-kDa soluble lytic transglycosylase complexed with bulgecin A. Implications for the enzymatic mechanism*. Biochemistry, 1995. 34(39): p. 12729-37.
92. Callewaert, L. and C.W. Michiels, *Lysozymes in the animal kingdom*. J Biosci, 2010. 35(1): p. 127-60.
93. Vollmer, W., et al., *Bacterial peptidoglycan (murein) hydrolases*. FEMS Microbiol Rev, 2008. 32(2): p. 259-86.
94. Doyle, R.J., J. Chaloupka, and V. Vinter, *Turnover of cell walls in microorganisms*. Microbiol Rev, 1988. 52(4): p. 554-67.
95. Muller, A., A. Klockner, and T. Schneider, *Targeting a cell wall biosynthesis hot spot*. Nat Prod Rep, 2017. 34(7): p. 909-932.
96. Dziarski, R. and D. Gupta, *The peptidoglycan recognition proteins (PGRPs)*. Genome Biology, 2006. 7(8).
97. Fritz, J.H., et al., *Nod-like proteins in immunity, inflammation and disease*. Nat Immunol, 2006. 7(12): p. 1250-7.

98. Meylan, E., J. Tschopp, and M. Karin, *Intracellular pattern recognition receptors in the host response*. Nature, 2006. 442(7098): p. 39-44.
99. Franchi, L., et al., *Function of Nod-like receptors in microbial recognition and host defense*. Immunol Rev, 2009. 227(1): p. 106-28.
100. Girardin, S.E., et al., *Nod1 detects a unique muropeptide from gram-negative bacterial peptidoglycan*. Science, 2003. 300(5625): p. 1584-7.
101. Girardin, S.E., et al., *Nod2 is a general sensor of peptidoglycan through muramyl dipeptide (MDP) detection*. J Biol Chem, 2003. 278(11): p. 8869-72.
102. Troll, J.V., et al., *Taming the symbiont for coexistence: a host PGRP neutralizes a bacterial symbiont toxin*. Environ Microbiol, 2010. 12(8): p. 2190-203.
103. Goodson, M.S., et al., *Identifying components of the NF-kappaB pathway in the beneficial Euprymna scolopes-Vibrio fischeri light organ symbiosis*. Appl Environ Microbiol, 2005. 71(11): p. 6934-46.
104. Viala, J., et al., *Nod1 responds to peptidoglycan delivered by the Helicobacter pylori cag pathogenicity island*. Nat Immunol, 2004. 5(11): p. 1166-74.
105. Bielig, H., et al., *NOD-like receptor activation by outer membrane vesicles from Vibrio cholerae non-O1 non-O139 strains is modulated by the quorum-sensing regulator HapR*. Infect Immun, 2011. 79(4): p. 1418-27.
106. Marina-Garcia, N., et al., *Clathrin- and dynamin-dependent endocytic pathway regulates muramyl dipeptide internalization and NOD2 activation*. J Immunol, 2009. 182(7): p. 4321-7.
107. Lee, J., et al., *pH-dependent internalization of muramyl peptides from early endosomes enables Nod1 and Nod2 signaling*. J Biol Chem, 2009. 284(35): p. 23818-29.
108. Girardin, S.E., et al., *Peptidoglycan molecular requirements allowing detection by Nod1 and Nod2*. J Biol Chem, 2003. 278(43): p. 41702-8.
109. Le Bourhis, L., S. Benko, and S.E. Girardin, *Nod1 and Nod2 in innate immunity and human inflammatory disorders*. Biochem Soc Trans, 2007. 35(Pt 6): p. 1479-84.

110. Bernard, E., et al., *Identification of the amidotransferase AsnB1 as being responsible for meso-diaminopimelic acid amidation in Lactobacillus plantarum peptidoglycan*. J Bacteriol, 2011. 193(22): p. 6323-30.
111. Dagil, Y.A., et al., *The Dual NOD1/NOD2 Agonism of Muropeptides Containing a Meso-Diaminopimelic Acid Residue*. PLoS One, 2016. 11(8): p. e0160784.
112. Rubino, S.J., et al., *Nod-like receptors in the control of intestinal inflammation*. Curr Opin Immunol, 2012. 24(4): p. 398-404.
113. Fritz, J.H., et al., *Synergistic stimulation of human monocytes and dendritic cells by Toll-like receptor 4 and NOD1- and NOD2-activating agonists*. Eur J Immunol, 2005. 35(8): p. 2459-70.
114. Hasegawa, M., et al., *A critical role of RICK/RIP2 polyubiquitination in Nod-induced NF-kappaB activation*. EMBO J, 2008. 27(2): p. 373-83.
115. Magalhaes, J.G., et al., *Nucleotide oligomerization domain-containing proteins instruct T cell helper type 2 immunity through stromal activation*. Proc Natl Acad Sci U S A, 2011. 108(36): p. 14896-901.
116. Magalhaes, J.G., et al., *Nod2-dependent Th2 polarization of antigen-specific immunity*. J Immunol, 2008. 181(11): p. 7925-35.
117. Fritz, J.H., et al., *Nod1-mediated innate immune recognition of peptidoglycan contributes to the onset of adaptive immunity*. Immunity, 2007. 26(4): p. 445-59.
118. Hasegawa, M., et al., *Differential release and distribution of Nod1 and Nod2 immunostimulatory molecules among bacterial species and environments*. J Biol Chem, 2006. 281(39): p. 29054-63.
119. Clarke, T.B., et al., *Recognition of peptidoglycan from the microbiota by Nod1 enhances systemic innate immunity*. Nat Med, 2010. 16(2): p. 228-31.
120. Yu, Y., et al., *Diversity of innate immune recognition mechanism for bacterial polymeric meso-diaminopimelic acid-type peptidoglycan in insects*. J Biol Chem, 2010. 285(43): p. 32937-45.
121. Park, J.H., et al., *RICK/RIP2 mediates innate immune responses induced through Nod1 and Nod2 but not TLRs*. J Immunol, 2007. 178(4): p. 2380-6.
122. Sophocleous, A. and A.I. Idris, *Rodent models of osteoporosis*. Bonekey Rep, 2014. 3: p. 614.

123. Kim, J., et al., *Serum amyloid A inhibits osteoclast differentiation to maintain macrophage function*. J Leukoc Biol, 2016. 99(4): p. 595-603.
124. Lee, E., et al., *Lactobacillus plantarum Strain Ln4 Attenuates Diet-Induced Obesity, Insulin Resistance, and Changes in Hepatic mRNA Levels Associated with Glucose and Lipid Metabolism*. Nutrients, 2018. 10(5).
125. Schultz, M., et al., *Lactobacillus plantarum 299V in the treatment and prevention of spontaneous colitis in interleukin-10-deficient mice*. Inflamm Bowel Dis, 2002. 8(2): p. 71-80.
126. Kwak, S.H., et al., *Cancer Preventive Potential of Kimchi Lactic Acid Bacteria (Weissella cibaria, Lactobacillus plantarum)*. J Cancer Prev, 2014. 19(4): p. 253-8.
127. McElroy, J.F. and G.N. Wade, *Short- and long-term effects of ovariectomy on food intake, body weight, carcass composition, and brown adipose tissue in rats*. Physiol Behav, 1987. 39(3): p. 361-5.
128. Felis, G.E. and F. Dellaglio, *Taxonomy of Lactobacilli and Bifidobacteria*. Curr Issues Intest Microbiol, 2007. 8(2): p. 44-61.
129. Irazoki, O., S.B. Hernandez, and F. Cava, *Peptidoglycan Muropeptides: Release, Perception, and Functions as Signaling Molecules*. Front Microbiol, 2019. 10: p. 500.
130. Baik, J.E., et al., *Differential profiles of gastrointestinal proteins interacting with peptidoglycans from Lactobacillus plantarum and Staphylococcus aureus*. Mol Immunol, 2015. 65(1): p. 77-85.
131. Hankiewicz, J. and E. Swierczek, *Lysozyme in human body fluids*. Clin Chim Acta, 1974. 57(3): p. 205-9.
132. Yuan, H., et al., *Pivotal role of NOD2 in inflammatory processes affecting atherosclerosis and periodontal bone loss*. Proc Natl Acad Sci U S A, 2013. 110(52): p. E5059-68.
133. Gilbert, L., et al., *Inhibition of osteoblast differentiation by tumor necrosis factor-alpha*. Endocrinology, 2000. 141(11): p. 3956-64.
134. Cavallari, J.F., et al., *Muramyl Dipeptide-Based Postbiotics Mitigate Obesity-Induced Insulin Resistance via IRF4*. Cell Metab, 2017. 25(5): p. 1063-1074 e3.

135. Macho Fernandez, E., et al., *Anti-inflammatory capacity of selected lactobacilli in experimental colitis is driven by NOD2-mediated recognition of a specific peptidoglycan-derived muropeptide*. Gut, 2011. 60(8): p. 1050-9.
136. Honma, K., et al., *Interferon regulatory factor 4 negatively regulates the production of proinflammatory cytokines by macrophages in response to LPS*. Proc Natl Acad Sci U S A, 2005. 102(44): p. 16001-6.
137. Jiao, Y., et al., *Induction of bone loss by pathobiont-mediated Nod1 signaling in the oral cavity*. Cell Host Microbe, 2013. 13(5): p. 595-601.
138. Chaves de Souza, J.A., et al., *NOD1 in the modulation of host-microbe interactions and inflammatory bone resorption in the periodontal disease model*. Immunology, 2016. 149(4): p. 374-385.
139. Schricker, M.E., G.H. Thompson, and J.R. Schreiber, *Osteomyelitis due to Bacillus cereus in an adolescent: case report and review*. Clin Infect Dis, 1994. 18(6): p. 863-7.
140. Asagiri, M. and H. Takayanagi, *The molecular understanding of osteoclast differentiation*. Bone, 2007. 40(2): p. 251-64.
141. Vollmer, W., *Structural variation in the glycan strands of bacterial peptidoglycan*. FEMS Microbiol Rev, 2008. 32(2): p. 287-306.
142. Lyte, M., *Microbial Endocrinology: The Microbiota-Gut-Brain Axis in Health and Disease Foreword*. Microbial Endocrinology: The Microbiota-Gut-Brain Axis in Health and Disease, 2014. 817: p. Vii-Vii.
143. Loehry, C.A., et al., *Permeability of the small intestine to substances of different molecular weight*. Gut, 1970. 11(6): p. 466-70.
144. Cao, J., et al., *Expression of RANKL and OPG correlates with age-related bone loss in male C57BL/6 mice*. J Bone Miner Res, 2003. 18(2): p. 270-7.
145. Moschen, A.R., et al., *The RANKL/OPG system is activated in inflammatory bowel disease and relates to the state of bone loss*. Gut, 2005. 54(4): p. 479-87.
146. Petnicki-Ocwieja, T., et al., *Nod2 is required for the regulation of commensal microbiota in the intestine*. Proc Natl Acad Sci U S A, 2009. 106(37): p. 15813-8.

147. Biswas, A., T. Petnicki-Ocwieja, and K.S. Kobayashi, *Nod2: a key regulator linking microbiota to intestinal mucosal immunity*. J Mol Med (Berl), 2012. 90(1): p. 15-24.
148. Rizzo, G. and L. Baroni, *Soy, Soy Foods and Their Role in Vegetarian Diets*. Nutrients, 2018. 10(1).
149. Arjmandi, B.H., et al., *Bone-sparing effect of soy protein in ovarian hormone-deficient rats is related to its isoflavone content*. Am J Clin Nutr, 1998. 68(6 Suppl): p. 1364S-1368S.
150. Bawa, S., *The significance of soy protein and soy bioactive compounds in the prophylaxis and treatment of osteoporosis*. J Osteoporos, 2010. 2010: p. 891058.
151. Picherit, C., et al., *Dose-dependent bone-sparing effects of dietary isoflavones in the ovariectomised rat*. Br J Nutr, 2001. 85(3): p. 307-16.
152. Morabito, N., et al., *Effects of genistein and hormone-replacement therapy on bone loss in early postmenopausal women: a randomized double-blind placebo-controlled study*. J Bone Miner Res, 2002. 17(10): p. 1904-12.
153. Ikeda, Y., et al., *Intake of fermented soybeans, natto, is associated with reduced bone loss in postmenopausal women: Japanese Population-Based Osteoporosis (JPOS) Study*. J Nutr, 2006. 136(5): p. 1323-8.
154. Putignani, L., et al., *The human gut microbiota: a dynamic interplay with the host from birth to senescence settled during childhood*. Pediatr Res, 2014. 76(1): p. 2-10.
155. Kim, H.J., et al., *Lipoteichoic acid and muramyl dipeptide synergistically induce maturation of human dendritic cells and concurrent expression of proinflammatory cytokines*. J Leukoc Biol, 2007. 81(4): p. 983-9.
156. Leemans, J.C., et al., *Lipoteichoic acid and peptidoglycan from Staphylococcus aureus synergistically induce neutrophil influx into the lungs of mice*. Clin Diagn Lab Immunol, 2003. 10(5): p. 950-3.

국문초록

목적

최근 장내 미생물과 건강과의 상관관계가 주목을 받고 있으며, 특히 프로바이오틱스의 섭취가 장내 세균을 조절하여 노화에 따른 성호르몬 감소나 감염에 따른 골소실을 완화한다는 다양한 연구결과가 보고되고 있다. 하지만 장내 세균에 의한 골대사 조절이 세균의 어떤 구성성분에 의해 매개되는가에 대한 부분은 명확히 밝혀진 바가 없다. 기존 연구 결과에 따르면 장내 세균 유래의 펩티도글리칸이 혈류를 따라 이동하여 골수 내의 면역세포 활성을 조절할 수 있다고 보고된 바 있으며, 펩티도글리칸의 최소 활성단위인 muramyl dipeptide 가 nucleotide-binding oligomerization domain (NOD) 2 를 통하여 조골세포와 파골세포 분화를 직접 매개한다는 것이 제시된 바 있다. 따라서, 이 논문에서는 기존 연구결과를 바탕으로, 세균으로부터 유래하는 펩티도글리칸이 직접적으로 혈류를 따라 이동하여 조골세포와 파골세포의 분화를 조절할 수 있을 것이라는 가설을 설정하고 이를 증명하기 위한 연구를 수행하였다.

실험방법

세균의 펩티도글리칸이 골대사 조절에 관여하는지 확인하기 위하여 *Lactobacillus* spp.와 *Bacillus* spp.로부터 펩티도글리칸을 분리하였다.

펩티도글리칸의 분리는 세균균질기를 이용해 세균을 깨뜨린 후, sodium dodecyl sulphate, DNase, RNase, trypsin 을 순차적으로 처리하여 지질단백질, DNA, RNA 를 제거하였다. Trichloroacetic acid 처리로 펩티도글리칸을 침전시킨 후, acetone 처리로 다른 세포벽 구성 분자를 제거하고, 동결건조 후 중량을 측정하여 사용하였다. 수용성 펩티도글리칸은 mutanolysin 처리를 통해 준비하였다. NOD1 또는 NOD2 의 신호전달 활성을 조사하기 위하여 NOD1 또는 NOD2 가 과발현된 HEK 293 T 세포에 펩티도글리칸을 처리하고 nuclear factor- κ B (NF- κ B) 활성을 리포터 유전자 분석기법으로 확인하였다. 동물모델에서 *L. plantarum* 으로부터 분리한 펩티도글리칸(Lp.PGN)의 효과를 확인하기 위하여 골소실 모델로 난소절제모델과 receptor activator of NF- κ B ligand (RANKL)을 선정하고, 불용성 펩티도글리칸을 4 주에 걸쳐 주 3 회 위관 투여하였다. Lp.PGN 의 직접적인 영향을 확인하기 위한 실험에서는 불용성 펩티도글리칸을 4 주에 걸쳐 주 1 회, 복강 또는 정맥투여하였다. 한편, *B. cereus* 와 *B. subtilis* 로 부터 분리한 펩티도글리칸을 4 주에 걸쳐 주 3 회 위관투여하여 마우스 대퇴골 내 소주골 변화를 미세단층촬영을 통해 분석하였다. 난소절제모델의 경우, 마우스 몸무게와 자궁 무게 측정, 혈청 내의 17β -estradiol 양 측정을 통해 난소 절제에 의한 성호르몬 감소가 유도되었음을 확인하였다. 골량 변화를 측정하기 위하여 마우스의 대퇴골과 요추골을 분리하여 미세단층촬영을 통해 대퇴골 내 소주골 또는 요추골 내 소주골을 분석하였다. 마우스 대퇴골은 탈회 후 조직절편을 얻어 조골세포 분화를 Runx2 면역형광염색법으로 확인하고, 파골세포의 분화를 tartrate-

resistant acid phosphatase (TRAP) 염색법을 이용해 측정하였다. 한편, 펩티도글리칸 투여 시, 일정 간격으로 calcein 을 투여한 후, 마우스 대퇴골 비탈회 조직절편을 얻어 신생골의 형성 정도를 분석하였다. 또한, 대퇴골의 골조직과 골수를 분리하여 조골세포와 파골세포 분화 관련 인자의 유전자 발현을 real-time RT-PCR 을 통해 측정하였다. 펩티도글리칸 투여에 의한 골세포 분화관련 사이토카인의 단백질 발현을 확인하기 위하여 펩티도글리칸을 투여한 마우스에서 serum 과 bone marrow extracellular fluid 를 얻어 TNF- α , interleukin (IL)-6, IL-1 β , RANKL, P1NP, 또는 osteoprotegerin (OPG)의 발현을 enzyme-linked immunosorbent assay 를 통해 확인하였다. *In vitro* 실험을 위한 조골세포 분화는 마우스 두개골에서 분리한 조골전구세포에 ascorbic acid 와 β -glycerophosphate 를 처리하여 유도하였으며, 파골세포 분화는 골수세포 유래의 대식세포에 macrophage colony-stimulating factor 와 RANKL 을 처리하여 유도하였다. 한편, 파골세포와 조골세포의 공배양 조건에서는 ascorbic acid, β -glycerophosphate, 1 α ,25-dihydroxyvitamin D₃ 를 처리하여 배양하였다. 조골세포의 활성화는 alizarin red S 염색법을 통해 확인하였으며, 파골세포 분화는 TRAP 염색법을 통해 세포를 염색하고, 핵을 세 개 이상 포함하는 다핵세포의 수를 측정하여 확인하였다. 각 세포의 분화와 활성화에 관련된 인자의 유전자 발현 정도는 real-time RT-PCR 로 관찰하였다.

결과

골소실 마우스 모델인 난소절제모델에 Lp.PGN 을 투여하였을 때, 대퇴골과 요추골의 소주골 골량과 소주골의 수의 증가가 관찰되었다. Lp.PGN 투여는 난소절제로 인해 감소한 소주골 주변의 runt-related transcription factor 2 발현 증가를 유도한 반면, 난소절제로 인해 증가한 소주골 주변의 TRAP 발현을 억제하였다. RANKL 로 유도한 골소실 모델에서의 Lp.PGN 위관투여 실험에서도 RANKL 에 의해 감소된 대퇴골 내 소주골의 골량이 Lp.PGN 투여에 의해 증가하는 것을 확인하였다. Calcein 투여 실험을 통해 Lp.PGN 투여에 의한 골량 증가가 신생골 형성을 통해서 유도된다는 것을 확인할 수 있었다. *In vitro* 실험을 통해 Lp.PGN 이 직접적으로 조골세포의 미네랄화 증가를 유도한다는 것을 확인하였으며, 파골세포와 조골세포의 공배양 조건에서 Lp.PGN 이 조골세포가 발현하는 RANKL 을 감소시켜 간접적으로 파골세포 분화를 억제함을 관찰하였다. Lp.PGN 은 NOD2 를 선택적으로 활성화하였으며, NOD2 가 결손된 골다공증 모델 마우스에 Lp.PGN 을 투여하였을 때, 야생형에서 나타난 골량 증가가 나타나지 않는 것을 관찰할 수 있었다. 이 때, Runx2 의 발현증가나 TRAP 발현 억제 또한 관찰되지 않았다. 뿐만 아니라, Lp.PGN 의 직접적인 역할을 확인하고자 수행한 Lp.PGN 의 복강투여나 정맥투여에서도 난소절제에 의해 감소한 대퇴골 내 소주골의 골량이 Lp.PGN 에 의해 증가됨을 관찰할 수 있었다. 또한, Lp.PGN 의 위관투여는 serum 에서의 난소절제에 의해 증가한 TNF- α 와 IL-6 의 발현을 감소시켰으며, bone marrow extracellular fluid 의

RANKL/OPG ratio 를 감소시킴을 확인하였다. 한편, *B. cereus* 유래의 펩티도글리칸(Bc.PGN)과 *B. subtilis* 유래의 펩티도글리칸(Bs.PGN)은 NOD1 을 선택적으로 활성화하였으며, Bc.PGN 을 주 3 회, 4 주동안 위관투여한 결과에서 Bc.PGN 에 의해 대퇴골 내 소주골 골량이 감소하였다. 이 때, Bc.PGN 투여에 의해 소주골 주변의 TRAP 발현이 증가함을 확인할 수 있었다. 파골세포와 조골세포의 공배양 조건에서 Bc.PGN 에 의한 파골세포 분화영향을 관찰하였을 때, Bc.PGN 은 조골세포가 발현하는 RANKL 을 증가시켜 파골세포의 분화를 증가시킨다는 것을 알 수 있었다. 뿐만 아니라, Bc.PGN 이 파골세포에 직접적으로 영향을 줄 수 있는지 확인하였을 때, Bc.PGN 이 파골세포에 직접적으로 파골세포에 작용하여 ERK 인산화를 통해 파골세포의 분화 증가를 유도함을 관찰하였다. Bc.PGN 은 조골세포에 직접적으로 작용하여 조골세포의 분화를 억제하는 것을 확인하였다.

결론

이상의 연구결과를 통해 NOD2 의 활성화를 유도하는 펩티도글리칸이 조골세포 분화 유도과 파골세포 분화 억제를 통해 골량을 증가시키고, 반대로 NOD1 의 활성화를 유도하는 펩티도글리칸은 조골세포 분화 억제와 파골세포 분화 유도를 통해 골량을 감소시키는 것을 확인할 수 있었다. 이러한 결과는 장내세균총 유래의 펩티도글리칸이 NOD1 과 NOD2 를 통해 골대사를 조절할 수 있을 것이라는 가능성을 제시하며, NOD2 를 활성화하는

펩티도글리칸의 경우 골질환 치료 제어를 위한 타겟 물질로 작용할 수 있을 것으로 기대된다.

주요어: 세균 펩티도글리칸, NOD1, NOD2, 파골세포, 조골세포

학번: 2011-31195